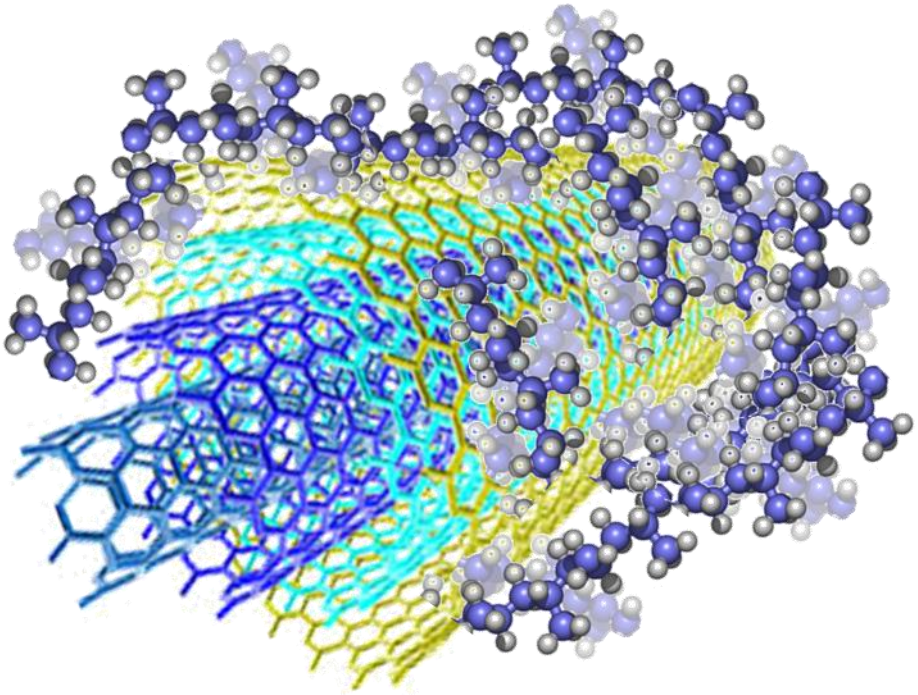

Preparation and Characterization of Polypropylene-Based Systems With Enhanced Thermal Conductivity

Antonella Patti

UNIVERSITY OF NAPLES FEDERICO II

Department of Chemical, Materials and Production Engineering

Preparation and Characterization of Polypropylene-Based Systems With Enhanced Thermal Conductivity

ANTONELLA PATTI

PhD in Materials and Structure Engineering

Dissertation

Supervisors

Ch.mo Prof. Giuseppe Mensitieri

Ch.mo Prof. Domenico Acierno

Ch.mo Dott. Pietro Russo

2013-2016

Preface

The increasing demand of thermally conductive plastics, together with growing spread of polypropylene as basic material for industrial plastics' world are the *leit motiv* of this research focused on improving thermal transport behavior of commercial polypropylene (PP) resins. An approach to solve this question could be the development of suitable nanosystems including extremely high thermally conductive fillers in neat PP matrices. This task could be well-accomplished by carbonaceous nanosized additives as carbon nanotubes, characterized by exceptionally high thermal conductivity. Yet, thermal conduction properties of a common binary PP/CNTs system could be further strengthened by the introducing of secondary fillers, different in size and shape with respect to the primary one.

In this framework, the structure of this dissertation is divided in five chapters. The whole is preceded by a brief description on the benefits of thermally conductive plastics, on how to get them and main reasons for choosing polypropylene resins as matrices: the Introduction.

The state of art, including general aspects on the thermal conductivity of matrix, carbon nanotubes and composites, is given in Chap. I.

In Chap. II, details on chosen materials, preparation and characterization techniques of obtained compounds are reported. All formulations are prepared by conventional melt-compounding procedures, generally less effective in filler dispersion but more attractive from industrial and environmental points of view, with respect to other routes as *solution mixing* and *in situ polymerization.*

Two experimental sections follow: the first one focused on the preparation and characterization of CNTs-binary systems, the second one dedicated to hybrid formulations obtained by adding to polypropylene, in addition to not

functionalized CNTs, a secondary filler, chosen for its previous applications in the same fields, as reported in literature [1-5].

The starting point, of the first experimental part, is an analysis on the influence of raw materials and processing conditions on the thermal transport behavior of nanocomposites. At this regard, two commercial polypropylene grades with different melt flow rate, the addition of a compatibilizer, different melt-compounding and molding conditions as temperature, dwell time, screw speed, pressure, filler drying and so on, are considered to optimize nanocomposites preparation in order to enhance their thermal conductivity (Chap. III). Three different commercial MWNTs, with the same aspect ratio but different chemistry and primary agglomerates are tested in order to verify how their features affect the final filler distribution and, consequently, the thermal transport of the hosting matrix (Chap. IV). In details, with the awareness that filler-matrix covalent compatibilization, improving the interface adhesion, hinders heat conduction along particles, carbon nanotubes modified with polar groups as amino (MWNT-NH_2) and carboxyl (MWNT-COOH) ones have been chosen in spite of the matrix non polarity. Thus, the polar nature of both functionalizations, reducing the affinity with the non-polar polypropylene, is responsible for poor wetting and infiltration of carbon nanotubes agglomerates and may give rise to agglomerates with higher cohesive strength and, consequently, more resistant to dispersion mechanisms than pristine ones. The actual filler dispersion is estimated by dynamic rheological measurements and morphological observations collected by electron microscopy (SEM and TEM), and also quantified through a well established approach, using images elaboration by optical microscopy (OP). Since both these two techniques are time-consuming and require analysis on cut or fractured surface, the possibility of adopting another alternative non-destructive technique, Terahertz (THz) Time Domain Spectroscopy (TDS), to get qualitative information on filler

dispersion, is also evaluated. To validate this innovative idea, specific parameters as the refractive index (n) and the absorption coefficient (α) are correlated with dispersion index, calculated by optical microscopy.

Calorimetric scanning tests (DSC) are also carried out on the same systems, analyzing any possible action of CNTs on the matrix crystallinity. Finally, taking into account the excellent mechanical properties of CNTs, static bending tests for all prepared systems are considered.

In the second experimental part (Chap. V), hybrid systems, including not functionalized MWNTs and secondary fillers as Boron Nitride (BN), Talc, Calcium Carbonate ($CaCO_3$) or Zinc Oxide (ZnO), respectively, are prepared and systematically characterized by analogous techniques. In particular, interest is devoted to thermal conductivity measurements, thermal characterization by TGA and DSC, and morphological aspects by EDS/SEM analysis. The influence of two included particles on the final processability of matrix is also analyzed by torque measurements, during melt compounding, and capillary rheological tests. Electrical conductivity measurements and rotational rheological tests are performed to clarify the rule of percolated structures on heat transport conduction.

Finally, an overall conclusion on the original contribution, intended as results of this work, is reported.

Acknoledgements

Con il titolo “Doctor of Philosophy ” è iniziato un altro lungo capitolo della mia vita, vissuto tutto d’un fiato, senza respiro, di corsa….. per poi aprire gli occhi ed accorgermi che sono passati tre anni! I progetti fatti?!…tutti inaspettatamente stravolti e cose nuove, imprevedibili, sono arrivate. Tanti ricordi, nuove esperienze ed emozioni che devo tutte alle persone incontrate.

Innanzitutto desidero ringraziare il Prof. Domenico Acierno ed il Prof.Giuseppe Mensitieri per avermi dato l’opportunità di raggiungere anche quest’altro insospettabile traguardo, credendo in me e dimostrandomi fiducia. Ringrazio poi l’Ing. Pietro Russo per avermi seguito in questo percorso, con disponibilità e costanza. Voglio ancora ringraziare il Prof. Stefano Acierno per avermi sempre offerto il suo aiuto e la sua competenza ogni volta che ne avevo bisogno. Come non ricordare e ringraziare Francesca, per la sua disponibile presenza nella dura fase iniziale di preparazione…delle miscele!...e Peppe per il suo supporto in più di qualche circostanza.

Ed infine….“Non dimentico chi ha toccato con mano, almeno per una volta la mia vita, perchè se lo ha fatto, significa che il destino ha voluto che mi scontrassi anche con loro”.

CONTENTS

INTRODUCTION

- *Why thermally conductive plastics?* 10
- *How to get thermally conductive plastics* 13
- *Why polypropylene as matrix?* 17

CHAPTER I - THERMAL CONDUCTIVITY OF NANOCOMPOSITES: GENERAL ASPECTS

1.1 Thermal conductivity of polymers 20

1.2 Thermal conductivity of carbon nanotubes 22

1.3 Thermal conductivity issues in CNTs-based composites 26

1.3.1 Thermal Interfacial Resistance

1.3.2 Thermal Contact Resistance

1.3.3 Dispersion of primary agglomerates

1.3.4 Secondary Agglomeration

1.3.5 CNTs Functionalization: a route for changing conditions of thermal transport

1.4 Theoretical models for thermal conductivity predictions 38

1.4.1 The Maxwell model

1.4.2 The Lewis-Nielsen model

1.4.3 The percolation model

1.4.4 Thermal conductivity models for composites containing carbon nanotubes

1.5 Hybrid systems 47

CHAPTER II - PREPARATION METHOD AND CHARACTERIZATION TECHNIQUES

2.1 Materials: polypropylene, carbon nanotubes, additional fillers for hybrid systems 51

2.2 Composites preparation 52

2.3. Characterization techniques 53

2.3.1 Thermal conductivity measurements

2.3.2 Differential scanning calorimetric tests

2.3.3 Thermogravimetric analysis

2.3.4 Scanning Electron Microscopy

2.3.5 Optical microscopy

2.3.6 MWNT Packing density evaluation

2.3.7 Terahertz (THz) Time Domain Spectroscopy (TDS)

2.3.8 Rotational Rheology

2.3.9 Capillary Rheology

2.3.10 Transmission Electron Microscopy

2.3.11 Three point bending tests

2.3.12 Electrical measurements

CHAPTER III - EXPERIMENTAL RESULTS AND DISCUSSION: PRELIMINARY INVESTIGATIONS FOR OPTIMIZING NANOCOMPOSITES PREPARATION

3.1 Influence of matrix features 61

3.2. Influence of a compatibilizer 63

3.4 Influence of carbon nanotubes drying 65

3.3 Influence of melt compounding conditions 66

3.5 Influence of compression molding conditions 68

3.6 Influence of test temperature 70

CHAPTER IV - EXPERIMENTAL RESULTS AND DISCUSSION: EFFECT OF FUNCTIONALIZED CARBON NANOTUBES ON FINAL PROPERTIES OF NANOCOMPOSITES

4.1 Effect of filler type and content on thermal conduction of nanocomposites 72

4.2 Differential scanning calorimetric results 75

4.3 Morphological aspects by Electron Microscopy 76

4.3.1 SEM of primary agglomerates

4.3.2 SEM on polypropylene-based nanocomposites

4.3.3 TEM on polypropylene-based nanocomposites

4.4 Quantitative analysis of filler dispersion by optical microscopy 83

4.4.1 Packing density evaluation

4.4.2 Optical microscopy analysis on nanocomposites at a filler concentration of 0.5% in vol.

4.5 Absorption coefficient and refractive index of nanocomposites by THz spectroscopy 86

4.6 Rotational rheological response of MWNT/PP nanocomposites 91

4.6.1 Storage modulus of PP/MWNT nanocomposites

4.6.2 Complex viscosity data

4.6.3 Rheological percolation threshold

4.6.4 Physical Gelation: rule of the filler

4.6.5 Effect of temperature on rheological behavior

4.7 Flexural Properties 101

CHAPTER V - EXPERIMENTAL RESULTS AND DISCUSSION: **CHARACTERIZATION ON NEW POLYPROPYLENE-BASED HYBRID SYSTEMS**

5.1 Thermal conductivity measurements on hybrid systems 103

5.2 Morphological observations by EDS/SEM analysis 105

5.3 Thermogravimetric analysis on hybrid systems 107

5.4 Differential scanning calorimetric analysis on hybrid systems 108

5.5 Torque measurements during mixing 109

5.6 Rheological measurements on hybrid materials 111

5.6.1 Viscoelastic behavior of hybrid systems

5.6.2 Role of carbon nanotubes in ternary formulations

5.6.3 Comparison between complex and shear viscosity

5.7 Electrical conductivity measurements for hybrid compounds 118

CONCLUSION 122

REFERENCES 127

INTRODUCTION

Why thermally conductive plastics?

In aerospace and automobile industry, every additional weight of components, implying more fuel to move vehicles, involves slow performance and is expensive in terms of energy, cost and pollution (CO_2 emissions). Demands on modern vehicles are very challenging because they need to fulfill several different criteria from regulations and legislations with environmental and safety concerns, together with requirements of customers. In many occasions, high performance, reliability and safety, greater comfort, fuel efficiency, style, competitive pricing, low environmental impact are conflicting factors that require optimized and balanced solution. [6] In this context, the easiness of plastics application, to replace heavier materials, like alumina, steel, ferrous metals and alloys is obvious. In fact, plastics are lightweight, versatile and flexible allowing technological innovation and design freedom. Moreover, these materials facilitate also production of complex parts on large scale and operations like assemblage of injection and blow molded parts, helping complicated structural design [7].

In electronic packaging industry and consumer electronic devices, thermoplastic materials have been considered for their excellent properties

including thermal stability at high temperature, low moisture absorption, low flammability. Their processability, during injection molding, is easier and requires short cycle times compared to thermosetting ones, whose viscosity, instead, during transfer molding, evolves in complicated manners, having hundreds of cavities [8, 9]. Furthermore, low density is desirable in the case of portable systems such as laptops and hand-held phones, because the reduction of weight, also minimizes potentially damaging stresses resulting from shock loads that could occur during shipping and from other causes [10].

In heat exchangers fields, the development of polymer materials is grown given their ability to handle liquids and gases, their resistance to fouling and corrosion, and their possible use in both humidification and dehumidification systems. Then, substantial weight, volume, space, and cost savings have provided a competitive edge over heat exchangers usually manufactured with metallic alloys [11].

Therefore, plastics could be considered a good compromise in terms of reduced weight, together with corrosion resistance, toughness, design flexibility, resilience without forgetting economic gain related to their relatively low cost.

However, as the diffusion of electronic equipments density is increased, power dissipation becomes a great problem. Heat could be conducted away from chips through materials with high thermal conductivity. Metals and ceramics are relatively good thermal conductors, but polymers are insulator. Concerning automobile production, the main industrial process for the production of plastic items is the injection molding, during which compounds are melted and injected at high pressure into a closed mold, opened after the cooling of products. Overall the process implies a remarkable heat transfer rate through employed materials to accelerate these operations and to reduce both production costs and cycle times. Clearly, also when new heat exchanger are

designed, thermal conductivity of constituent materials becomes the main issue to be considered [8, 11, 12].

In this context, to apply efficiently plastics in all above-mentioned industrial fields, the improvement of their thermal conductivity is the first target to achieve and the most important problem to solve.

Typical conductivity values, required for electrical and electronic applications, are between 1 and 30 W/(mK) [13]. These values are far, one or two orders, from intrinsic thermal conductivity of some polymers, which oscillate instead around 0.1 to 0.4 W/(mK) at a temperature of 25 °C (as seen in Tab.1).

Materials	Thermal Conductivity [W/(mK)]
Low density polyethylene (LDPE)	0.30
High density polyethylene (HDPE)	0.44
Polypropylene (PP)	0.11
Polystyrene (PS)	0.14
Polymethylmethacrylate (PMMA)	0.21
Nylon-6 (PA6)	0.25
Nylon-6.6 (PA66)	0.26
Poly(ethylene terephthlate) (PET)	0.15
Poly(butylene terephthlate) (PBT)	0.29
Polycarbonate (PC)	0.20
Poly(acrylonitrile-butadiene-styrene) copolymers (ABS)	0.33
Polyetheretherketone (PEEK)	0.25
Polyphenylene sulfide (PPS)	0.30
Polysulfone (PSU)	0.22
Polyphenylsulfone (PPSU)	0.35
Polyvinyl chloride (PVC)	0.19
Polyvinylidene difluoride (PVDF)	0.19
Polytetrafluoroethylene (PTFE)	0.27
Poly(ethylene vinyl acetate) (EVA)	0.34
Polyimide, Thermoplastic (PI)	0.11
Poly(dimethylsiloxane) (PDMS)	0.25
Epoxy resin	0.19

Tab. 1-Thermal conductivity values at a temperature of 25°C for same polymers [11], [14] , [15].

How to get thermally conductive plastics

A general approach for improving thermal transport behavior of plastics is the inclusion of fillers with a high thermal conductivity with respect to the hosting matrix. Usually, composites offer the possibility to realize new material systems, having unique features, from the combination of their individual constituents properties. By changing fillers type and content, a specific adjustment of composite final properties could be obtained.

In general, three classes of fillers can be used for this purpose: metallic powders (aluminum, silver, copper, nickel), ceramic particles (aluminum nitride, silicon carbide and beryllium oxide) and carbon-based ones (graphite, carbon fibers and carbon black). Exceptional thermal and electrical properties have mainly been developed in a matrix, by adding carbon-based and metallic particles, while electrical insulation and thermal conduction have been achieved by ceramic ones. Yet, metallic particles, having high specific gravities, cannot be applied in the case of the lightness target. So, carbon-based reinforcements seem to be the best choice when lighter thermal conductor compounds may be wished.

In the following table (Tab.2), thermal conductivity values for different fillers are summarized.

Generally, a relevant amount of the above cited fillers (more than 30% in vol.) is required to achieve the desired thermal conductivity, representing a significant processing challenge. In fact, higher filler loadings, affecting mechanical and viscoelastic behavior of the hosting matrix, compromise the final processability of thermally conductive composites. In these conditions, extrusion and injection molding processes are often difficult and not always possible.

Materials	Thermal Conductivity [W/mK]
Graphite	100-400 (on plane)
Carbon black	6-174
Diamond	2000
PAN-based Carbon Fibre	8-70 (along the axis)
Pitch-based Carbon Fibre	530-1100 (along the axis)
Copper	483
Silver	450
Gold	345
Aluminum	204
Nickel	158
Boron Nitride	250-300
Aluminum nitride	200
Beryllium oxide	260
Alluminum oxide	20-29

Tab. 2 - Thermal conductivity values at a temperature of 25 °C for same thermally conductive fillers [16, 17].

Recently, considerable attention is devoted to nanocomposites, i.e. compounds containing dispersed particles, with at least one dimension in the order of 1-100 nanometers. Small size and large surface area (for a given volume) of nanofillers are key factors for the development of exceptional unexpected properties with respect to macroworld.

The nanometric fillers are classified into three categories, depending on their geometry -nanoparticles, nanotubes, nanolayers- and are dosed in matrix properly to modulate final product features. [16, 17]

Since their discovery by Iijima in 1991, carbon nanotubes (CNTs) attracted attentions of many researchers for their unique features, in term of mechanical, thermal and electrical properties. Applications for nanotubes encompassed many fields and disciplines such as medicine, nanotechnology, manufacturing, construction, electronics, and so on. The following applications can be noted: high-strength composites, actuators, energy storage and energy conversion devices, nanoprobes and sensors, hydrogen storage media, electronic devices, and catalysis [18].

As conductive fillers in advanced nanocomposites, due to their remarkable intrinsic high electrical conductivity (~10^6 S/m) and large aspect ratio (length to diameter ratio~1000), CNTs improve electrical properties of hosting polymer matrices, resulting in lower electrical percolation thresholds [19]. As mechanical reinforcement, combination of Young's modulus (1~TPa) [20], significant higher than steel modulus (200–400 GPa), with a density approximately one-sixth that of steel, makes carbon nanotubes suitable also in enhancements of composites mechanical behavior.

In summary, while in case of mechanical load, CNTs could act as stress-transfer from low-strength matrix, in case of electric and thermal load, they become charge and phonons transfer through continuous conductive paths.

Usually, final properties of polymer nanocomposites and, in particular, of carbon nanotubes-based composites are lower than ones predicted by rule of mixture model. According to this rule, each phase contributes to final compounds properties proportionally to its volume fraction (Eq. 1):

$$p_c = \sum_{i=0}^{n} p_i \ \phi_i \qquad 1)$$

where p_c is composite property, p_i is the intrinsic property of each specific constituent and ϕ_i is their volume fraction in composite system.

This means that nanoscale unique properties cannot be reproduced on the macroscale probably for non-continuum effects at filler-polymer interfaces. A better knowledge of the relationships among process, interfacial optimization and final properties of a composite is the main goal of this research area [21].

This issue appears more evident if the thermal conductivity of CNTs-based nanocomposites is investigated. In fact, CNTs possess thermal conductivity, approximately in the range of 200-3000 W/mK [16]. Nevertheless experimental

measurements, on CNTs-based nanocomposites, revealed values almost, one or two order, smaller than expected.

Recent research revealed that, in order to employ the effectiveness of CNTs, as thermally conductor in nanocomposites, an optimal filler dispersion, good interfacial adhesion between filler-matrix ("*interfacial resistance"*) and properly gap between tubes ("*contact resistance"*) could be obtained. In fact, due to high surface energy and intrinsic Van deer Walls forces, CNTs are thermodynamically unstable and tend to entangle and agglomerate into ropes or bundles. In these conditions, every attempts toward homogeneous distribution of CNTs, adjacent one to each other, so to create one or more effective CNTs conductive paths, is hindered. In fact, the successful utilization of nanotubes in a composites in terms of properties enhancement depends primarily on their actual distribution. Within the industrial context, being melt-mixing the preferred method for compounds preparation, number and sizes of CNTs aggregates can be minimized by applying suitable shear stress levels. It was shown that melt mixing conditions as well as post mixing process (injection or compression molding) influence strongly the nanotubes dispersion and consequently the properties of final products.

The functionalization, i.e. the introduction of functional groups on carbon nanotubes surface, obtained by covalent or non-covalent means, is a common approach widely adopted for changing chemistry of inert CNTs. These methods may significantly affect the thermal conductivity of nanocomposites, by promoting filler dispersion and by reducing the interfacial thermal resistance and/or contact thermal resistance between adjacent CNTs. In fact, the presence of functionalities, such as hydroxyl, carbonyl, amino and carboxyl groups, modifying the CNTs affinity against the surrounding matrices, can affect stress-transfer during mechanical tests, as well as phonon and/or electron transport phenomena [21-22].

In summary, several parameters are recognized to play an important role in conductivity performance of nanocomposites, from features of raw materials to processes conditions [23], mentioned in Fig.1.

Currently, the development of hybrid compounds, by combining two fillers, different in geometry and scale, provides an interesting approach to obtain thermal conductors. The behavior of hybrid materials, joining together intrinsic properties of each part, can result in a superior effect respect to the sum of that achieved by individual elements ("*synergism*"). The effectiveness of a synergy, in conductive composites, could be due to interactions among dispersed particles, resulting in interconnected structures, suited for heat transport.

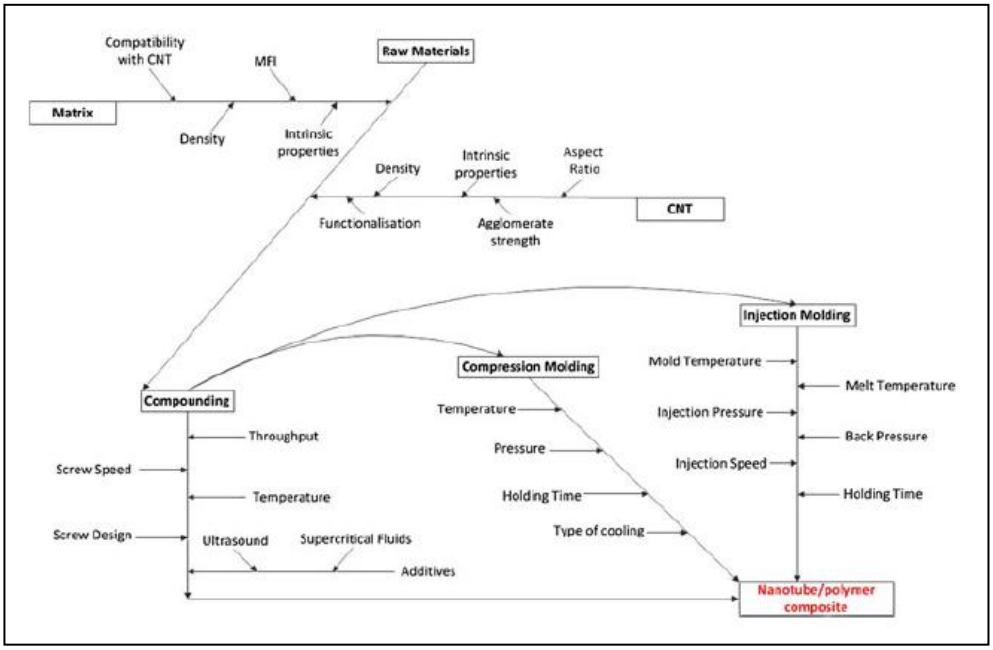

Fig. 1- Tailoring a CNT incorporated thermoplastic composites [23].

Why polypropylene as matrix?

Polypropylene grades are semicrystalline resins, largely utilized in industrial fields for several different applications, due to their relatively low cost, excellent processability, easy availability, flexibility to tailor-make desired properties and recyclability. A wide range of polypropylenes and their composites can be

found in everyday life, as constituent materials of automobile cabin interior, or external parts, like bumpers and tailgate, or still for boat components. In heat exchangers, polypropylene has a significant application in mechanical vapor compression desalination units for its excellent corrosion resistance. *"According to a report published by Transparency Market Research, the polypropylene market is expected to reach US$133.39 billion in 2023, expanding at a CAGR (Compound Annual Growth Rate) of 5.7% between 2015 and 2023. The rise in demand in the packaging industry, which accounted for over 45% of the demand in 2014, is likely to augment the global polypropylene market in the next few year, as is the increased demand for lightweight vehicles. The automobile industry was the second-largest consumer of polypropylene in 2014 as polypropylene can reduce the overall weight of the vehicle when used effectively.* (Angharad Lock, Energy Global Hydrocarbon Engineering, 2015)".

So, great research attention is devoted to overcome some drawbacks of this thermoplastic polyolefin, as its toughness and insulation features. Compounding of polypropylene, with additive or fillers, could be a method to improve its functional and structural properties, in order to obtain specific materials suitable for different applications. Using polypropylene with natural minerals such as calcium carbonate, zeolite, mica, and talc, an appropriate balance between successful reinforcement and cost optimization could be obtained.

Several works, in literature, analyzed the influence of CNTs on thermal, mechanical, electrical properties of polypropylene based-nanocomposites but only few are available on the effect of carbon nanotubes in improving PP thermal conductivity.

Additional particles (CNTs) can significant change crystallization behavior of isotactic polypropylene, in term of melt temperature, degree of crystallinity and crystallization temperature, that increased with filler content. In fact, CNTs,

acting as nucleating agents, may induce conformational changes in matrix structure [24]. Mechanical properties are reduced when CNTs content, exceeded over 2-3% in wt. Probably this is a result of a poor CNTs dispersion that, weakening polymer/CNTs interfacial adhesion, prevents an efficient load transfer from the polymer matrix to CNTs [25]. Instead, a significant enhancement of PP electrical features is observed with the addition of CNTs, for the formation of percolating structure even at relatively low loadings (below 3% in vol.), with respect to other carbon-based fillers, like graphite (G) and reduced graphene oxide (TrGO) [26]. Polypropylene-based hybrid composites have been also investigated, combining opportunely organic and inorganic fillers, in order to improve particles dispersion and reduce costs without compromising physical features. Bao *et al*. [27] investigated the effect, on electric percolation threshold and resistivity, of calcium carbonate ($CaCO_3$) together with carbon nanotubes (CNTs) in polypropylene matrix. They showed an interesting decrease of both parameters, attributing these results to excluded volume effect. H.Palza *et al.*, [28] instead, evaluated the effect of different geometrical nanoparticles (montmorillonite clay, copper nanoparticles and spherical silica) on electrical conductivity of CNTs/PP composites, concluding that excluded volume and bridges between particles could not explain satisfactorily their results. In fact, while in the case of spherical silica, by reducing free volume for CNTs dispersion, the effective concentration increased and so even for electric conductivity; in the case of layered clay, a higher aspect ratio of the secondary filler could hinder interconnections between CNTs, by acting as a wall between them and by damaging conductive pathways.

CHAPTER I

THERMAL CONDUCTIVITY OF NANOCOMPOSITES: GENERAL ASPECTS

1.1 Thermal conductivity of polymers

Thermal conductivity is a material's property, that indicates its capacity in transferring heat. It could be defined by Fourier's law (Eq. 1.1), in steady-state conditions, as the proportional factor (*k)* between "*heat flux" (*$\bar{q}$*),* across a conducting medium, and its respective "*temperature gradient"* (ΔT):

$$\bar{q} = -k\,\Delta T \qquad 1.1)$$

In a crystal, heat flux induces continuous fluctuations of atoms in the neighbourhood of their regular positions, becoming more pronounced at higher temperatures. During these oscillations, chemical bonds between atoms, are stretched and compressed, forcing them to vibrate together. Frequencies of vibrations, called "*normal modes*", produce vibrational waves, called "*phononos"*, that are the first mechanism, through which thermal energy is transmitted. The second mechanism is associated to motions of free or conducting electrons from hotter to colder areas. During this migration, electrons collide with phonons or other imperfections in the crystal, transferring kinetic energy to the atoms themselves, known as "vibrational energy".

In the case of electrically insulators, like polymers, since free movement of electrons is not possible, heat flows essentially due to phonons, accomplished by rotation and vibration of polymer chains. In this case, thermal conductivity can be evaluated by Debye equation (Eq. 1.2) based on the concept of mean free path of thermal waves:

$$k = \frac{c_p v l}{3} \qquad 1.2)$$

where c_p is the specific heat capacity per unit volume, v is the average velocity of wave and l is the mean free path of phonons. The phonon mean free paths, defined as the average distance travelled by phonon between two successive collisions, depend on phonon-phonon, phonon-boundary and phonon-defect scattering processes.

Thermal conductivity of polymers is affected by many factors, like: chemical constituents, bond strength, structure type, molecular weight and density distributions, type and strength of defects, temperature. Thus, by changing these parameters, the response, in terms of thermal conductivity, is not completely clear and univocal. In general, thermal conductivity of polymers increases with crystallinity and oriented chain length. These effects could be explained through the theory of "*phonons scattering"* event. Phonons, travelling along polymer backbone, may be hampered by random orientation, curvature and sequence of bends that, by creating tortuous paths for waves propagation, reduce phonon-mean free path and limit thermal conductivity values. Then, at the chain ends, because of accentuated phonon scattering phenomena ("*phonon scattering boundary"*), vibrational waves ride quickly through a longer molecular chain rather than between shorter polymeric ones. [29-31]

In general, the influence of all listed parameters on thermal conductivity is not completely available.

Dashora and Gupta [32] explained the variation of thermal conductivity with temperature for non-conducting linear amorphous polymers. Since the motions of structural polymeric units, as chain segments or side pendants, are affected by temperature, inevitably this influence pours also on the thermal conductivity. Increasing temperature, three different behaviors of thermal conductivity can be distinguished: (i) a maximum peak in the region of glass transition temperature (T_g); (ii) broad plateau; (iii) a linear increase with change in slope near T_g. In details, in the region below glass transition temperature, the predominant phonon scattering processes are: *structure scattering* and *chain-defect scattering*. However, the existence of same local order is well established so, by rising temperature, polymeric chains straighten out, phonons mean free paths increase and the thermal resistivity overall decreases. Above the glass transition temperature, thermal motions and torsional rotations of atomic groups, individual units and chain segments could lead to two opposite effects: (i) formation of defects, vacancies or microvoids; (ii) augmentation of chains alignments and bridging. For polymers, having longer branches, stronger bonds and heavier segment units, the formation of defects becomes the predominant mechanism resulting in a higher phonon scattering. As a result, thermal transport phenomenon decreases with temperature. On the contrary, for polymers with feeble interactions and shorter branch chains, improvements of the thermal conductivity with temperature are the main consequence of orientation and alignment of polymeric chains, that prevail on defects formation.

1.2 Thermal conductivity of carbon nanotubes

Individual carbon nanotubes can be visualized as cylinders, obtained by wrapping one-atom-thick layer of graphite, called graphene. Depending on the number of graphene sheets concentrically wrapped, CNTs are categorized as

single-walled carbon nanotubes (SWCNTs) or multi-walled carbon nanotubes (MWCNTs) (Fig. 1.1).

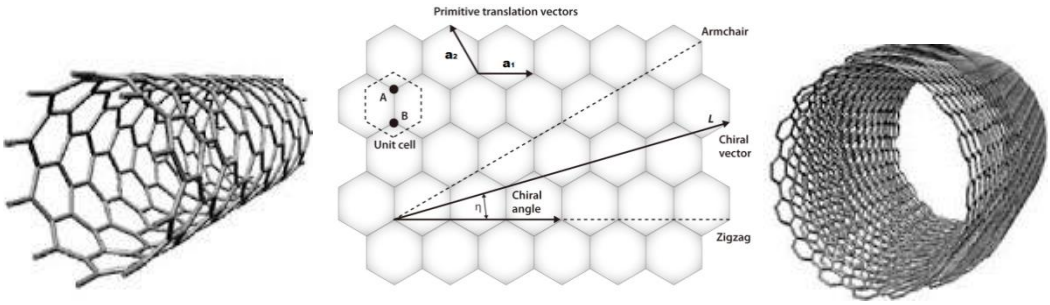

Fig. 1.1- Single walled carbon nanotubes (on the left) Multi walled carbon nanotubes (on the right) and schematic representation of chiral structures.

The atomic structure of nanotubes can be described in terms of the tube chirality, or helicity, which is defined by the chiral vector $\overline{C_h}$, also known as the roll-up vector, ($\overline{C_h} = n\,\overline{a_1} + m\overline{a_2}$ where: n and m are integers, representing the number of steps along the unit vector of the hexagonal lattice , a_1 and a_2 are unit vectors), and the chiral angle θ, which determines the amount of twist in the tube. The chiral angles are 0°C and 30°C for the two limiting cases which are referred to as zigzag (m=0) and armchair (m=n), respectively. [33-34]

Nanotube morphology (sheets of graphene rolled) and atomic structure (chirality) together with size, impurities and defects represent the main factors influencing their thermal heat conduction. Thermal conductivity value of carbon nanotubes has not been well established although different studies concerning molecular dynamic simulations, experimental measurements and theoretical predictions, are performed in this direction. (see Tabs 1.1 and 1.2). The order of magnitude of these discrepancies, between predicted and evaluated values, are primarily attributed to length effect, temperature, boundary conditions and molecular dynamics simulation methodology. Others factors, like technological difficulties of synthesizing high-quality and well-ordered nanotubes, may be considered. Then, nanotubes can have natural

defects and vacancies, that should affect their thermal conductivity especially in one-dimension material.

	k (W/mk)	Tube length (nm)	Cross-sectional area (m^2)
Berber et al. (2000)	6600	2.5	29×10^{-19}
Osman et al. (2001)	1700	30	14.6×10^{-19}
Che et al. (2000)	2980	40	4.3×10^{-19}
Yao et al. (2005)	$1\text{-}4\times10^{23}$	6-60	14.6×10^{-19}
Padgett and Brenner (2004)	40-230	20-310	14.6×10^{-19}
Maruyama (203)	260-400	10-400	14.6×10^{-19}

Tab. 1.1- Thermal conductivity of single wall carbon nanotube with chirality (10, 10) obtained through simulation techniques [35].

		k (W/mk)	Tube length (nm)	Diameter (nm)
Kim et al.(2001)	MWNT	3000	2500	14
Yu et al. (2005)	SWNT	2000	2600	1
		10000	2600	3
Pop et al. (2008)	SWNT	3400	2600	1.7
Choi et al. (2006)	MWNT	300	1400	20

Tab. 1. 2-Thermal conductivity value obtained by experimental measurements on carbon nanotubes with unknown chirality [35].

Clearly, it is therefore important to know how these parameters influence the thermal conduction properties of carbon nanotubes.

Heat conduction in CNTs is essentially due to phonon transport, that dominates over electron transport, even if metallic properties are evident in these chiralities structures. The phonon conductivity is an overall result between two opposite effects: *"coupled-vibration"* of carbon atoms, by which is explained

conduction phenomena, and "*phonon-dispersion"* in relationship with phonon mean-free paths and scattering rates.

Whereas an increase in temperature or CNTs length is performed, a change in mean free path is brought and conductive regime switches from ballistic to diffusive ones. While in ballistic regime, phonons scatter rarely along length of carbon nanotubes, in diffusive one phonons scatter many times. So, when the length of carbon nanotubes is major respect to phonon mean-free path, diffusive heat conduction dominates. A general trend could be established regarding CNTs thermal conductivity in function of their length. In the ballistic regime, increasing length, thermal conductivity increases up to a saturated value, at which corresponds a diffusive behavior. [36-37]

At low temperatures, ballistic conduction rules and thermal conductivity increases with temperature. This behavior is evident up to room temperature, then scattering processes take over and the value drops. In fact, at high temperatures more number of phonon participate to collision reducing mean free paths and so also the thermal conductivity. Osman *et al.* [38], through dynamic simulations, showed that thermal conductivity of (10,10) SWNT increased slowly up to 300 K, then reached a peak around 400K and dropped until 500K.

About the influence of diameter on CNTs thermal conductivity, experimental results on SWNT and MWNT, reported by Marconnet *et al*. [36], showed a decrease of thermal conductivity by increasing the diameter size.

Several models [39] investigated the effect of nanotube chirality on the CNTs thermal conductivity, verifying no significant changes in thermal conductivity with CNTs atomic structures. On the contrary, other works [40] supported that in armchair and chiral structure, the stretch of sigma bonds between carbon atoms, by causing excessive strain along nanotube axis, reduces mean free paths and lowers the thermal conductivity.

Theoretical predictions are based on perfect structures, but it is quite impossible to obtain defect-free CNTs samples. In fact, due to synthesis processes, inevitably structural imperfections in atomic arrangements can be derived, some of which cause a strong impact on final properties. Defects can be classified [41] as: (i) topological defects, like non exagonal carbon rings or vacancies, (ii) rehybridization defects, and (iii) incomplete bonding. Even at low concentrations, both vacancies and Stone-Wales defects significantly reduce the thermal conductivity. The Stone-Wales defect is induced by a rotation of C-C bond resulting in the transformation of four hexagons of graphene sheets, in two pentagons and two heptagons. Even if in many cases, the chirality of the structure could be changed, its detrimental effect on thermal conductivity is smaller with respect to vacancies, because of no significant changes in basic bonds and, consequently, less structural deformations [42].

1.3 Thermal conductivity issues in CNTs-based composites

As above mentioned, the thermal conductivity of CNTs has been measured between 300 and 10,000 W/(mK) (Tab.1.2). By applying a simple rule of mixtures to a typical polymer, having a thermal conductivity around 0.2-0.3 W/(mK) (see Tab.1 in Introduction) the thermal conductivity of CNTs/polymer nanocomposites may be in the order of 10 W/(mK), at 1% loading, and in the hundreds of W/(mK) at 10% loading. However, experimental evidences do not confirm these expectations, showing an increase in thermal conductivity typically less than 1 W/(mK). So, even if remarkable improvements are enriched, the predicted effectiveness of carbon nanotubes has not been proven [43].

At this regard, different research efforts have been spent and reported in the literature. Wu *et al.* [44] showed a linear increase in thermal diffusivity of high-

density polyethylene (HDPE) based composites, by increasing multiwalled carbon nanotubes (MWNT) content up to 40% in vol. Results were discussed through an effective medium approach model and the intrinsic longitudinal thermal conductivity of an individual as-grown MWNT was found in the range of 40~60 $Wm^{-1}K^{-1}$. Chen *et al.* [45] measured the thermal conductivity of high density polyethylene/multiwall carbon nanotube (HDPE/MWNT) composite films by laser pulse method, founding firstly a rapid increase for MWNT contents up to 3.35% in volume; over which, the increasing rate became slow. Authors interpreted this irregular trend as a sort of percolation. Kim *et al.* [46] analyzed different samples prepared by melt-blending polypropylene (PP) with non-treated, nitric acid (HNO_3)-treated, and potassium hydroxide (KOH)-treated nanotubes, respectively, in terms of thermal conductivity and diffusivity. Thermal conductivities were enhanced by a factor of about two in the case of acid-functionalized and base-treated carbon nanotubes with respect to non treated ones. Kashiwagi *et al.* [47] studied thermal and flammability properties of melt compounded polypropylene/multi-walled carbon nanotube (PP/MWNT) nanocomposites, with a filler content up to 20 in wt. %. In details, authors measured thermal conductivities as a function of temperature in the range from 30 to 260°C, confirming higher values for nanocomposites with respect to pure PP. A particularly pronounced effect was recorded above 160°C. Yang *et al.* [48] discussed the correlation between dispersion behavior and thermal/electrical conductivities of CNTs-polystyrene nanocomposites. Results showed that the thermal conductivity linearly increased with CNTs content. Nanocomposites, loaded with 5 wt% of CNTs, exhibited an enhancement in thermal conductivity around 120%, even if less remarkable with respect to that recorded for electrical conductivity. Abbassi *et al.* [49] realized multiwalled carbon nanotubes/polycarbonate composites by diluting a masterbach of 15% in wt. with melt-mixing method. They found that, at low concentrations, the

thermal conductivity gradually increased with nanotubes content, while a remarkable jump was observed around 1-2 % in wt. of filler loading. This stepwise change in conductivity was attributed to the formation of interconnected structures and regarded as thermal percolation thresholds. Cai et Song [50], by following the colloidal physics method, utilized semicrystalline polyurethane (PU) dispersions as latex host to accommodate multi-walled carbon nanotubes (MWNT). The thermal conductivity increased from 0.15 $Wm^{-1}K^{-1}$ to 0.47 $Wm^{-1}K^{-1}$, as the addition of MWNT increased up to 3 wt%. On the contrary, going over 3% in wt. of filler content, the thermal conductivity of composite system underwent a slight decrease. Probably, by increasing MWNT concentration, the settlement of more single nanotubes in the void space among latex particles could increase the size of their bundles resulting in more nanotube–nanotube interfacial phonon scattering.

In the light of this drawback, clearly, proper exploitations of the thermal conductivity of CNTs-based nanocomposites require a very careful control of the microstructure. At this regard, different parameters are recognized to play an important role, such as: the interfacial resistance between filler-filler and filler-polymer or distribution, dispersion and alignment of fillers in the matrix. Functionalization of carbon nanotubes is considered a successful tool for improving dispersion and for reducing the interfacial resistance, because of an improvement of the wettability between two phases. In principle, it also may be oriented to reduce the thermal contact resistance between adjacent CNTs. In fact, although few works are carried out on this way, it is not excluded that between functional groups may arise interactions, stronger than Van der Walls forces, which, binding more CNTs between them, also promote a reduction in the contact resistance [17].

1.3.1 Thermal Interfacial Resistance

Interfacial resistance is also known as "*Kapitza Resistance*" from the name of discoverer, that in 1941 found the temperature discontinuity at the interface between metal (Copper) and liquid (superfluid Helium). It represents a barrier to heat flow at the interface between two different phases, due to possible weak contact and difference in the phonon spectra [51].

The thermal contact resistance is attributed to phonons losses during heat transmission from one medium to another. Two limiting models allow a qualitative evaluation of thermal boundary resistance: acoustic mismatch model (AMM) and the diffuse mismatch model (DMM), representing the upper bound and lower bound for Kapitza resistance, respectively. The former assumes that all phonons propagate as a planar wave, so the transmitted energy is related to different acoustic impedances of two materials. Instead, the latter assumes that all phonons, colliding into the interface, are randomly scattered. If the acoustic impendences between materials are very different, the phonons scattering will contribute to further increase the thermal resistance. Because of high sensitivity of phonons to surface defects, Kapitza resistance is affected by interface conditions. [52-53]

For CNTs-based nanocomposites, the order of magnitude of boundary resistance has been valued around 10^{-8} W/(mK). This value is approximately equal to the resistance of an insulating polymer layer with a thickness of 10-20 nm [54].

In principle, a good thermal contact particles/polymer can lead to a highly efficiency in heat transferring. However, perfectly dispersed CNTs, having no contact between them and exchanging energy only with surrounding matrix, not seem to be a good choice in terms of thermal conduction due to lower phonons mean free paths in the polymers with respect to fillers. Indeed,

preferential heat conduction across percolated CNTs networks could be the basic idea for realizing actually conductive materials [17].

1.3.2 Thermal Contact Resistance

Two solid bodies, which are apparently in contact, actually touch together only in a few point for their roughness and geometrical defects. In this case, when heat flows normally from hotter body to colder one, between contact points, an interstitial zones exist, that limits the thermal conduction. In fact heat transport takes place only between effective contact points. The physical consequence is a constriction of flux lines (Fig. 1.2), which are responsible of a heat resistance best known as "thermal contact resistance" [55].

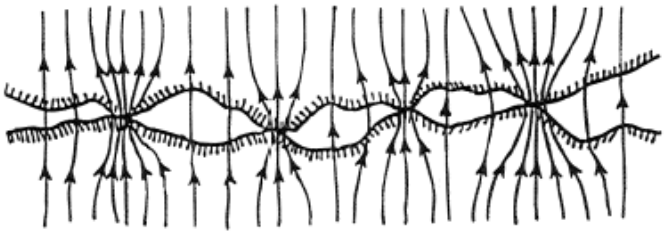

Fig. 1.2-Constriction of heat flow paths between contact points of two bodies.

Accurate models are devoted to investigate thermal transport conduction in carbon nanotubes, as randomly oriented mats or vertically aligned arrays. Thermal conductivity of these assemblies materials is affected by packing fraction of CNTs, boundary resistance related to CNT-CNT contact ("*thermal contact resistance*") and possibly damage or defects resulting from production processes [56]. These factors prevent mats from having the high thermal conductivity measured for an individual carbon nanotube. For example, Prasher *et al.* [57] reported thermal conductivities of randomly oriented CNTs films in the order of 0.13 to 0.19 W/(mK).

Zhong *et al.* [58] estimated, using classical MD simulation, the interfacial thermal resistance between two parallel single walled carbon nanotubes (SWNT) as a function of nanotubes spacing, overlap and length. They found a reduction in thermal transport resistance for longer nanotubes and with an increased overlap area. A reduction in the interfacial thermal resistance, approximately of four order of magnitude, is performed by bringing tubes in close and intimate contact.

1.3.3 Dispersion of primary agglomerates

Because of their synthesis process, CNTs, far from being perfect idealized cylinders, are characterized, instead, by structural defects and curved geometries. In these conditions, they are held together by a highly cohesive resistance, due to Van deer Walls interactions and physical entanglements. Consequently, they are produced in form of agglomerates, called "*initial primary agglomerates*", with possible different packing structures, such as: "combed yarns", i.e. larger and more loosely packed agglomerates, or "bird nests", i.e. denser but smaller ones [59].

The cohesive strength (σ) of agglomerates [60] is calculated through the "Rumpf equation", as reported below:

$$\sigma = \frac{(1-\varepsilon)}{\varepsilon} \frac{F}{a^2} \qquad \textit{for spherical particles} \qquad 1.3)$$

$$\sigma = (1-\varepsilon)\, k\, \frac{F}{A} \qquad \textit{for convex shaped particles} \qquad 1.4)$$

where:

- a is diameter of particles forming agglomerates;
- ε is agglomerate porosity defined through bulk density (ρ_{bulk}) and particle density ($\rho_{particle}$)

$$\varepsilon = 1 - \frac{\rho_{bulk}}{\rho_{particle}} \quad 1.5)$$

- F is the adhesive force, which, in case of dry agglomerates, is predominantly represented by Van deer Walls force. Its expression depends by particles geometry as below:

$$F_{sphere} = -\frac{H}{6\,D^2}\left(\frac{R_1 R_2}{R_1+R_2}\right) \quad 1.6)$$

$$F_{Cylinder} = -\frac{H}{8\sqrt{2}}\,\frac{L}{D^{5/2}}\left(\frac{R_1 R_2}{R_1+R_2}\right)^{1/2} \quad 1.7)$$

In these formulas, H is the Hamaker's constant (for nanotubes equal to 60E-20J); D is the inner distance of the particles (assumed 0.4 nm equal to inter graphite layer separation); L and R are respectively length and radius of the particle (in general assuming R_1=R_2=R); k is the coordination number (equal to 10 for rigid pipes with an aspect ratio of 100);

- A is the surface area of particles forming agglomerates ($2\pi RL$ for rods).

Dispersion involves different steps (Fig. 1.3), which occur simultaneously during mixing processes and are affected by materials features, mixing parameters, procedure and equipments [59, 60]:

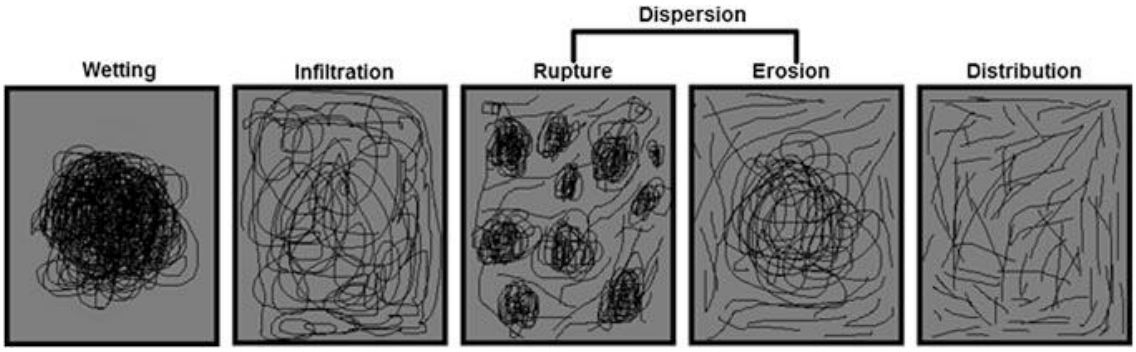

Fig. 1.3-Mechanism of CNT dispersion.

- **wetting of initial agglomerate**, mainly dependent on the interfacial energy between CNTs and liquids or melts. Functional groups, presented on CNTs surface, in general due to synthesis processes, make them rather polar [61]. This feature can influence CNTs wettability and represents an hindrance especially in case of non polar melts, like polyolefins;
- **polymer infiltration,** i.e**.** polymer chains diffusion in pores of primary agglomerates, which reduces the cohesive strength favouring their disintegration. This mechanism is favoured by agglomerates with large pores (low packing density) or by polymer with low melt viscosity. Since the latter feature depends, in turn, by parameters such as the average molecular weight, molecular weight distribution, shear rate and temperature, the infiltration results affected by processing conditions and choice of materials, too.
- **dispersion** occurring through rupture and erosion processes. The *rupture* is a bulk phenomenon, during which the agglomerates are broken, in a short time, into smaller ones; instead, *erosion* is a surface phenomenon, during which individual nanotubes or bundles are removed from agglomerates in a longer time. The dispersion phase is influenced by both operating conditions and matrix viscosity, regulating together the shear force responsible of these phenomena. A threshold value exists for shear stress that must be overcome for the occurrence of these two mechanisms. In general, the required value for rupture is greater than the one for erosion.
- **distribution** in which nanotubes are individually dispersed in melt.

As already discussed in the introduction, different techniques are utilized for dispersing CNTs in a matrix: mixing in solution or in the molten state and in situ polymerization. Among them, even if polymerization in situ, starting from monomer, is more effective; in an industrial context, mixing in the molten state

or "melt mixing" is preferred. In this last case, number and size of primary agglomerates can be minimized, using a suitable shear stress, induced not only by operating conditions [60] but also through matrix structural features, as melt viscosity and molecular weight [62].

In details, Kasaliwal *et al.* [62] studied the influence of molecular weight and melt viscosity on nanotube dispersion, utilizing three different polycarbonates (PCs). At low mixing speeds, they observed smaller un-dispersed agglomerates only in the case of high melt viscosity, concluding that remarkable shear stress is necessary for better dispersion. Moreover, lower viscosity and/or matrix molecular weight play an important rule during infiltration step. As a consequence a lower cohesive strength, facilitating rupture and erosion processes, leads to a better dispersion.

The influence of viscosity, on the state of dispersion of MWCNTs, was also investigated by Socher *et al*. [63], correlating final results with electrical properties of nanocomposites. They chose five different thermoplastic matrices, having each three levels of viscosity: polyamide 12, polybutylene terephtalate, polycarbonate, polyetheretherketone and low density polyethylene. By increasing the matrix viscosity, a higher input of mixing energy was available to break primary agglomerates resulting in a better CNTs dispersion but in a pronounced CNTs shortening. In terms of electrical properties, this effect led to a higher amount of CNTs necessary for reaching the electrical percolation threshold.

Krause *et al.* [64] studied the effect of melt mixing conditions on different properties of CNT filled composites based on polyamide 6 (PA6) and polyamide 6.6 (PA66), especially in term of electric resistivity. As expected, variation in temperature, rotation speed and mixing time, influenced dispersion and distribution of MWCNTs and consequently the electrical resistivity of composites. They found that overall conditions, resulting in a higher mixing

energy and in a better state of filler dispersion, not implied improvements of electrical volume resistivity. This effect could be related to CNTs shortening and their encapsulation in polyamide chains. In fact, polymer wrapping can isolate nanotubes to each other, resulting in a higher electric volume resistivity even in the case of a good dispersion.

In this context, this main aspect should be highlighted: dispersion of CNTs into isolated particles with little or no contact to each other not always represented the best direction to follow for efficient nanocomposites performance. It's very difficult to provide generals rules for the relationship between the dispersion of nanotubes and final properties of their nanocomposites**.** Dispersion is a relative concept that depends by author's interpretation; little or no quantitative parameters are used in literature for a comparison between results [17]. Few experimental data underline a clear and univocal relation between thermal conductivity and dispersion. Yang *et al*. [65] conducted studies on CNTs dispersion in a oil. They found that the optimal shear rate for maximizing dispersion corresponded to a minimization in thermal conductivity values. Microscopy images also confirmed that a higher thermal conductivity was achieved in correspondence of larger agglomerates.

By increasing the mixing energy, a better dispersion and CNTs shortening could be obtained, simultaneously [66]. If shorter CNTs are more easily dispersible, defects caused by breakage are detrimental for their intrinsic thermal conduction [41].

Thus, final overall conclusions on relationship between dispersion and thermal conductivity cannot be given easily.

1.3.4 Secondary Agglomeration

The dispersion is probably the main critical aspect during the process of composite preparation. From the technological point of view, there are two reasons determining a particles spatial arrangement not homogeneous in a polymer: (i) inability in destroying completely primary agglomerates; (ii) impossibility to control the so called "*secondary agglomeration"*, i.e. re-formation of the cluster by external forces, such as electric fields and shear deformation, or particles diffusion promoted by attractive interactions [59].

It has been experimental established that the secondary agglomeration of CNT can occur in quiescent melt as well as under shear deformation during mixing or in secondary processes, like compression molding [67]. During melt mixing only high shear forces can provide suitable MWNT dispersion because firstly the disentanglement is facilitated and then secondary agglomeration is prevented.

Instead, during hot pressing, MWNT networks or their arrangements can be manipulated by the processing conditions like melt temperature and pressing speed. In details, low pressing speed as well as high temperatures can enhance secondary agglomeration [68].

1.3.5 CNTs Functionalization: a route for changing conditions of thermal transport

In CNT structures, atoms are chemically stable because of aromatic nature of their bonds. The chemical feature of non-polar material, containing only few functional groups, renders them inert and unable to establish strong interactions with the surrounding matrix (except Van deer Walls forces, too weak to ensure a good transfer across CNT/polymers interface). Significant efforts have been spent to modify CNTs surface by introducing functional groups, suitable to react with matrix [69]. Surface's functionalizations could be

both chemical and physical, depending on interactions between active molecules and carbon atoms.

The chemical functionalization, based on covalent bonds of functional groups, exploits extremely reactive ends cap of nanotubes or surface defects and it is categorized as: (i) direct covalent sidewall functionalization, associated with a change of hybridization from sp2 to sp3, and a creation of active sites for effective interactions with polymer; and, (ii) defect functionalization, during which intrinsic defects are supplemented by strong acids oxidization, resulting in holes functionalized with oxygenated groups [71].

On the contrary, the physical functionalization implies non-covalent modifications realized through a physical adsorption and/or wrapping of polymers on CNTs surface. The latter consists in a suspension of CNTs in presence of a polymer. From a thermodynamic point of view, the driving force for polymer wrapping is the elimination of hydrophobic interface between CNTs and an aqueous medium; contemporary, CNTs agglomeration is kinetically prevented by long ranged entropic repulsion among polymer-modified tubes [69]. Other non covalent methods include surfactant adsorption and endohedral method. While in the first case, a surfactant on CNT surface can lower surface tension and promote electrostatic/static repulsive forces preventing agglomeration; in the second one, guests or molecules are introduced into CNT inner cavity through capillary effects so to integrate properties of two components [69].

When functionalized CNTs are adopted in nanocomposites, an increase in dispersion can be achieved [72], but structural defects, occurring on CNTs surface, due to chemical treatments [69], can be harmful for their final thermal transport behavior. In fact, Padgett *et al.* [73] studied, by molecular dynamic simulation, the thermal conductivity of single-walled CNTs functionalized with phenyl rings. Results showed that functionalization of carbon nanotubes

drastically reduces their thermal conductivity, almost entirely for a reduction in the scattering length. Instead, in the case of non-covalent functionalization, CNTs structures are not damaged because additives, essentially coupling agents or compatibilizers [74], only adhere on their surface. In general, due to differences in chemical nature and polarity, poor adhesion between polymer and CNTs restricts separation of filler aggregates and hinders an uniform filler dispersion. In presence of a suitable coupling agent, instead, CNTs surface energy is changed so to improve wetting and adhesion characteristics and to reduce the tendency to agglomeration. A common compatibilizer for polyolefins is maleic anhydride grafted to polymer (Ma-g-PO). Maleic anhydride functionalities, reacting with carboxyl, amine and/or hydroxyl groups on MWNT's surface, stabilize the morphology and improve the interfacial interaction between particles and surrounding polymer. Diez-Pascual *et al.* [76] analyzed the effect of polyetherimide (PEI) as a compatibilizing agent on the morphology, thermal, electrical and dynamic mechanical properties of poly(ether ether ketone) (PEEK)/single-walled carbon nanotube (SWCNT) nanocomposites. In presence of the compatibilizer, a more homogeneous distribution of the CNTs was observed together with an enhancement in the storage modulus and in the rigidity of products. This effect was attributed to an improved interfacial adhesion between reinforcement and matrix. On the contrary electrical and thermal conductivities decreased with the incorporation of PEI probably for a polymeric coating formed on the tubes.

1.4 Theoretical models for thermal conductivity predictions.

In literature, different models have been suggested, for predicting the thermal conductivity of nanocomposites. Some of them are discussed in this section, neglecting details of fundamental theories, based on acoustic or diffusive

mismatch models. In each reported formula, k_c, k_p and k_m are thermal conductivities of composites, particles and matrix, respectively, while Φ_p and Φ_m are volume fractions of particles and matrix.

First of all, two basic models may be described: parallel model, well-known as "*rule of mixture*" and the so-called "*series model*". For composites, most of experimental results fell between these two references, thus the first one is considered a lower bound, while the second represents an upper bound.

The rule of mixture assumes a perfect contact between particles in a fully percolated network. Each phase contributes independently to the overall conductivity, proportionally to its volume fraction and the thermal conductivity of a composite can be predicted as following in Eq. 1.8:

$$k_c = k_p\Phi_p + k_m\Phi_m \qquad 1.8)$$

On the contrary, the series model confined particles contribution only to the region of embodying matrix, by assuming no contact between particles. Its expression is described below in Eq. 1.9:

$$k_c = \frac{1}{\left(\frac{\Phi_m}{k_m}+\frac{\Phi_p}{k_p}\right)} \qquad 1.9)$$

In these two opposite models, thermal conductivity of a composite is expressed as a function of volume fraction and intrinsic features of each constituent. Since also composite microstructure, particle dimension and geometry, matrix-filler interphase affect this thermal parameter, further models have been proposed.

1.4.1 The Maxwell model

By following the effective medium theory (EMT), also referred as effective medium approximations (EMA), Maxwell carried out analytical investigations on conduction properties of particles embedded in a base medium. This model [77], described in Eq. 1.10, considers only interactions between matrix and spherical particles .

$$k_c = k_p\left(\frac{1+2\beta\phi_p}{1-\beta\phi_p}\right) \quad 1.10)$$

and

$$\beta = \frac{k_p-k_m}{k_p-\alpha k_m} \quad 1.10.a)$$

$$\alpha = \frac{2k_m R_k}{d} \quad 1.10.b)$$

where d is particle diameter and R_k is the Kapitza Resistance.

Later, for highly anisotropic, stiff rods with random orientation, an extension of EMA was given, taking into account the effective thermal conductivity of an individual particle: parallel $(k_{p,l})$ and perpendicular $(k_{p,d})$ to the rod long axis.

$$k_c = k_m\left(\frac{3+\phi_p(\beta_x+\beta_z)}{3-\beta\phi_p}\right) \quad 1.11)$$

in which:

$$\beta_x = \frac{2(k_{p,d}-k_m)}{k_{p,d}+k_m} \quad 1.11.a)$$

$$\beta_z = \frac{k_{p,l}}{k_m} - 1 \quad 1.11.b)$$

$$k_{p,l} = \frac{k_p}{1+\left(\frac{2R_k k_p}{l\ k_m}\right)} \quad 1.11.c)$$

$$k_{p,d} = \frac{k_p}{1+\left(\frac{2R_k k_p}{d\ k_m}\right)} \qquad 1.11.d)$$

Maxwell's formula has been validated only in the case of low filler content (under 25 vol. %).

In case of dilute solution ($i.e. \phi_c < 0{,}01$), as reported in literature by Nan *et al.* [78], Eq. 1.11 can be simplified in Eq. 1.12**:**

$$\frac{k_c}{k_m} = 1 + \frac{\Phi_f p}{3} \frac{\frac{k_p}{k_m}}{p+\frac{2a_k}{d}\frac{k_p}{k_m}} \qquad 1.12)$$

where $p\left(=\frac{L}{d}\right)$ is the aspect ratio of particles and $a_k(=R_k k_m)$ is the Kapitza radius. In this model, improvements of the composite thermal conductivity is mainly limited by the interface thermal resistance. Experimental results, on nanotubes suspension in oil, showing a good correlation between predicted and measured values, demonstrated the validity of this simple model for describing the thermal conductivity in nanotubes-based composites.

1.4.2 The Lewis-Nielsen model

Lewis and Nielsen modified the Halpins-Tsai equation, by including effects of particles shape, orientation and packing type for a two-phase systems, containing up to 40% in vol. of filler loading [79]. The effective thermal conductivity of a composite is calculated by Eq. 1.13:

$$k_c = k_m \left[\frac{1+AB\phi_f}{1-B\psi\phi_f}\right] \qquad 1.13)$$

where

$$B = \frac{\frac{k_f}{k_m} - 1}{\frac{k_f}{k_m} - A} \quad 1.13.a)$$

$$\psi = 1 + \left(\frac{1-\phi_{max}}{\phi_{max}^2}\right) \phi_f \quad 1.13.b)$$

In particular, ϕ_m is the maximum filler volume fraction (reported in Tab.1.3 for different packing types) and A is the shape coefficient (reported in Tab.1.4 for sphere and random oriented rods as a function of the aspect ratio).

Shape of particles	Type of packing	ϕ_m
Spheres	Face-centered cubic	0.7405
	Hexagonal close	0.7405
	Body-centered cubic	0.6
	Simple cubic	0.524
	Random close	0.637
	Random loose	0.601
Rods or fibers	Uniaxial hexagonal close	0.907
	Uniaxial simple cubic	0.785
	Uniaxial random	0.82
	Three-dimensional Random	0.52

Tab. 1.3-Maximum packing fractions for different arrangements [77].

Shape	Aspect ratio of particles (length/diameter)	A
Spheres	1	1.5
Randomly oriented rods	2	1.58
	4	2.08
	6	2.8
	10	4.93
	15	8.38

Tab. 1.4-Values of A for several dispersed types of particles [77].

1.4.3 The percolation model

Percolation is one of simplest models in probability theory [80], firstly used to describe the passing of a liquid through a porous substance or small holes, then extended to explain the formation of conducting channels in many types of transport problems, e.g., electric circuits, public transport or spread of a disease [77]. The term percolation is also applied to composites microstructure for

indicating the critical point, at which particles form a continuous network, changing drastically materials features. The minimum filler content, corresponding to the formation of these networks, is called percolation threshold.

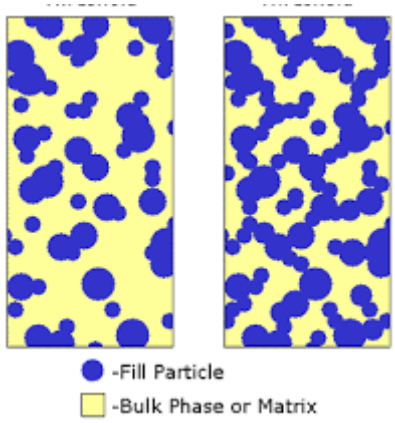

Fig .1.4-Schematic representation in a composite material of: interconnected particles, forming continuous network (on right), and particles connected in part without realizing network (on left).

The percolation theory is a classical approach in describing electrical behavior of a composite [81]. In fact, near the percolation threshold, the enhancement in electrical conductivity becomes by several orders of magnitude, obeying the conventional power-law relationship:

$$\sigma \sim (p - p_c)^{\alpha} \qquad 1.14)$$

where σ is the composite electric conductivity, p is the filler volume fraction and p_c is volume fraction at the percolation threshold.

While electrical measurements are an indication of topologically percolating networks; surprisingly, no experimental evidences confirm the existence of percolation phenomena in the case of thermal conductivity measurements. The different behavior between these two kind of conductions was attributed to the conductivity ratio between filler and matrix (k_p/k_m). In fact, while this parameter is approximately in the order of magnitude of 10^4, in the case of thermal conductivity, it enriches until 10^{12}-10^6 in the case of electrical

conductivity. Thus, the effective channel for electrical transport is along the percolating tube network. Instead, for thermal transport the dominant channel of heat flow always involves in matrix [82]. Another reason, for justifying the lack of percolation in the thermal conduction, is the thermal resistance between two adjacent tubes, too high to allow an efficient direct heat transport [78] [82].

Yet, Bonnet *et al.* [83] considered percolation a pertinent approach to describing heat transport in SWNT/PMMA composites. They found a good correlation between experimental thermal conductivity values, in term of Δk ($= k_c - k_m * (1 - \phi)$), and the percolation model, reported in Eq. 1.15, for a filler content up to 2% in volume:

$$\Delta k = k_0 \left[\frac{(\phi - \phi_c)}{(1 - \phi_c)}\right]^{\beta} \qquad 1.15)$$

where prefactor k_0 represents the contribution of the filler network alone, β is an exponent accounting for effective percolated network characteristics and ϕ_c is the percolation threshold.

Paleo *et al.* [84] described thermal conduction in polypropylene reinforced with carbon nanofibers (CNFs) by means of reologically percolated microstructures. They demonstrated that thermal conductivity and diffusivity values of percolated composites were greater than the ones of non-percolated systems. Thermal conductivity values were well-fitted by Eq. 1.15 considering ϕ_c equal to the rheological percolation threshold. A prefactor k_0, approximately equal to 6,5 W/(mK), was correlated to the thermal conductivity of CNF networks, nearly 100 times greater than PP. This result would support the reasonable use of percolation for describing thermal conduction phenomena and suggested that, in these composites, above a certain critical content of carbon nanofiber ϕ_c, the thermal conductivity is mainly controlled by CNF networks.

Kole *et al*. [85] measured the effective thermal conductivities of HDPE/LBSMO composites as a function of the filler loading. Various thermal models, including effective medium theory and Lewis model, fitted results with good

agreement for a filler content below 8% in volume. Large deviations were observed for a filler volume fraction higher than 10%. This discrepancy was due to the basic assumptions of an homogeneously distribution of fillers in the matrix without considering fillers percolating paths. In fact, percolation theory provides a remarkable prediction of the measured effective thermal conductivity of HDPE/LBSMO composites at high volume fraction. According to Zhang et *al*. (2009) model [86], the effective thermal conductivity was derived as following in Eq. 1.16:

$$k_c = k_p \left(\frac{k_{\phi_c}}{k_p}\right)^{\left[\frac{1-\phi}{1-\phi_c}\right]^n} \quad 1.16)$$

where k_{ϕ_c} is the thermal conductivity of composite system at percolation threshold and ϕ_c is the filler volume fraction at which the effective thermal conductivity of the composites starts to increase rapidly. In this case, ϕ_c is determined by taking the value corresponding to maximum of double-derivative curve of the measured effective thermal conductivity $\left(\frac{d^2k_c}{d\phi^2}\right)$ as a function of the filler volume.

It may be noted that Zhang model predicts the percolation threshold of thermal conductivity only if the ratio between electrical conductivities of fillers and polymer is larger than 10^5.

1.4.4 Thermal conductivity models for composites containing carbon nanotubes

Simple specific models are developed for predicting thermal conductivity of CNTs-based composites, taking in account different parameters, as: their

volume fraction, anisotropic thermal conductivities, aspect ratio, non straightness and interfacial thermal resistance [87].

In the case of composites with low loading of randomly oriented CNTs, the effective thermal conductivity can be given by:

$$\frac{k_c}{k_m} = 1 + \frac{\phi_f}{3}\left[\frac{1}{\left(\frac{k_{p,l}}{k_m}-1\right)^{-1}+H} + \frac{2}{\left(\frac{k_{p,d}}{k_m}-1\right)^{-1}+\left(\frac{1-H}{2}\right)}\right] \quad 1.17)$$

where H reflects the influence of aspect ratio p, in the following way:

$$H(p) = \frac{1}{p^2-1}\left[\frac{p}{\sqrt{p^2-1}}\, ln\left(p+\sqrt{p^2-1}\right) - 1\right] \quad 1.17.a)$$

Considering aspect ratio in the order of 1000 or even larger, the function H tends to zero ($H(p) \to 0$) and the last equation can be approximate as:

$$\frac{k_c}{k_m} = 1 + \frac{\frac{f}{3}}{\frac{k_m}{k_{p,l}}+H} \quad 1.18)$$

This model is derived in an ideal case by considering straight CNTs. On the contrary, in a composites, CNTs are curved and entangled, consequently an approximation is required. Thus, each carbon nanotube can be regarded as an equivalent straight thermal cable, in which the same thermal flux is conducted between the two ends at a distance L^{ce}, by considering end to end entangled CNT length. In this case, the thermal conductivity can be described by following formula:

$$\frac{k_c}{k_m} = 1 + \frac{\frac{\eta\phi_c}{3}}{\frac{k_m}{\eta k_{p,l}}+H(\eta p)} \quad 1.19)$$

where $\eta\left(=\frac{L^{ce}}{L}\right)$ is defined as the straightness ratio of CNTs.

Then, taking into account the Kapitza resistance, $k_{p,l}$ is modified in $k_{p,l}^{e}$, as following:

$$k_{p,l}^{e} = \frac{k_{p,l}}{1+\frac{2R_K k_{p,l}}{L}} \quad 1.20)$$

Finally, interaction effects between carbon nanotubes are considered, through interaction direct derivative (IDD) micromechanics scheme, and an analytical expression for thermal conductivity k^{IDD} can be written in Eq. 1.21:

$$\frac{k^{IDD}}{k_m} = 1 + \left[1 - H(q)\left(\frac{k_c}{k_m} - 1\right)\right]^{-1}\left(\frac{k_c}{k_m} - 1\right) \quad 1.21)$$

where k_c/k_m is the non-interaction evaluation by Eq. 1.17); 1.19), and H(q) is a function in the form of 1.17.a), with q=1 corresponding to the random isotropic distribution.

1.5 Hybrid systems

The term "hybrid material" is widely employed as an indication of different systems such as crystalline ordered polymers, amorphous sol-gel compounds, materials with or without interconnection between organic and inorganic phases as so on. In general, an hybrid material is constituted by two moieties blended on molecular scale, inorganic and organic, respectively. Thus, no clear borderline separates nanocomposites and hybrid systems. In fact large molecular inorganic clusters in hybrid material can already be of nanometer size [88].

Asby and Brèchet [89] created the following definition for an hybrid material: ''a combination of two or more materials in a predetermined geometry and scale, optimally serving a specific engineering purpose.'' They conceived an

hybrid as addition between the choice of raw materials with own intrinsic properties, their different shape and size ("*A+B+shape+scale*"). All these aspects, suitably combined together, can be used to enhance or diminish physical, mechanical, thermal and electrical properties, as stiffness or strength, and also to manipulate the percolation limit.

The final properties of hybrid materials could be a combination between individual component ones, or a result of synergy. Synergism is intended a total effect greater than the sum of single components. In other words, synergy is the joint action between fillers, supplied by distinct geometry of shape, aspect ratio as well distribution peculiarity, that can increase the effectiveness of both when combined [90].

Inert materials, such as calcium carbonate ($CaCO_3$), talc and wollastonite, are commonly used as hard particles to improve significantly the modulus of polymers and also to affect their crystallization process.

For example, mechanical and thermal properties of polypropylene filled with calcium carbonate and talc, compounded with a twin screw extruder, are analyzed by Leong *et al.* [91]. The aim was to replace talc with calcium carbonate, being the latter cheaper, without gain loss in reinforcement features. A synergistic effect was observed in term of flexural and impact strength when 50% of talc was substituted with $CaCO_3$. Significant improvements in nucleating ability were also demonstrated.

Incorporation of the same inert fillers into CNTs/polymers has been also investigated for enhancing electric properties. In fact, Bao *et al.* [92] demonstrated that the addition of $CaCO_3$ to polypropylene based composites containing carbon nanotubes, leads to a reduction in electrical resistivity and percolation threshold. They explained these results with excluded volume effects: after being incorporated, $CaCO_3$ could occupy a specific amount of space, reducing the one available for CNTs. This inclusion, by allowing

connections between MWNTs, facilitated movements of electrons through composites. Analogous results were also achieved utilizing talc and wollastonite in substitution of $CaCO_3$.

Melt-compounding hybrid composites were also prepared by combining boron nitride (BN) and carbon fiber (CF) in polybuthylene terephthalate (PBT), in order to obtain a high thermal conductivity together with an electrical resistivity [93]. In fact, BN was used for a dual action: on one hand, for hindering electrically conductive network, and on the other, for facilitating thermally conductive one. Since BN was too expensive, CF was added to support thermal conduction and contemporary to limit cost. The results showed that, even if a considerable reduction of electrical conductivity was obtained, any improvements were visible in thermal conductivity with respect to PBT/BN. Probably this was due to CF breakages during extrusion or to a possible alignment during sample preparation by injection molding. Moreover, hybrid composites possessed better tensile properties and processability with respect to PBT/BN.

Muller *et al.* [94] examined the effect of talc and multiwall carbon nanotubes (MWCNTs) in linear-low density polyethylene (LDPE) with regards to electrical percolation behavior. The state of dispersion of MWNT seemed to be improved by adding talc with lower particles size. As a results a decrease of the electrical percolation was observed. Yet, the effect of better dispersion wasn't reflected in an enhancement of mechanical features. In fact, modulus and stress values increased with hybrid fillers but not in a synergistic manner.

Hybrid fillers represent a good choice also in enhancing thermal conductivity of composites probably for a higher connectivity of structuring filler with a high aspect ratio. At this regard, Lee *et al.* [95] attempted to maximize the abundance of thermally conducting paths by using filler concentration at maximum packing loading. Various inorganic fillers, with different size and shape,

including roughly spherical aluminum nitride (AlN), acicular wollastonite, whiskers of silicon carbide (SiC) and lamellar boron nitride (BN), were tested, alone or together, in high density polyethylene (HDPE) matrix. When the filler content was below its maximum packing fraction, the role of structuring filler in hybrid system was more pronounced. On the contrary, when filler content overcame the maximum packing fraction, abundant conductive paths can be formed and the effect of mixed fillers became weak.

Pak *et al.* [96] detected synergic improvements in thermal conductivity of polyphenylene sulfide (PPS) based composites, with addition of boron nitride (BN) and multi-wall carbon nanotubes (MWNT) surface modified with hydrogen peroxide and acid treatments. Good results were attributed to the generation of three dimensional thermal transfer paths between fillers and surface treated MWNTs, that, strongly affected the interfacial interaction and the interfacial thermal resistance. Finally, many other researchers verified synergic effects of mixed fillers, with distinct shapes and dimensions, on the thermal conductivity of relative composites, as: Aluminum oxide (Al_2O_3) and Aluminum Nitride (AlN) with large and small size [97]; graphite (G) and silicon carbide (SiC) in epoxy resins, both in microparticles, the first considered for its ability in dispersion and low cost, the second for high temperature and high power applications [98]; Boron Nitride (BN) flakes and tetrapod-shaped ZnO (T-ZnO) whiskers for thermally conductive but electrically insulating phenolic formaldehyde resin (PF) [99]; graphene (nanofiller) and graphite (microfiller) in epoxy resins at different overall concentration [100].

CHAPTER II

PREPARATION METHOD AND CHARACTERIZATION TECHNIQUES

2.1 Materials: polypropylene, carbon nanotubes, additional fillers for hybrid systems

The matrix, used in this study, is a commercial polypropylene resin (Monsten MA524, melt flow index 24,0 g/10min at 230°C, 2,16 Kg) supplied by UNIPETROL RPA. In specific tests, a further polypropylene grade (Monsten MA712, melt flow index 12,0 g/10min at 230°C, 2,16 Kg - UNIPETROL RPA, Litvínov-Czech Republic) and maleic anhydride-grafted polypropylene (Polybond 3200, melt flow index 115,0 g/10min at 190°C, 2,16 Kg, maleate content 1% in wt., ADDIVANT, Danbury, USA), are considered, too.

Three types of multi-wall carbon nanotubes: non functionalized (3150), functionalized with carboxyl groups (3151) and functionalized with amino groups (3152), supplied by Nanocyl S.A. (Sambreville - Belgium), are chosen, as fillers, to prepared polypropylene based nanocomposites. Their features are summarized in Tab. 2.1.

In the case of hybrid systems, additional particles of zinc oxide (assay~80% Zn basis; nanopowder < 100 nm; density: 5.61 g/cm^3), calcium carbonate (assay: 98%; powder < 30μm; density: 2.71 g/cm^3), boron nitride (assay: 98%; powder < 1μm; density: 2.93 g/cm^3) and talc (powder < 10μm; density: 2.78 g/cm^3) are

utilized, as secondary fillers in PP/MWNT mixtures. All powders are purchased from Sigma Aldrich Co. LLC. (Milan-ITALIA). Their intrinsic thermal conductivity is reported in Tab. 2.2.

	Nanocyl 3150	Nanocyl 3151	Nanocyl 3152
Functionalization	None	-COOH	$-NH_2$
Carbon Purity	>95%	>95%	>95%
Average Lenght (μm)	<1	<1	<1
Average Diameter (nm)	9.5	9.5	9.5
True density (g/ml)	1.94	1.94	1.94
Bulk density (g/l)	100	250	150
Porosity*	0.95	0.87	0.92

Tab. 2.1-Nanocyl datasheets for different types of carbon nanotubes utilized. *Porosity was calculated by Eq.1.5.

Thermal conductivity of additional fillers at a room temperature	
Zinc Oxide	micron/submicron/ nano powder [101]
	60 [102]
	29 [103]
Calcium Carbonate	2.25 [104]
Talc	⊥ 1.76 ∥ 10.69 [105]
Boron nitride	250-300 [16,17]

Tab. 2.2-Thermal conductivity values for secondary fillers.

2.2 Composites preparation

Compounds are prepared by melt-blending, in a batch mixer (Brabender Plastograph EC- Brabender GmbH & Co. KG, Germany). The matrix, as received, is added in the fed chamber and processed for 2 min so that all polymeric pellets are melted. At this point, the filler is included and mixing continued for further 5 min. In the case of hybrid systems, fillers are manually

premixed together and then introduced in the melt PP matrix. Operating at a temperature of 190°C, with a screw speed of 60 rpm, binary systems containing up to 5% in vol. of each type of selected carbon nanotubes, and ternary systems containing 1.5% in vol. of non functionalized multiwalled carbon nanotubes (MWNT) and 10% in vol. of additional fillers, are prepared. For each batch, the mixing chamber is filled more than 80% of its total volume. Systematic evaluations of the actual filler content by thermogravimetric analysis always confirmed an appreciable agreement between the effective and the nominal filler content. When required, total mechanical energy (TME), involved in the mixing process, is determined with the following equation [107]:

$$TME = 2\pi N \int_0^t M dt \qquad 2.1)$$

where N is the rotor speed used in the process (r/min), M (Nm) is the torque value obtained as a function of mixing time *t* (min), during nanocomposites preparation, directly by Reomixer software.

2.3. Characterization Techniques

2.3.1 Thermal conductivity measurements

Steady-state thermal conductivity measurements are performed using a thermal conductivity meter (UNITHERM MODEL 2022 from THERMAL CONDUCTIVITY INSTRUMENT, fabricated according to the ASTM E1530 [108]). This instrument allows to measure the thermal conductivity in through-plane modality.

A specimen and a heat flux transducer (HFT) are sandwiched between two flat plates controlled at different temperatures, to produce a heat flow through the test stack. A reproducible load is applied to the test stack by pneumatic or

hydraulic means, to ensure that there is a reproducible contact resistance between the specimen and plate surfaces. A cylindrical guard surrounds the test stack and is maintained at a uniform mean temperature of the two plates, in order to minimize lateral heat flow to and from the stack. At steady-state, the difference in temperature between the surfaces contacting the specimen is measured with temperature sensors embedded in the surfaces, together with the electrical output of the HFT. This output (voltage) is proportional to the heat flow through the specimen, the HFT and the interfaces between the specimen and the apparatus. The proportionality is obtained through prior calibration of the system with specimens of known thermal resistance measured under the same conditions, such that contact resistance at the surface is made reproducible.

Disc-shaped specimens, with a diameter of 40 mm and a thickness of 1.4 mm, are prepared by compression molding.

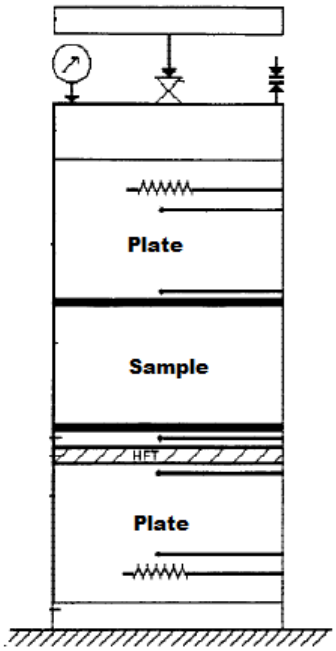

Fig. 2.1-Schematic representation of a typical device.

2.3.2 *Differential scanning calorimetric tests*

Calorimetric tests are carried out by using a DSC, Model Q20 from TA Instrument. Samples, typically measuring between 8-10 mg, are first heated from room temperature to 200 °C (1st run) at a heating rate of 10°C/min and kept at the end temperature for 2 min, in order to erase the thermal history of the material. Then specimens are cooled at the constant rate of 10 °C/min up to 30 °C (2nd run) and, finally, reheated at the same rate up to 200 °C (3rd run) to observe the melting signal. All tests are performed under a nitrogen atmosphere. The degree of cristallinity is determined using the following equation:

$$x_c = \frac{\Delta H_f}{\Delta H_f^0 (1-\phi)} * 100 \qquad 2.2)$$

where $(1-\phi)$ is the weight fraction of polymer and ΔH_f^0 is the theoretical enthalpy value for a 100% crystalline, taken to be 209 J/g [109].

2.3.3 *Thermogravimetric analysis*

Thermogravimetric analysis are conducted by using TGA, model Q2000, from TA Instruments. A sample of about 10 mg is heated from 40 to 700°C with a heating rate of 20°C/min under nitrogen purge.

2.3.4 *Scanning Electron Microscopy*

Microscopic analysis are performed by field emission scanning electron microscope (SEM), Mod. FEI QUANTA 200F, equipped with an energy dispersion spectrometer (EDS) Oxfor INCA Energy System for element analysis of no-carbonaceous particles. Micrographs have been obtained operating at

high vacuum condition at voltage of 20 kV. Cryo-fractured surfaces of each sample are metalized with Au-Pd alloy before testing.

2.3.5 *Optical microscopy*

For each nanocomposite, 10 slices with an average thickness of about 7 microns are obtained by using a Leica CM1850 microtome at room temperature and analyzed by optical microscope Olympus BX53. Slices are taken from different regions of the same compression molded sample in order to check the achieved level of uniformity in terms of MWCNTs agglomerate size distribution. For each slice, the dispersion index D of the nanofillers in matrix is evaluated according to the following equation [110]:

$$D = \frac{V_{VD}}{V_{VT}} \qquad 2.3)$$

in which V_{VD} and V_{VT} are the dispersed and total volumetric fraction of carbon nanotubes in a thin slice, respectively.

The evaluation of V_{VD} is difficult because it represents only isolate nanotube usually observable just with nanometric resolution device like electron microscopy in transmission (TEM).

Thus, to obtain the same information by a simple and more practical method, like optical microscopy, agglomerates in the range of 1-5 microns are necessarily included in the dispersed phase.

The volumetric fraction of non dispersed CNTs could be evaluated through the expression 2.4), being known agglomerates volume fraction (V_{VA}) and packing density (f), i.e. volumetric fraction of carbon nanotubes in agglomerates:

$$V_{VD} = V_{VT} - f\, V_{VA} \qquad 2.4)$$

Consequently, the definition of the dispersion index becomes:

$$D = \frac{V_{VT} - fV_{VA}}{V_{VT}} * 100 = \left(1 - f\frac{\frac{A}{A_0}*100}{V_{VT}}\right) * 100\% \quad 2.5)$$

where A and A_0 represent the area occupied by agglomerates and the total investigated area, respectively, measured for each observed section through the Java-based free software ImageJ (National Institutes of Health, United States), neglecting agglomerates with diameters smaller than 5 μm. Number of agglomerates, their mean size and cumulative percentage are also evaluated. The agglomerate mean size is assumed as circle equivalent diameter, under the hypothesis of spherical geometry.

2.3.6 *MWNT Packing density evaluation*

The packing density of each MWNT type is evaluated by the following procedure [111]. An aluminium cup is filled with the MWNT-powder and vacuum infiltrated with epoxy resin. After curing the volume fraction of MWCNTs agglomerates V_A is estimated by optical microscopy images, considering the area fraction approximately equal to the volume fraction. The corresponding infiltrated MWNT volume fraction (V_{im}) is known or calculated by knowing the mass of epoxy and carbon nanotubes as well as their densities. The packing density is given by the following ratio between V_{im} and V_A.

$$f = \frac{V_{im}}{V_A} \quad 2.6)$$

2.3.7 *Terahertz (THz) Time Domain Spectroscopy (TDS)*

A customised THz-TDS system (EKSPLA, Lithuania), based on a 1064 nm fiber laser with 120 fs pulse width and 60 MHz repetition rate, is used for the

measurements carried out on freestanding samples. The spot diameter is about 2 mm. Thickness of bulk samples for the THz measurements has been set to a minimum (1.4 mm), in the attempt to enhance as much as possible the THz transmission band [112]. All measurements are performed in a nitrogen-controlled atmosphere, to reduce or eliminate the water absorption lines caused by signal transmission in air. The dielectric properties, in term of refractive index and adsorption coefficient, of polypropylene-based composites loaded with 0.5 vol.% MWNT, functionalized and not, are measured in the frequency band 0.3 – 1.4 THz, with a maximum dynamic range of about 60 dB.

The refractive index quantifies the reduction of propagation rate and a change in direction, when a radiation crossed a medium. Instead, the adsorption coefficient indicates the energy of radiation, adsorbed inside the material.

2.3.8 *Rotational Rheology*

Linear viscoelastic characterization of melts is performed using a parallel plate rheometer (ARES, TA Instruments, USA). Small amplitude oscillations, in the frequency range from 0.01 to100 rad/s, are performed at 190°C, by using 25 mm parallel plates, under dry nitrogen atmosphere. Preliminary strain sweep tests are developed to establish linear viscoelastic region (LVE). Specimens are discs, prepared by compression molding at a temperature of 190°C and under a pressure of 70 bar.

2.3.9 *Capillary Rheology*

Capillary rheological measurements are conducted, in a shear rate range of 100-10000 s^{-1}, at a temperature of 190°C, using a CEAST SmartRheo (Instron ITW Test and Measurement Italia S.r.l.), equipped with a capillary die of 1 mm

diameter and a length of 30 mm. The entrance pressure drops are neglected but Mooney-Rabinowitsch corrections for non-parabolic velocity profile are applied. Therefore, data are presented in terms of shear viscosity as a function of shear rate.

2.3.10 *Transmission Electron Microscopy*

TEM micrographs of selected formulations are obtained by using a Tecnai G2 Instrument with an acceleration voltage of 120 kV. All specimens are microtomed into 70 nm thick slices and deposited on a 400 mesh copper nets for observations.

2.3.11 Three point bending tests

Three-point bending tests have been performed by using an Instron, electromechanical machine, under displacement control, at room temperature with a constant crosshead rate of 2 mm/min and a span length ratio of 40 mm. All measurement are conducted up to a flexural strain equal to 5%, according to the ASTM D790 standard. Dimensions of prismatic specimens is 10×80×1.3 mm. All the reported results are averaged on at least five specimens for each investigated material. Samples are obtained by compression molding under a pressure of 70 bar and a temperature of 190°C

2.3.12 Electrical measurements

Electrical resistivity measurements are performed through an apparatus Hewlett Packard 6516A Power Supply equipped with an adjustable direct voltage generator in a range 0-3000 V. Test are developed by applying a

constant DC voltage equal to 100 V in the case of insulators (binary systems without carbon nanotubes and matrix), and equal to 5V in the case of conductors (compounds containing carbon nanotubes). The current intensity, through samples, is evaluated after a period of 2 min by picoammeter HP4140B with resolution of 10-15 A and flow rate up to 100 mA.

Relative permittivity (ε) and loss factor (tanδ) are measured, instead, by impendence analyzer HP 4192A, connected to a measuring cell, Agilent 16451B Dielectric Text Fixture, suitable for frequencies between 5 Hz and 13 MHz.

CHAPTER III- EXPERIMENTAL RESULTS AND DISCUSSION:

PRELIMINARY INVESTIGATIONS FOR OPTIMIZING NANOCOMPOSITES PREPARATION

Several tests are performed in order to identify how raw materials and processing conditions affect the thermal transport behavior of polypropylene based-nanocomposites. In this section, except for specified cases, not functionalized carbon nanotubes are adopted in compounds preparation.

3.1 Influence of matrix features

Two polypropylene grades, different in MFI, and consequently with different molecular weights (Mn, Mw, Mz), polydispersity index (PI - parameter reflecting the width of the molecular weight distribution) and intrinsic viscosity (see Tab.3.1), are chosen to verify their effect on thermal conduction of CNTs-filled nanocomposites.

	Mn [g/mol]	**Mw [g/mol]**	**Mz [g/mol]**	**PI (Mw/Mn)**	**Mz/Mw**	**[η] [dL/g]**
PP MA524	32,400	250,084	727,230	7.7	2.9	0.692
PP MA712	33,519	301,727	834,012	9.0	2.8	0.803

Tab. 3.1-Molecular Weight Distribution of two different matrices, in term of Mn (number average molecular weight); Mw (weight average molecular weight); Mz (zed average molecular weight); Mw/Mn and Mz/Mw (polidispersity), η (intrinsic viscosity). Results are carried out by ISMAC (CNR).

Thermal parameters derived from preliminary calorimetric tests are collected in Tab.3.2.

	First Heating			Cooling		Second Heating		
	T_m^1	ΔH_f^1	x_c^1	T_c^1	ΔH_c^1	T_m^2	ΔH_f^2	x_c^2
PP MA524	168.2	73.9	35%	126.9	82.7	164.7	81.7	39%
PP MA712	166.3	81.5	38%	128.3	92.2	166.4	83.6	40%

Tab. 3. 2 -Differential scanning calorimetric results of two commercial polypropylene resins: PP MA524 and PP MA721.

In details, PPMA712 ($MFI_{230°C/2.16Kg}$ = 12 g/10 min), shows higher average molecular weights and dispersion index but is characterized by similar thermal parameters in comparison with PPMA524 ($MFI_{230°C/2.16Kg}$ = 24 g/10 min),.
Polymeric compounds, containing 1.5% vol. of carbon nanotubes (MWNT), are prepared with PPMA524 and PPMA712, respectively, and characterized in term of thermal conductivity. Results are reported in Fig. 3.1.

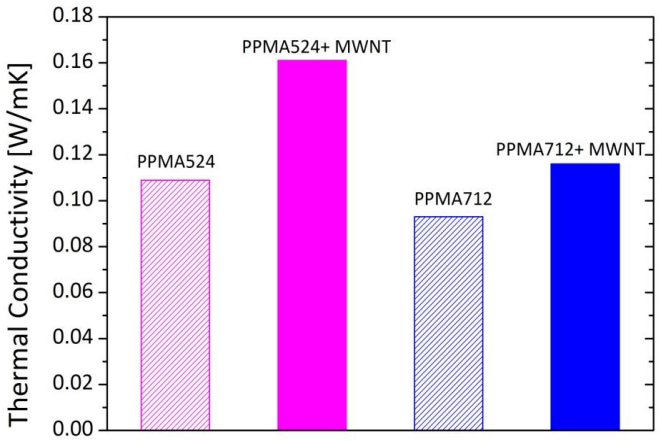

Fig. 3.1- Thermal conductivity values, at a temperature of 30°C, for nanocomposites realized with matrices different in fluidity containing the same type and amount of filler.

At the same filler content, considerable increases in thermal conductivity, equal to 47.7% with respect to the neat PP matrix, are revealed for nanocomposites prepared with the higher MFI resin (PPMA524), against the recorded enhancement equal to 24.7% for formulations based on the lower MFI matrix (PPMA712). This behavior has been explained assuming that a higher polymer fluidity probably facilitates the melt matrix infiltration into primary nanotubes agglomerates, playing an important role in the reduction of their strength. In these conditions, also fragmentation, by rupture and erosion mechanisms, is favored. Consequently, a better state of filler dispersion, useful for conduction networks, may be achieved, as verified by Kasaliwal *et al.* (2011) in term of electrical properties [113].

3.2. Influence of a compatibilizer

The inclusion of a small amount (10% in wt.) of maleic anhydride-grafted polypropylene (MA-g-PP), to basic formulations containing PPMA524 and 1.5 vol.% of carbon nanotubes, both amino-functionalized (MWNT-NH_2) and neat ones (MWNT), respectively, have been considered. Results, in term of thermal conduction, are plotted in Fig. 3.2.

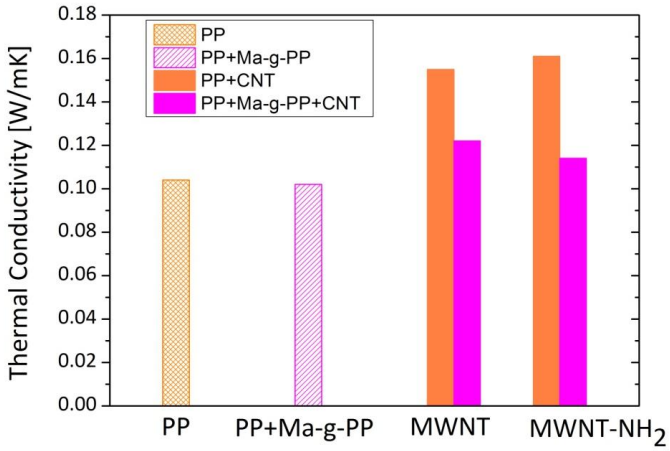

Fig. 3.2-Comparison between thermal conductivity of systems with or without compatibilizer measured at 30°C.

Experimental tests demonstrate that the presence of Ma-g-PP does not alter the intrinsic thermal conductivity of the matrix, that remains almost equal to 0.1 W/(mK) but, unexpectedly, reduces improvements coming from the inclusion of carbon nanotubes. In details, the addition of carbon nanotubes gives rise to an increase of the thermal conductivity equal to about 42.2% (MWNT) and 47.7% (MWNT-NH_2) but, in presence of Ma-g-PP, the same enhancements are reduced to 19.6% (MWNT) and 11.7% (MWNT-NH_2).

In light of these considerations, it is possible to assume that although in general compatibilizers favor the filler dispersion, the same agents may adversely affect the thermal conductivity of products probably altering the interfacial resistance and/or forming a polymeric coating on nanotubes that reduces contact point between them [76].

Rotational rheological tests, reflecting the internal structure of polymers and polymeric compounds, can provide information about dispersion state of particles and interfacial interaction between particles and matrix. At this regard, steady-state rheological measurements are performed on all materials, reporting results in term of complex viscosities ratio between nanocomposite and its respective polymer.

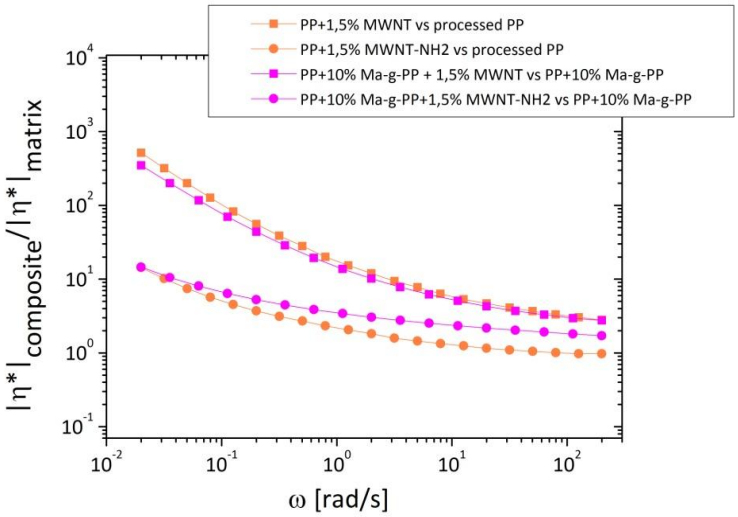

Fig. 3.3- Complex viscosities ratio between nanocomposite and its respective polymers with or without compatibilizer at a temperature of 190°C.

Clearly, the addition of the compatibilizer containing maleic anhydride does not significantly alter the rheological behavior of PP/MWNT (*pink squares*) compared with those realized without compatibilizer (*orange squares*). Probably only weak interaction is given by grafting reaction between maleic anhydride and carbon nanotubes [114]. In the case of functionalized carbon nanotubes, instead, the complex viscosity ratio of PP/Ma-g-PP/MWNT-NH_2 compounds (*orange circles*), almost higher than PP/MWNT-NH_2 (*pink circles*) can be assumed as an indication of improved interfacial adhesion, achieved by stronger interactions between amino-groups and maleic anhydride functionalities [115-116].

3.3 Influence of carbon nanotubes drying

In Fig. 3.4, a comparison among thermal conductivity of nanocomposites containing 1.5% in vol. of carbon nanotubes, as received and after vacuum drying at 80°C for one hour and overnight, respectively, is reported.

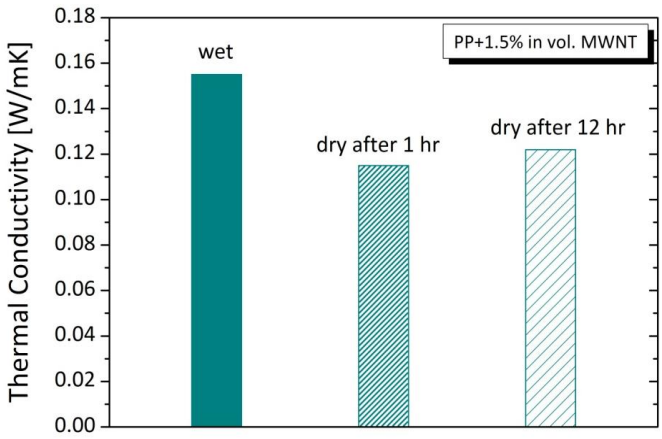

Fig. 3.4-Thermal conductivity values at 30°C for nanocomposites realized with 1.5% vol. of both dry and as received filler.

Moisture may affect in two ways the thermal conduction of CNTs/polymer nanocomposites. In fact, besides a reduction of adhesion between polymer and filler, water molecules, being physically present at the interface [6], could provoke also a reduction (~25-30%) of CNTs intrinsic thermal conductivity, as demonstrated by molecular dynamic simulation [117]. In our case, unexpectedly, pre-drying of MWNT results in a remarkable reduction of the thermal conductivity of PP composites with a detrimental effect (-21.3%). Probably, during heating-treatment, the evaporation of water molecules favors the establishment of cohesion forces between carbon nanotubes in primary agglomerates, especially in presence of functional reactive groups, hindering the next dispersion phase in the hosting matrix.

3.4 Influence of melt compounding conditions

Nanocomposites, at 1.5% in vol. of filler loading, are prepared in different melt-compounding conditions, by changing melt temperature, screw rotational speed and mixing time, in order to verify the effect of each parameter on the thermal conductivity of products and to optimize its choice. Results are presented in the following picture (Fig. 3.5).

Cleary, higher thermal conductivities are obtained by employing mixer temperature of 190°C, screw speed of 60 rpm and mixing time equal to 7 min.

By increasing the processing temperature from 190°C to 250°C, a slight reduction of the thermal conductivity (~ -14%) is recorded, probably as a consequence of the matrix viscosity reduction. In fact, this effect could play two opposite roles: it favors the polymer infiltration in primary agglomerates but worsen the disintegration effectiveness and the overall filler dispersion.

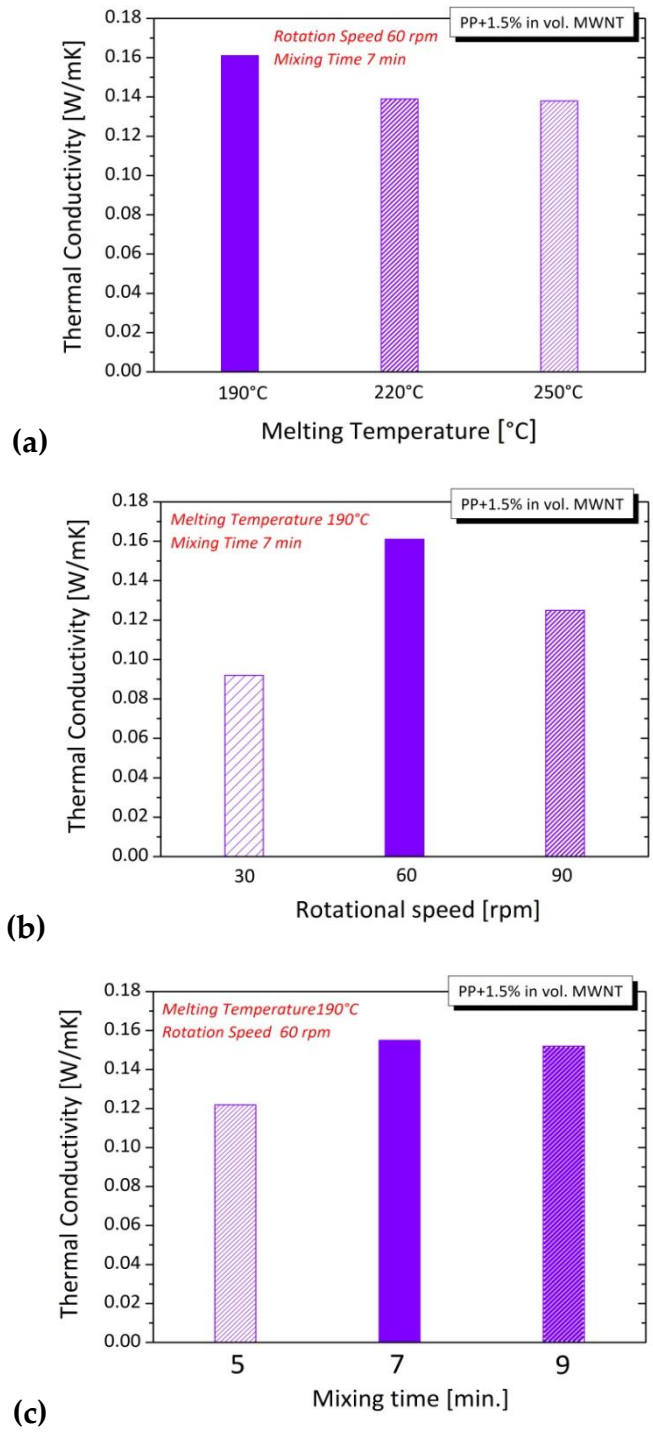

Fig. 3.5-Thermal conductivity values at 30°C of nanocomposites prepared at different process conditions: (a) speed (30, 60, 90 rpm) at a fixed time (7 min) and temperature (190°C); (b) temperature (190, 220, 250 °C) at a fixed speed (60rpm) and time (7min); (c) time (5 ,7 ,9 min) at a fixed temperature (190°C) and speed (60 rpm).

A different situation is highlighted by analyzing the influence of mixing time and screw speed. A non monotonic trend of the thermal conductivity is

observed by increasing separately the mixing time from 5 to 9 min and the screw speed from 30 to 90 rpm. This behavior could be explained taking into account that the increasing of screw speed and/or mixing time favor not only the breaking of primary agglomerates, but also re-agglomeration and/or the CNTs shortening, with a consequent deterioration of intrinsic filler conduction properties.

3.5 Influence of compression molding conditions

In Fig. 3.6, a comparison among thermal conductivity of nanocomposites, compounded under the same conditions but molded in different compression ways, is indicated.

Overall, the results highlight that:

- an increase equal to 17% is obtained by reducing the temperature. Probably in the quiescent melt, under a higher temperature, a lower material viscosity favors a secondary agglomeration of the filler, worsening its dispersion;
- no variation is verified by changing pressure time. Probably, under a fixed temperature, once applied the pressure, the state of dispersion remains unaltered in time;
- a slight increase of the thermal conductivity, approximately equal to 10%, is obtained by increasing the pressure.

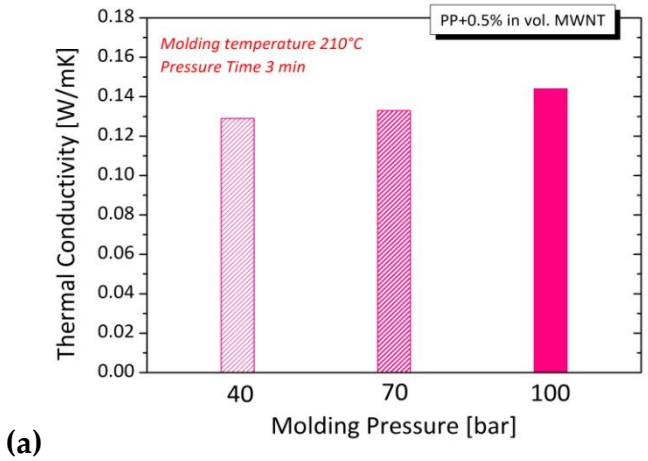

(a)

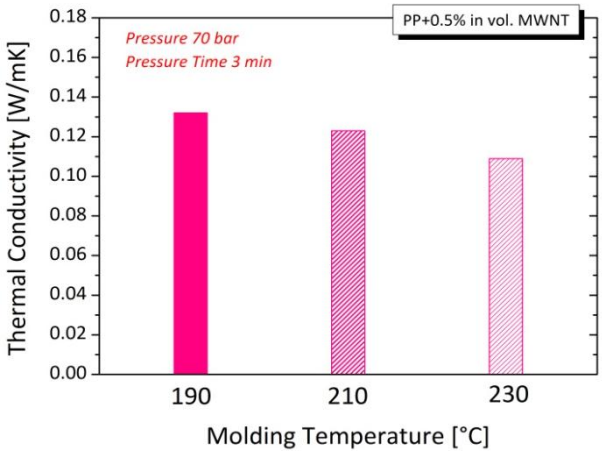

(b)

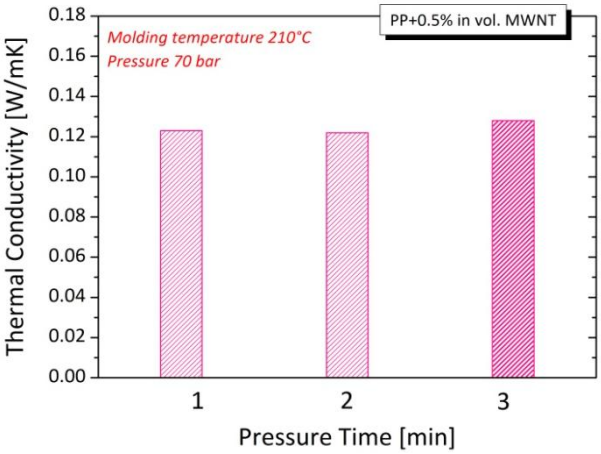

(c)

Fig. 3.6-Thermal conductivity of samples compressed in different conditions: (a) molding temperature (190, 210, 230°C) at a fixed pressure (70 bar) and time (3 min); (b) molding pressure (40, 70, 100 bar) at a fixed time (3 min) and temperature (210°C); (c) pressure time (1, 2, 3 min) at a fixed temperature (210°C) and pressure (70 bar).

3.6 Influence of test temperature

Fig. 3.7 shows thermal conductivity values for nanocomposites, containing up to 2.5% in vol. of MWNT, obtained at different test temperatures.

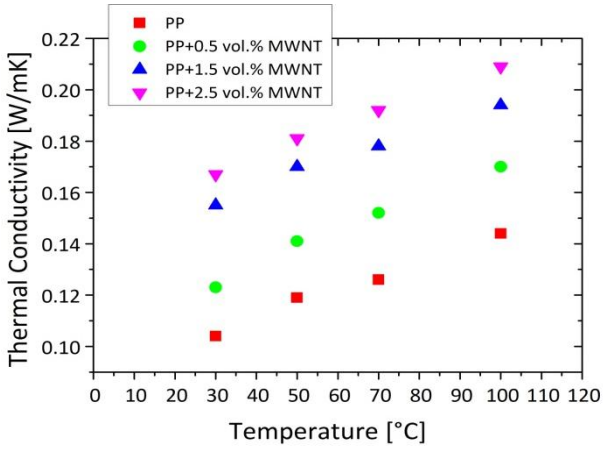

Fig. 3.7-Thermal conductivity of nanocomposites in function of test temperature.

Nanocomposites show always higher thermal transport properties than the neat matrix, even if enhancements appear to be reduced by increasing the test temperature. When the temperature grows up, the polymeric chains surrounded with CNTs began to vibrate and straighten out. As a result, the mean free path increases and enhances the phonon propagation length, implying the higher thermal conduction [119].

CHAPTER IV- EXPERIMENTAL RESULTS AND DISCUSSION:

EFFECT OF FUNCTIONALIZED CARBON NANOTUBES ON FINAL PROPERTIES OF NANOCOMPOSITES

All conclusive remarks on processing parameters and raw materials, collected in Cap.III, are adopted in this section to prepare nanocomposites in optimized conditions for thermal transport. In particular, previous considerations, highlighting the role of interfacial adhesion on thermal conduction of nanocomposites, bring to test two different types of chemically modified fillers in polypropylene: amino-functionalized carbon nanotubes (MWNT-NH_2) and carboxyl functionalized ones (MWNT-COOH). These polar functionalities, not ensuring any affinity with the non-polar hosting matrix, are responsible of different states of filler distribution with respect to that obtained for neat carbon nanotubes (MWNT). At this regard, compounds are prepared in pre-optimized melt-blending conditions and characterized in terms of thermal conductivity, morphological aspects (SEM, TEM, optical microscopy, THz, rheological measurements) and flexural properties.

4.1 Effect of filler type and content on thermal conduction of nanocomposites

In Figure 4.1 the thermal conductivity at room temperature of all investigated materials is reported as a function of the carbon nanotubes content [120].

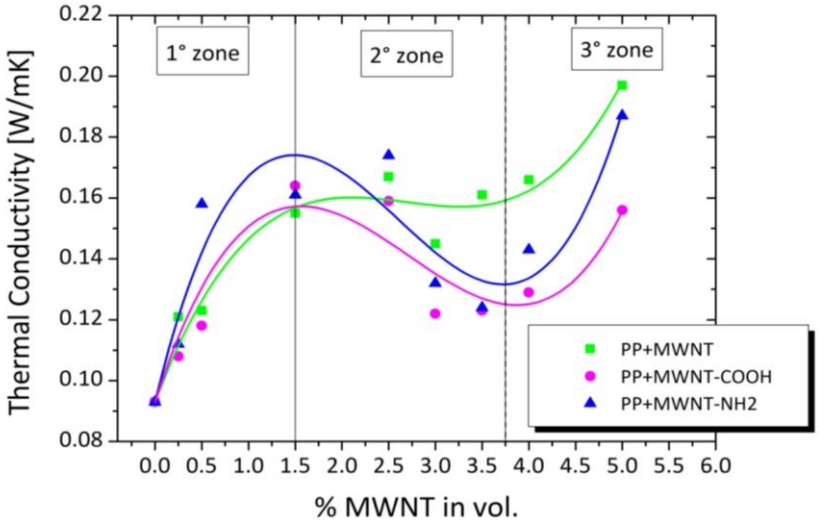

Fig. 4.1- Thermal conductivity of PP/MWNT composites as a function of volume fraction.

As far away from having a linear monotonic trend by increasing MWNT content, thermal conductivity data are affected by competitive phenomena that occur during the preparation of nanocomposites according to the filler concentration: dispersion and secondary agglomeration. These opposite processes influence average sizes of MWNT agglomerates and consequently, the distance between them, defined as the average inter-agglomerate distance (AID), in analogy with the well known geometrical parameter "*average inter-particles distance*" (AID). In literature, a lower AID gives rise to more chance for the formation of thermal conductive pathway [121]. At this regard, Fig. 4.1 can be divided in three ranges, depending on MWNT concentrations:

a) For MWNT contents up to 1.5 vol.% of MWNTs, a linear increase of the thermal conductivity is always detected with an effect more marked in presence of MWNT-NH_2 with respect to the presence of MWNT and

MWNT-COOH. Probably, low viscous forces developed in the mixing chamber could be not sufficient to ensure a significant disintegration of primary agglomerates, in spite of their porosity, lower in the case of functionalized carbon nanotubes. Therefore, the dispersion, taking place though erosion rather than rupture mechanisms, leads to non homogeneous filler distribution, characterized by dispersed and aggregates areas.

b) For MWNTs content in the range from 1.5 to 3.7 vol. %, different situations are proposed. In the case of MWNT, thermal conductivity seems to be stabilized to a constant value; while, a drastic reduction is observed for both functionalized fillers.

   Probably, the increased stress may enhance the infiltration of MWNT agglomerates and activate dispersion mechanisms (rupture and erosion) while the higher content may facilitate their aggregation. These opposite phenomena could become competitive to determine the extent of the final AID parameter. In particular, for MWNT, having higher affinity with respect to the hosting matrix than polar functionalized ones, their increased tendency to fragment in small size bodies may counterbalance aggregation phenomena, maintaining constant the mutual distance among agglomerates and, consequently, the thermal conductivity of samples. Instead, in the case of functionalized MWNT, due to intrinsic features of their initial agglomerates (lower porosity, higher agglomerates strength), a lower mutual tendency in fragmentation combined with a lower viscosity are such to prevail the aggregation phenomena with increases of both agglomerate mean sizes and AID, and consequent reductions of the thermal conductivity.

c) For filler contents over 3.7 vol. %, an overall increase in thermal conductivity is always shown.

In these conditions, the high stress at which agglomerates are subjected during the mixing and ever more probable collisions between them may further enhance the efficiency of dispersion mechanisms with respect to aggregation phenomena.

Finally, thermal conductivity trend could be always well fitted, as shown in the picture, by a cubic polynomial equation 4.1):

$$k\,(\emptyset) = A + B * \emptyset + C * \emptyset^2 + D * \emptyset^3 \qquad 4.1)$$

where $k(\emptyset)$ is the measured thermal conductivity of sample containing a filler volume, defined as $\emptyset$. Coefficients A, B, C, D are summarized in Tab. 4.1.

	MWNT	MWNT-NH_2	MWNT-COOH
A	0.093	0.093	0.093
B	0.081	0.126	0.09
C	-0.032	-0.059	-0.043
D	0.004	0.007	0.005
$\mathbf{R^2}$	0.997	0.991	0.994

Tab.4. 1-Coefficients A, B, C D (Eq. 4.1) for investigated PP/MWNTs systems.

Besides the coefficient A, representing the thermal conductivity of the neat PP, the coefficient B roughly reflects trends of the thermal transport behavior at low filler contents, at which last terms, scaling by a factor equal to 2 and 3, respectively, with the volume fraction of carbon nanotubes, can be neglected. About C and D coefficients, instead, more and more relevant by increasing the filler content, can be considered as a sign of the extent of competition between dispersion/collision and agglomeration phenomena. In particular, while both terms A and D represent two positive contributions in improving thermal conduction, the parameter B, being negative, involves in a drastic reduction of this latter. In this perspective, the third value of eq.1 could be probably

indented as an indication of re-agglomeration phenomena that inevitably take place during mixing phase. Supporting this hypothesis, the coefficient B results higher in the case of functionalized carbon nanotubes, for which stronger attractive interactions than Van der Waals forces can arise between chemical groups on CNTs surface, pushing isolate particles to merge.

4.2 Differential scanning calorimetric results

DSC analysis is one of the most convenient techniques to obtain a qualitative assessment of the crystallinity of polymer composites. In this work, DSC analyses are performed varying filler type and content to get, in addition to the crystallinity degree, also information about melt and crystallization temperature and associated enthalpy variations. All detected parameters are summarized in the following table (Tab. 4.2).

Many studies report on the nucleating effect of carbon nanotubes [122] as well as on their action on increasing the crystallization temperature of the matrix [123] even if opposite results, regarding their influence on degree of cristallinity, are also available [124].

In our case, both type and content of carbon nanotubes do not seem to affect the crystallization behavior of the matrix. In fact, not only melt and crystallization temperature but also the degree of crystallinity of nanocomposites remain almost equal to those detected for the neat matrix.

As a consequence, detected improvements in thermal conduction of nanocomposites, could not be attributed to a variation of polymer crystallinity in presence of carbon nanotubes.

	First Heating			Cooling		Second Heating		
	T_m^1[°C]	ΔH_f^1 [J/g]	x_c^1	T_c^1 [°C]	ΔH_c^1 [J/g]	T_m^2 [°C]	ΔH_f^2 [J/g]	x_c^2
PP	**168**	**73.9**	**35 %**	**127**	**82.7**	**164.7**	**81.7**	**39%**
PP+0.5 vol% MWNT	167	77.4	37%	124.9	87.6	165.9	85.4	41%
PP+1.5 vol% MWNT	167	75.7	37%	124.5	82.9	166.7	82.9	41%
PP+2.5 vol% MWNT	166	77.2	39%	124.7	81.2	166.1	77.6	39%
Average PP/MWNT	**166.7**	**76.8**	**37.7%**	**124.7**	**83.9**	**166.2**	**82.0**	**40.3%**
STD.Dv. PP/MWNT	**0.6**	**0.9**	**1.2**	**0.2**	**3.3**	**0.4**	**4.0**	**1.2**
PP+0.5 vol% MWNT-NH2	172	72.3	35%	125.0	83.7	165.9	76.7	37%
PP+1.5 vol% MWNT NH2	168	76.3	37%	124.8	82.4	166.3	78.2	39%
PP+2.5 vol% MWNT NH2	168	75.9	38%	124.8	80.9	166.4	76.3	38%
Average PP/MWNT-NH$_2$	**169.3**	**74.8**	**36.7 %**	**124.9**	**82.3**	**166.2**	**77.1**	**38.0%**
STD.Dv. PP/MWNT-NH$_2$	**2.3**	**2.2**	**1.5**	**0.1**	**1.4**	**0.3**	**1.0**	**1.0**
PP+0.5 vol% MWNT-COOH	170	77.5	37%	125.0	83.7	166.8	82.7	40%
PP+1.5 vol% MWNT-COOH	170	75.0	37%	125.8	84.2	166.6	78.8	39%
PP+2.5 vol% MWNT-COOH	169	72.4	37%	125.3	84.6	166.5	79.8	40%
Average PP/MWNT-COOH	**169.7**	**75.0**	**37.0**	**125.4**	**84.2**	**166.6**	**80.4**	**39.7%**
STD.Dv. PP/MWNT-COOH	**0.6**	**2.6**	**0.0**	**0.4**	**0.5**	**0.2**	**2.0**	**0.6**

Tab. 4.2- Crystallization temperature (T_c), crystallization enthalpy (ΔH_c), melting temperature (T_m), melting enthalpy (ΔH_f),degree of crystallinity (X_c) of PP/MWNT nanocomposites.

4.3 Morphological aspects by Electron Microscopy

4.3.1 SEM of primary agglomerates

First of all, attention is focused on analysis of carbon nanotubes powder, as received, to observe differences between primary agglomerates of each carbon nanotubes type (amino-, carboxyl- functionalized and pristine ones) through scanning electron microscopy. In Fig. 4.2, SEM micrographs, performed on powder of each type of multiwalled carbon nanotubes, as received, at two different magnifications, respectively 20 and 1 microns, are reported.

At magnification of 20 microns, not substantial differences seem to be evident among primary agglomerates, while a deeper magnification of 1 micron reveals a denser and more loosely packed structures for carboxyl modified carbon nanotubes with respect to other ones.

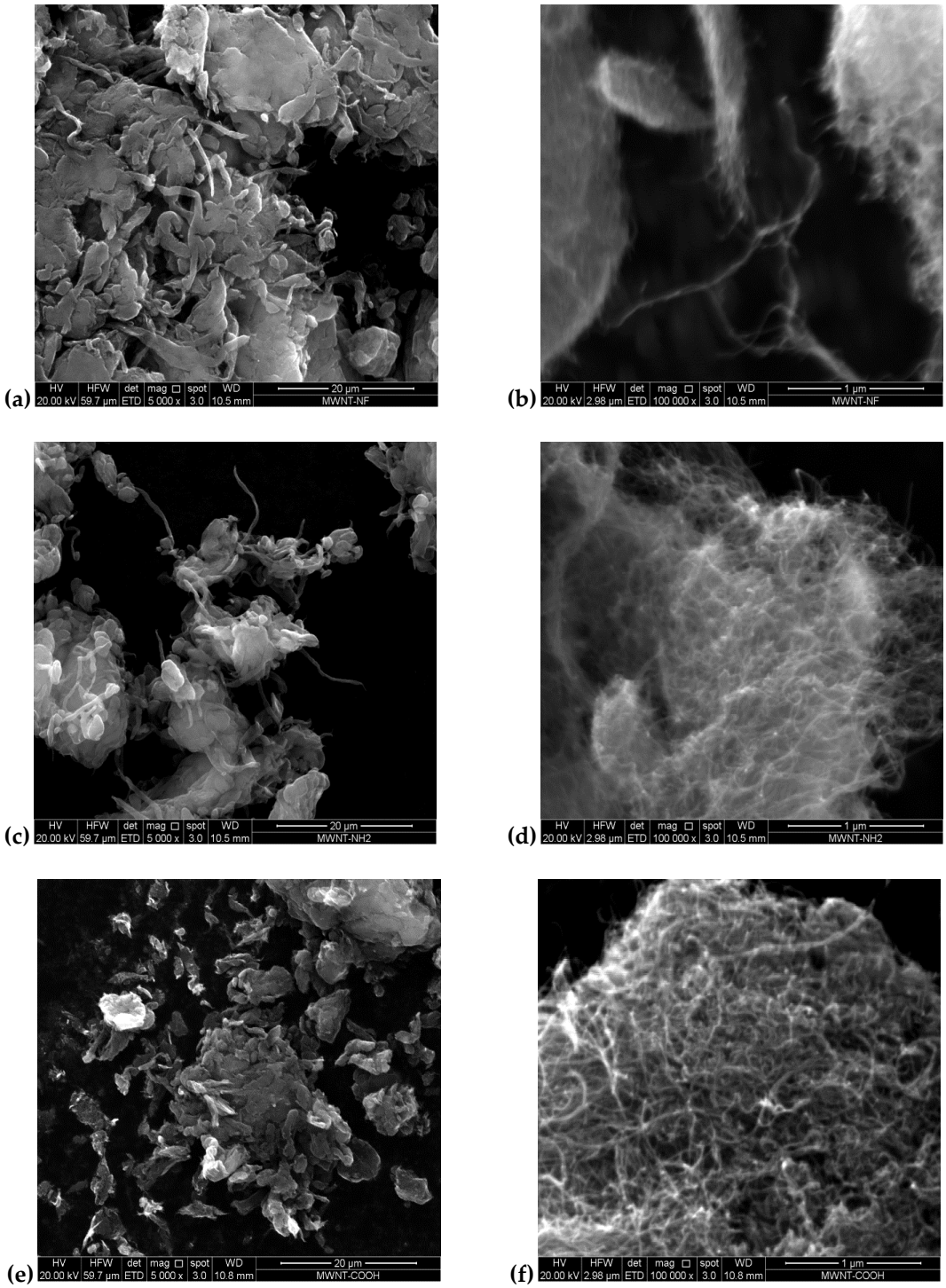

Fig. 4.2-SEM on carbon nanotubes powders at two different magnifications, 20 and 1 µm, respectively: (a) and (b) MWNT; (c) and (d) MWNT-NH_2; (e) and (f) MWNT-COOH.

4.3.2 SEM on polypropylene-based nanocomposites

SEM observations on cryofractured surfaces of PP composites, filled with different volume fractions of amino-, carboxyl- and neat multi-walled carbon nanotubes, are shown in Figs. 4.4, 4.5 and 4.6, respectively. With the exception of the pure PP micrograph (Fig. 4.3), showing typical features of a brittle fractured surface, it is always evident that nanotubes are mainly dispersed as bundles or/and aggregates, whose dimension increases with the amount of filler. In particular, at low filler contents (Figs. 4.4.a, 4.5.a, 4.6.a), MWNTs appear quite isolate in the matrix or in form of small aggregates. Instead, increasing the filler content up to 2.5% in vol., MWNT form agglomerates with gradually larger dimensions (Figs. 4.4.b, 4.5.b, 4.6.b, 4.4.c, 4.5.c, 4.6.c) . This is due to the usual tendency of carbon nanotubes to interact each other through surface forces, as Van deer Walls or also hydrogen bonding, especially if carboxyl and hydroxyl groups are present on their surfaces [125].

Finally, it is evident that, under the same filler content, smaller aggregates are obtained for functionalized carbon nanotubes with respect to not functionalized ones.

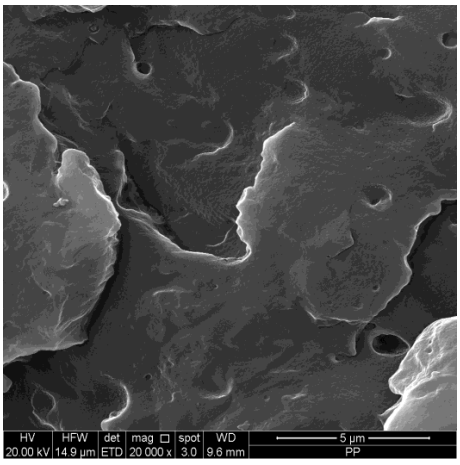

Fig. 4.3 - SEM micrographs of neat PP.

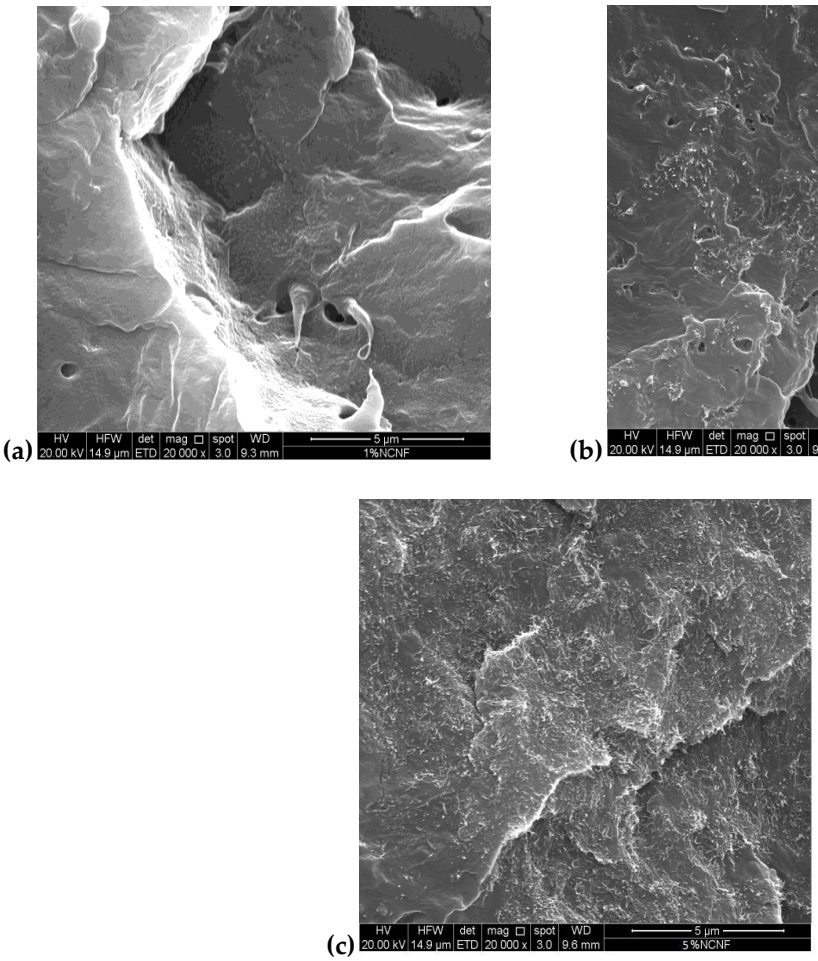

Fig. 4.4 - SEM micrographs of PP compounds containing a) 0.5 vol% (corresponding to 1% in wt.), b) 1.5 vol% (corresponding to 3% in wt.) and c) 2.5 vol% (corresponding to 5% in wt.) of MWNT.

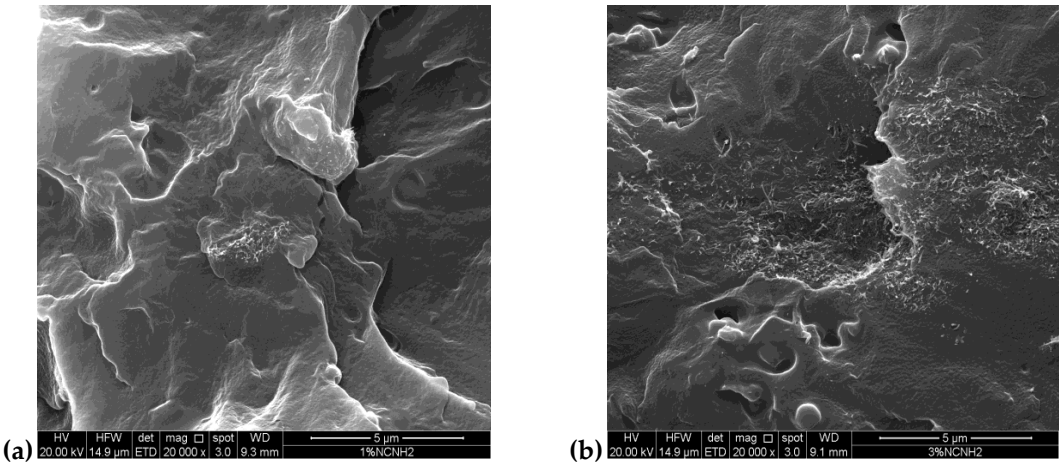

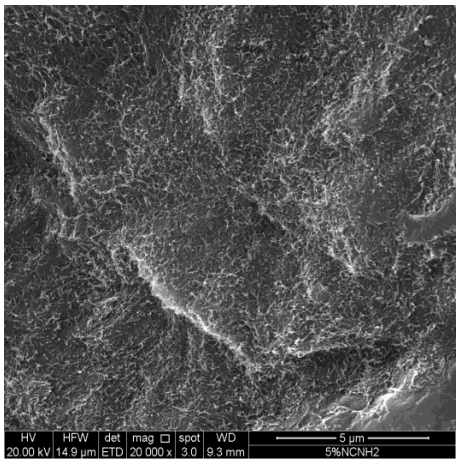

(c)

Fig. 4.5 - SEM micrographs of PP compounds containing a) 0.5 vol% (corresponding to 1% in wt.), b) 1.5 vol% (corresponding to 3% in wt.) and c) 2.5 vol% of MWNT-NH_2 (corresponding to 5% in wt.).

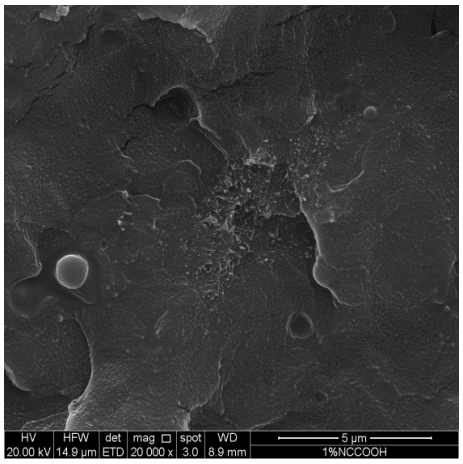

(a)

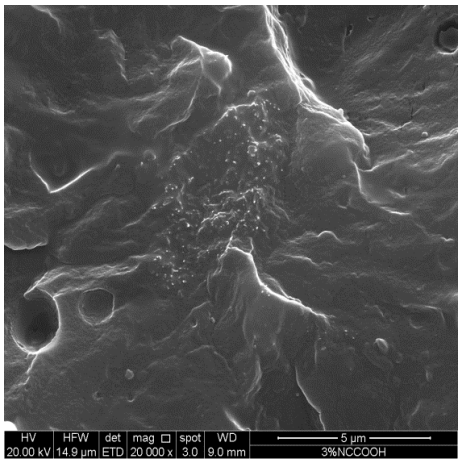

(b)

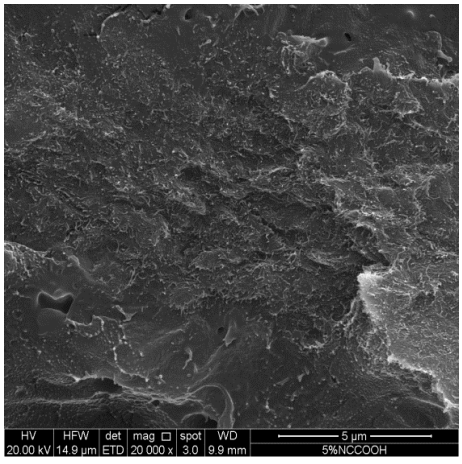

(c)

Fig. 4.6 - SEM micrographs of PP compounds containing a) 0.5 vol% (corresponding to 1% in wt.), b) 1.5 vol% (corresponding to 3% in wt.) and c) 2.5 vol% of MWNT-COOH (corresponding to 5% in wt.).

4.3.3 TEM on polypropylene-based nanocomposites [120]

In Figs. 4.7 - 4.9, TEM images of nanocomposites containing 0.5%, 2.5%, 5% in vol., respectively, of carbon nanotubes, functionalized and not, are reported. In details, not functionalized carbon nanotubes show swelled aggregates forming a network of particles, partially dispersed (Fig. 4.7.a) or aggregated at higher filler concentrations (Fig. 4.7.b). In case of functionalized carbon nanotubes, quite isolate elements can be distinguished, at low filler contents (Figs. 4.8.a, 4.9.a) while lower aggregates, surrounded by individual particles, become visible by increasing the concentration (Figs. 4.8.b, 4.9.b).

Finally, in all three cases, an homogenous distribution seems to be achieved at 5% in vol. of filler loadings (Figs. 4.7.c, 4.8.c, 4.9.c).

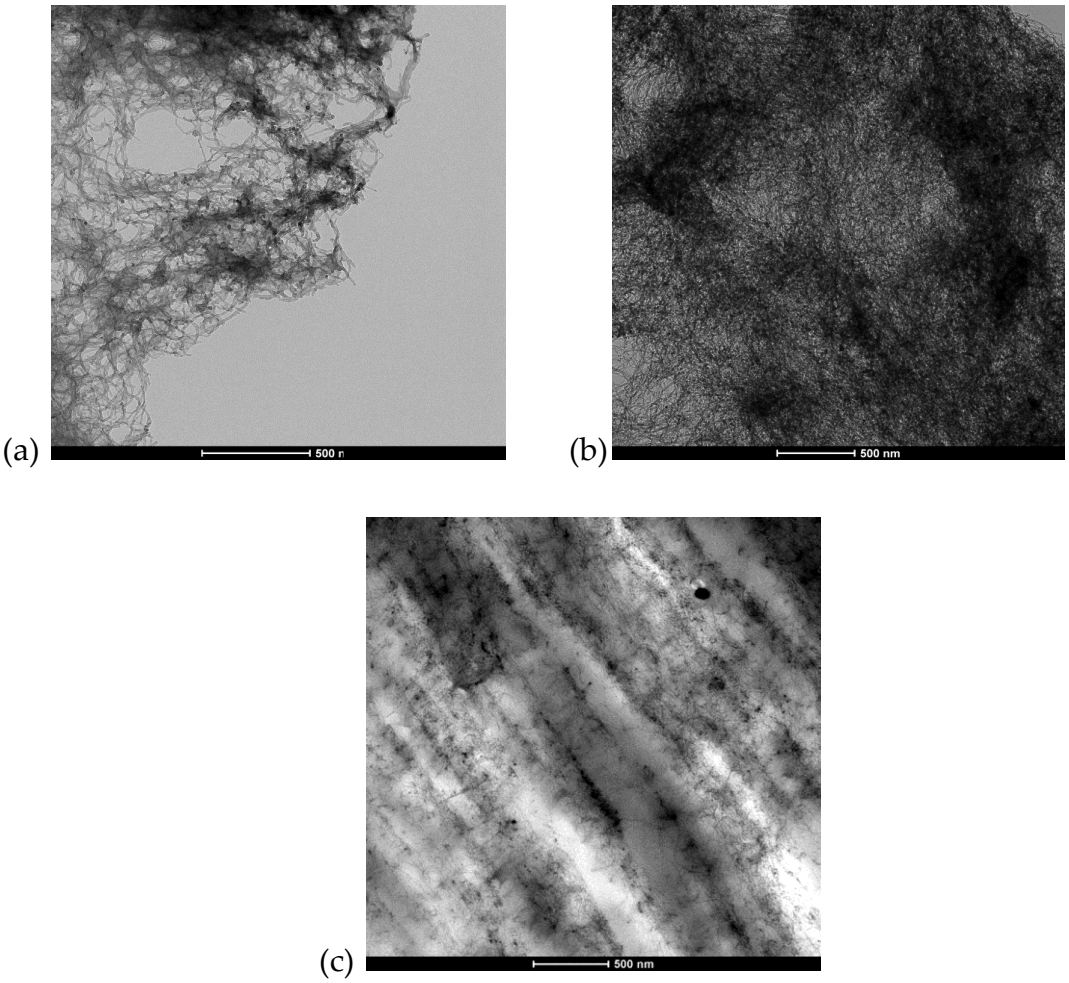

Fig. 4.7- TEM images of MWNT: (a) 0.5% in vol. (b) 2.5% in vol. (c) 5% in vol.

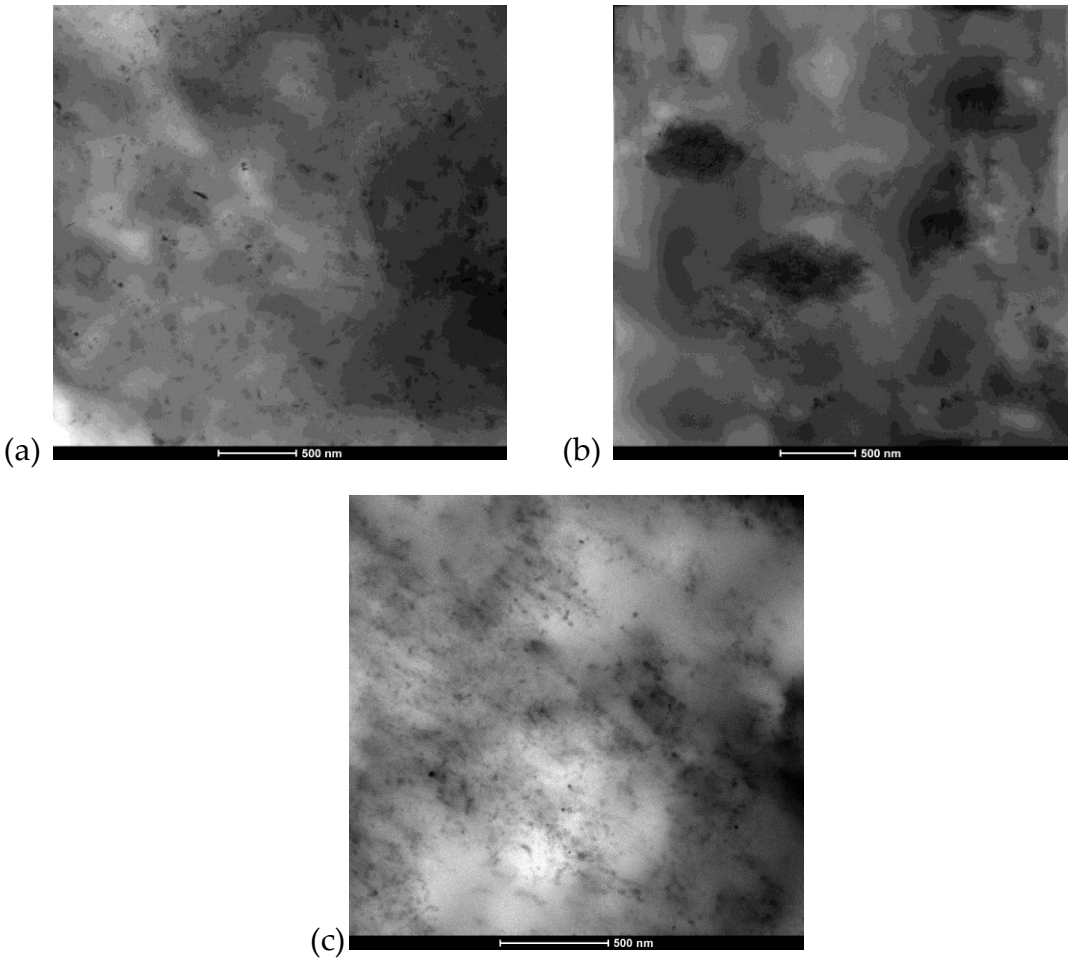

Fig. 4.8- TEM images of MWNT-NH2: (a) 0.5% in vol. (b) 2.5% in vol. (c) 5% in vol.

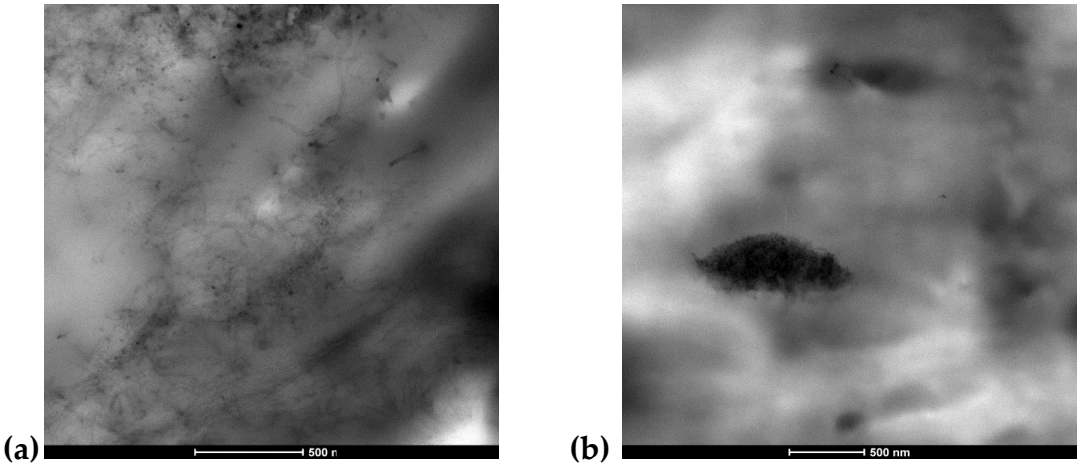

(c) 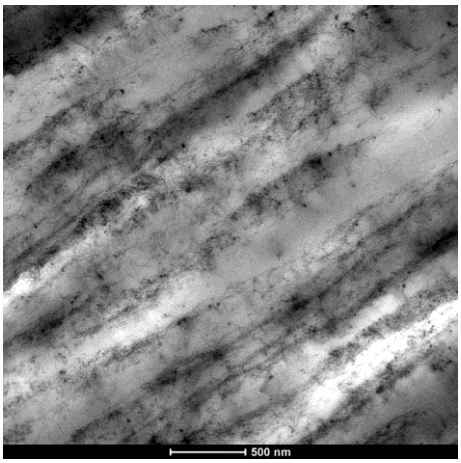

Fig. 4. 9-TEM images of MWNT-COOH: (a) 0.5% in vol. (b) 2.5% in vol. (c) 5% in vol.

4.4 Quantitative analysis of filler dispersion by optical microscopy

4.4.1 Packing density evaluation

As described in parag. 2.3.6., the packing density calculation requires samples of CNTs powder, infiltrated in epoxy resins. Thin slices of these materials are observed by optical microscopy (Fig. 4.10). The elaboration of collected pictures, by a freeware image processing software, allows to obtained packing density values, applying equation 2.6.

(a) 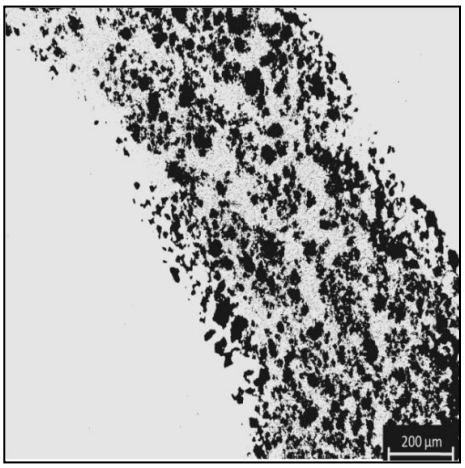

(b) 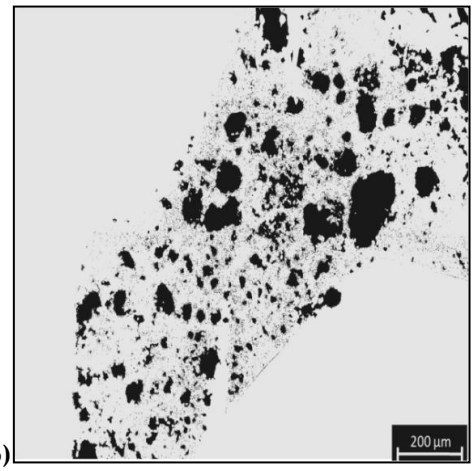

(c) 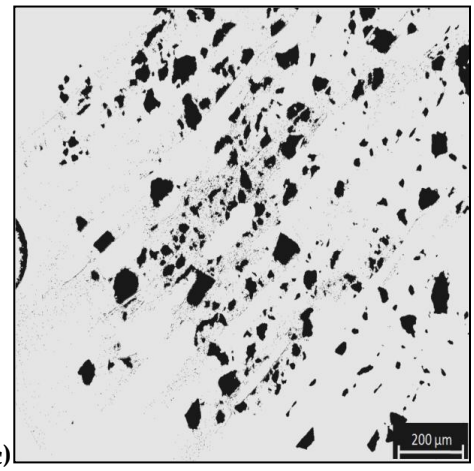

Fig. 4.10-Optical microscopy images of epoxy resins and carbon nanotubes type: MWNT (a); MWNT-NH2 (b); MWNT-COOH (c).

This parameter is equal to 0.025, for both MWNT and MWNT-NH_2; while it is 0.029 for MWNT-COOH aggregates, as summarized in following Tab. 4.11.

	Packing density
MWNT	0.025
MWNT-NH_2	0.025
MWNT-COOH	0.029

Fig. 4.11-Packing density values.

4.4.2 Optical microscopy analysis on nanocomposites at a filler concentration of 0.5% in vol. [126]

The image analysis, carried out on several slices of each investigated material, shows that a satisfactory MWNT aggregate size distribution is always achieved under the applied processing conditions. Figure 4.12 displays representative light microscopy images of compounds containing 0.5% in volume for each kind of carbon nanotubes, herein considered: non-functionalized,

functionalized with amino groups (-NH_2), functionalized with carboxyl groups (-COOH). Differences among investigated samples are clearly reflected in parameters as: the dispersion index (calculated according to Eq. 2.5), number of agglomerates and circle equivalent diameter (see Fig. 4.13). Further deeper evaluations, on agglomerates size distribution and cumulative percentage, are also reported (Fig. 4.14).

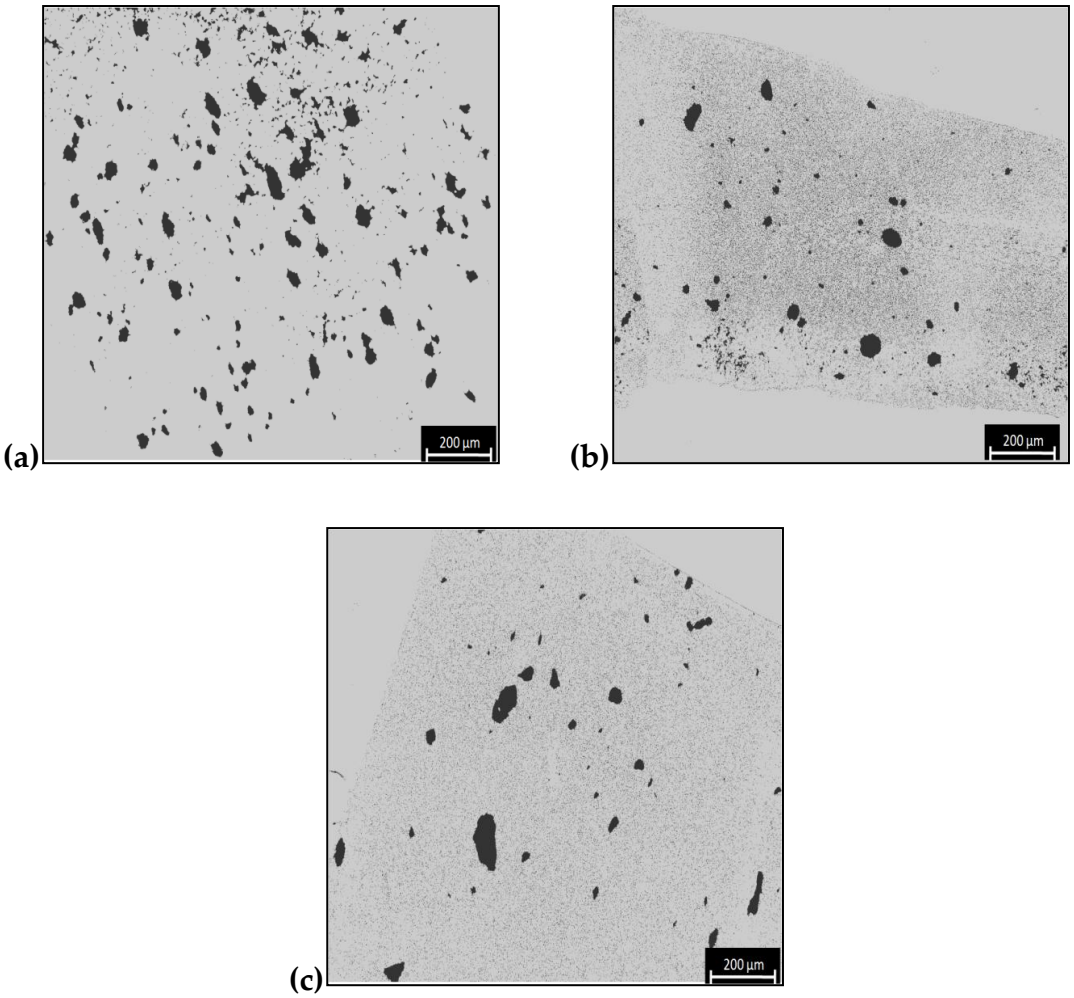

Fig. 4.12 -Optical micrographs for nanocomposites with MWNT: non-functionalized (a), functionalized with amino groups (b) and functionalized with carboxyl groups (c).

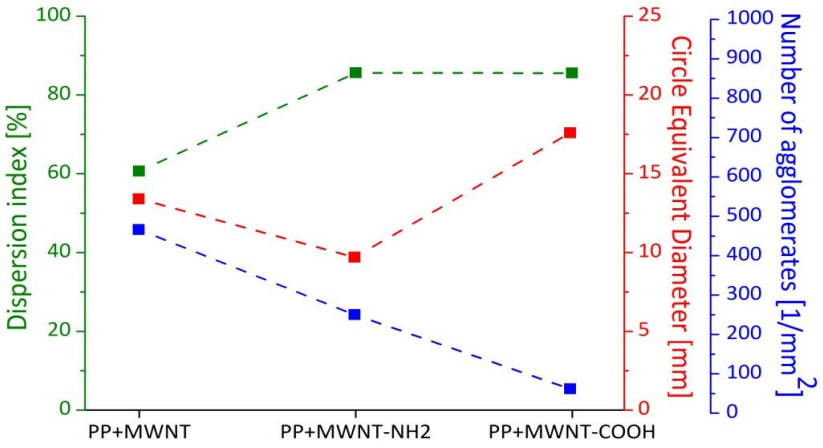

Fig. 4. 13-Dispersion index, circle equivalent diameter and number of agglomerates for three different nanocomposites at 0.5% vol. of filler loadings.

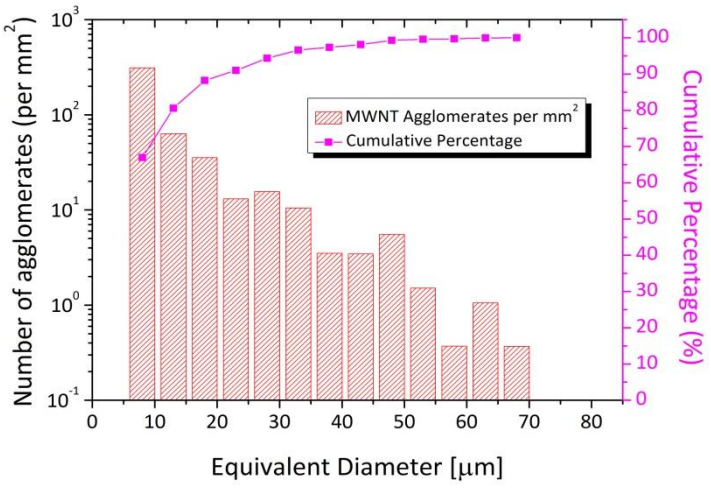

(a)

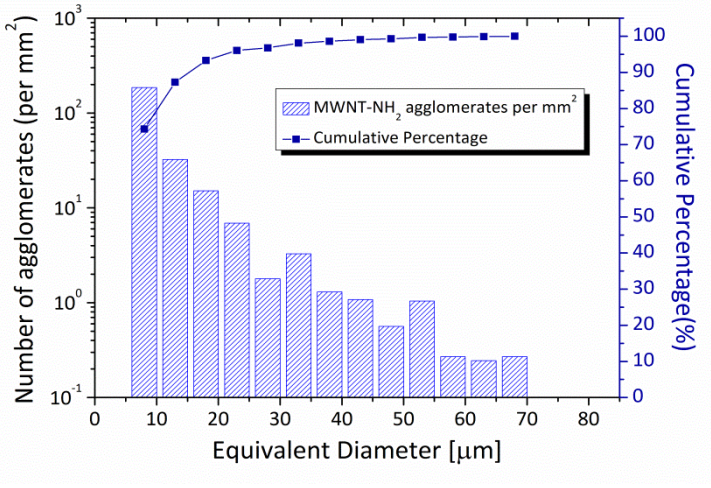

(b)

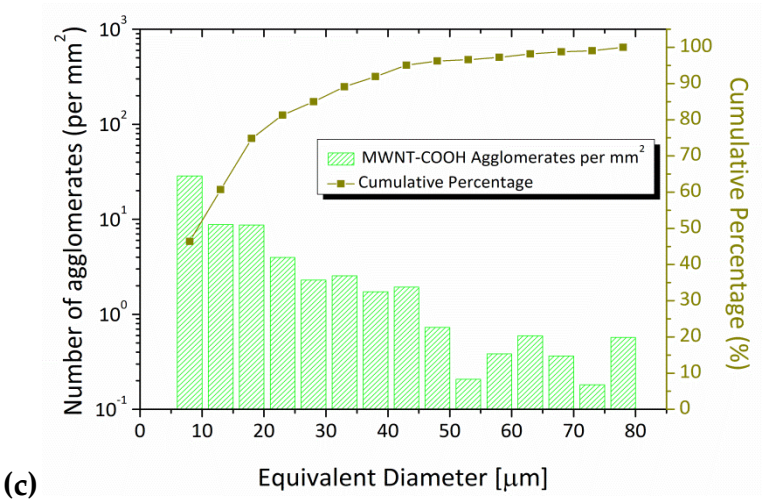

Fig. 4. 14-Size distribution of MWNT agglomerates in nanocomposites with different functionalized filler: nonfunctionalized (a), functionalized with amino groups (b), and functionalized with carboxyl groups (c).

From these results, clearly, the worst dispersion index *D* occurs in presence of non-functionalized carbon nanotubes (~60%), whereas for both types of surface modified nanotubes the same parameter increases and reaches a similar value (~87%). The number of agglomerates, instead, vary from 60 counts/mm² in case of compounds filled with carboxyl-modified carbon nanotubes up to 320 and 470 counts/mm² for systems containing the same amount of amino-modified and pristine carbon nanotubes, respectively.

Thus, non-functionalized MWNTs give rise to a higher number of agglomerates with an average size (equivalent diameter) larger than MWNT-NH_2, reducing the dispersion index of melted compounds. By cumulative percentage, it is observed that 90% of CNTs aggregates have mean sizes not exceeding 25 µm for MWNT, 15 µm for MWNT-NH_2 and 35 µm for MWNT-COOH, respectively.

Concluding, although the dispersion of carbon nanotubes seems to be favoured at the same extent in presence of two surface-modified carbon nanotubes, the type of functional groups apparently influences the number of MWNT agglomerates and their size distribution. This consideration can be ascribed to expected differences in terms of filler-matrix interactions and primary

agglomerates strength, that affect in different way wetting of primary agglomerates, polymer infiltration, erosion and rupture process. In fact, a lower agglomerates strength, due to better wetting phase and higher porosity, could be reasonably assumed for carbon nanotubes not functionalized. This could mean that fragmentation might arise easy through rupture process, leading a large number of agglomerates with medium dimensions. Instead, if the compatibility between filler and matrix is reduced by polar functional groups, as amino and carboxyl ones, the wetting phase becomes limited. In this situation, being also a higher porosity, primary agglomerates of MWNT-NH_2 and MWNT-COOH are linked by higher strength. Consequently, erosion mechanism could dominate fragmentation, resulting in a state of dispersion characterized by individual carbon nanotubes or smaller number of aggregates.

4.5 Absorption coefficient and refractive index of nanocomposites by THz spectroscopy

Terahertz Time Domain Spectroscopy has been widely employed as a characterization tool for a wide range of materials, including ceramics, semiconductors, polymeric compounds, useful for morphological studies [127], to monitor glass transitions [128] and compounding processes [129], for quality control [130].

In the Ref. [126], nanocomposites, containing 0,5% vol. of carbon nanotubes, amino, carboxyl functionalized and pristine ones, are analyzed through THz spectroscopy. Parameters, as refraction index and absorption coefficient, in function of frequency, are directly derived (Fig. 4.15), taking as reference the neat matrix, processed under the same conditions.

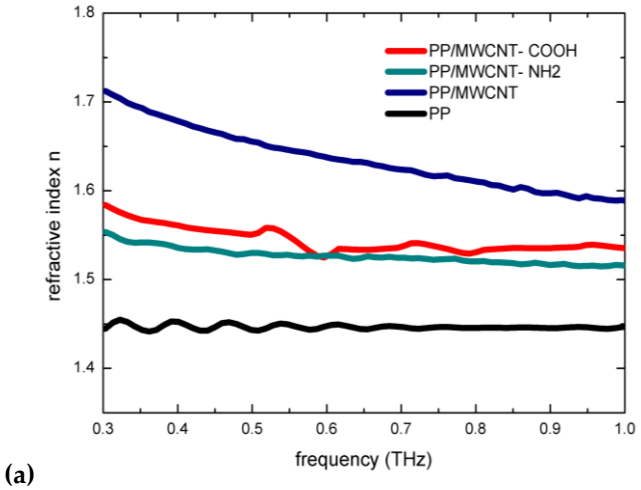

(a)

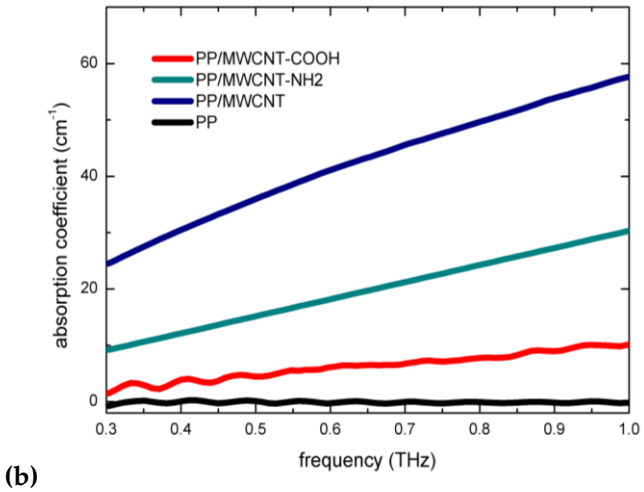

(b)

Fig. 4.15-Refractive index (a) and absorption coefficient (b) for nanocomposites at 0.5% in vol. of carbon nanotubes: not functionalized, amino and carboxyl functionalized, respectively.

The adsorption coefficient of neat polypropylene, around zero for all frequency range, allows to define the matrix as an "invisible" background medium, in which embedded MWCNTs can be easily characterized. For examined nanocomposites, the adsorption coefficient increases with the frequency in a way strongly dependent on the different degree of CNTs functionalization. The lowest value is observed for the sample functionalized with carboxyl groups (-COOH).

Concerning the refractive index of PP, its value is quite constant for all frequencies for the absence of any resonant band behavior in the analyzed

range of frequencies. When polypropylene is loaded with not functionalized MWNT, at every investigated frequency, the refractive index remained always higher than in presence of functionalized loading. Probably an increase of interaction between the medium and the THz wave takes place.

These results could be explained in the light of previous optical microscopy characterization, performed on the same samples. In fact, the high number of agglomerates, found in nanocomposites containing both non-functionalized and amino modified MWNT, probably, giving larger Rayleigh scattering phenomena, leads to a higher refractive index respect to samples containing carboxyl-modified carbon nanotubes, in which instead a less number of agglomerates are present. Moreover, a higher degree of dispersion is evaluated in the case of functionalized fillers, consisting probably in smaller entities, having dimensions comparable with the wavelength. These, in turn, might reduce the number of significant scattering sources, in the investigated frequency region, also for the same level of nanofiller content.

These considerations have prompted attention to combine results of THz spectroscopy with those of light optical microscopy. In fact, by increasing dispersion index D a decrease of the refractive index seems to be achieved, so to imply a possible correlation between these two parameters (Fig. 4.16).

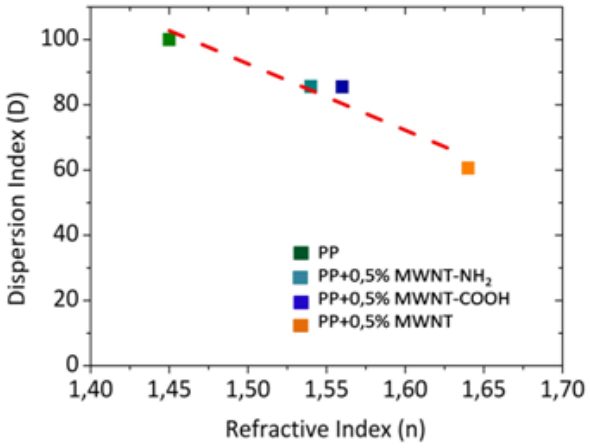

Fig. 4.16-Plot of dispersion index in function of refractive index. Dashed line is a guide for eyes.

4.6 Rotational rheological response of MWNT/PP nanocomposites [120]

The rotational rheological response of polypropylene-based nanocomposites is studied in order to verify microstructure in the melted states [131], and to obtain information on filler percolation within the composite [132].

4.6.1 Storage modulus of PP/MWNT nanocomposites

The elastic moduli (G′) of all investigated systems, as a function of angular frequency and filler content, are shown in Fig. 4.17.

The storage modulus always decreases with angular frequency; but, by increasing the CNTs content, a gradual reduction in the G′ slope at low frequencies is observed.

In particular, at low frequencies, the fully relaxed neat polypropylene exhibits scaling properties of approximately $G' \alpha \omega^{1,6}$, with factor lower than theoretically expectation ($G' \alpha \omega^2$), because of the polymer polydispersity [133]. By increasing the filler content, the melt behavior gradually changes from "*liquid-like*" to "*solid-like*"; the storage modulus becomes almost frequency independent (see Tab. 4.3), by showing a low-frequency slope that tends to zero ($G' \rightarrow \omega^0$). This phenomenon takes place at a particular filler content, defined as "*rheological percolation threshold*", and corresponds to the formation of interconnected structures, dominated by filler-filler and filler-matrix interactions, that strongly restrict the motion of macromolecular chains [134]. Data suggest that MWNT and MWNT-NH_2 have a very similar tendency to network formation, with a slope that nullify at 2.5% vol. of filler, while MWNT-COOH show a reduced tendency to network formation with a positive slope for the explored range.

Quantitative differences may be highlighted among storage modulus values, detected for each class of carbon nanotubes. In particular, at a frequency of 0.01 rad/s, for an amount of filler equal to 2.5 vol.%, G′ of PP/MWNT is 2 order of

magnitude higher respect to PP/MWNT-NH_2, and 3 order respect to PP/MWNT-COOH. These differences could be ascribed probably to two reasons:

- polymer affinity with not functionalized MWNT is less compromised with respect to functionalized ones. In fact the presence of amino or/and carboxyl groups, by increasing polar features of nanotube surface, reduces the interfacial adhesion with non-polar matrix and consequently the stress-transfer from polymer to filler [135].
- the presence of a network, more interconnected, for neat MWNT with respect to functionalized ones, that requires more energy for the deformation and the microstructural rearrangement, at constant deformation [136].

This behavior provides an indication of the relative quality of filler dispersion and/or mutual affinity between filler and matrix. In general a homogeneous dispersion of MWNT results in a higher storage modulus compared to the case in which poor dispersion is achieved. Consequently in this case, rheological measurements confirm a better dispersion of MWNT with respect to functionalized ones.

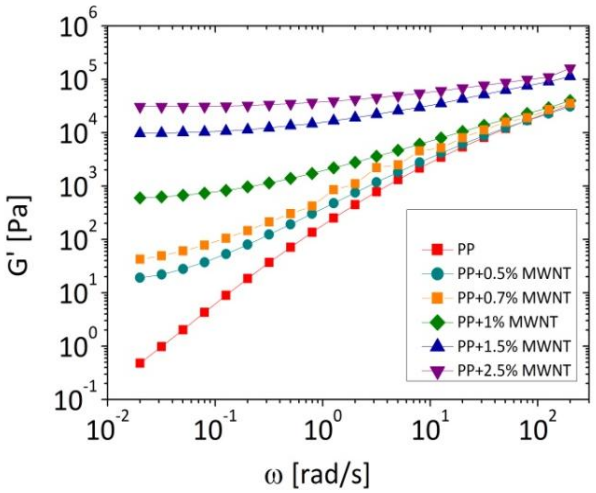

(a)

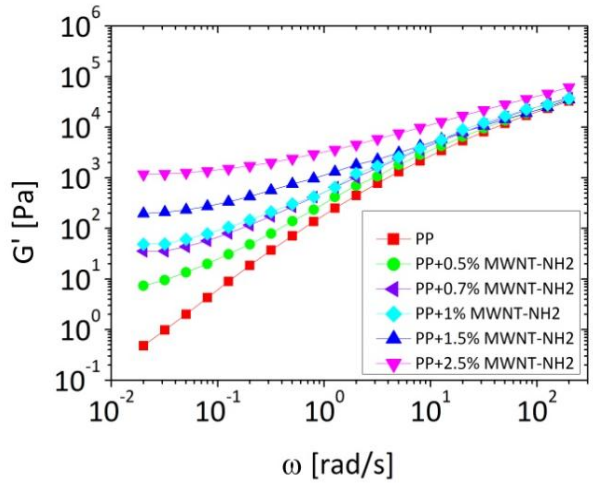

(b)

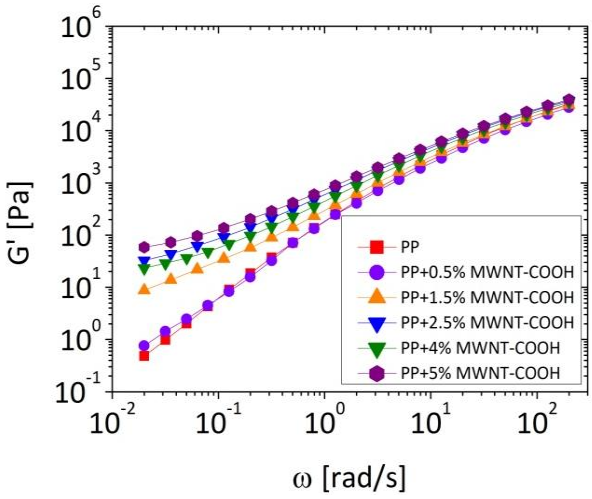

(c)

Fig. 4.17- Storage moduli as a function of frequency at 190°C for nanocomposites: (a) PP/MWNT; (b) PP/MWNT-NH_2; (c) PP/MWNT-COOH.

MWNTs content (vol. %)	G′ Slope at ω<0.1 rad/s		
	MWNT	MWNT-NH_2	MWNT-COOH
0	1.588	1.588	1.588
0.5	0.300	0.548	1.335
0.75	0.076	0.041	/
1	0.055	0.033	/
1.5	0.022	0.025	0.806
2.5	0	0	0.454
4	---	---	0.470
5	---	---	0.289

Tab. 4.3- Low frequency slope of storage moduli trend for PP/MWNT systems.

4.6.2 Complex viscosity data

In Figs. 4.18, complex viscosity data are reported as a function of the frequency. As expected, the complex viscosity of composites is always higher than for neat PP all over the investigated frequency range with values increasing with the filler content. While the neat PP shows a plateau at low frequency (corresponding to the Newtonian region in shear flow) and a thinning region at high frequency, the composite systems show very remarkable differences. Indeed, for the systems containing nanotubes, as the filler concentration is increased, the low frequency plateau rapidly shifts towards lower frequencies until it disappears thus showing a yield stress behavior. These effects, which are particularly pronounced in presence of non-functionalized CNTs, are clearly reduced for the systems containing amino-functionalized nanotubes and are almost negligible for PP/MWNT-COOH composites.

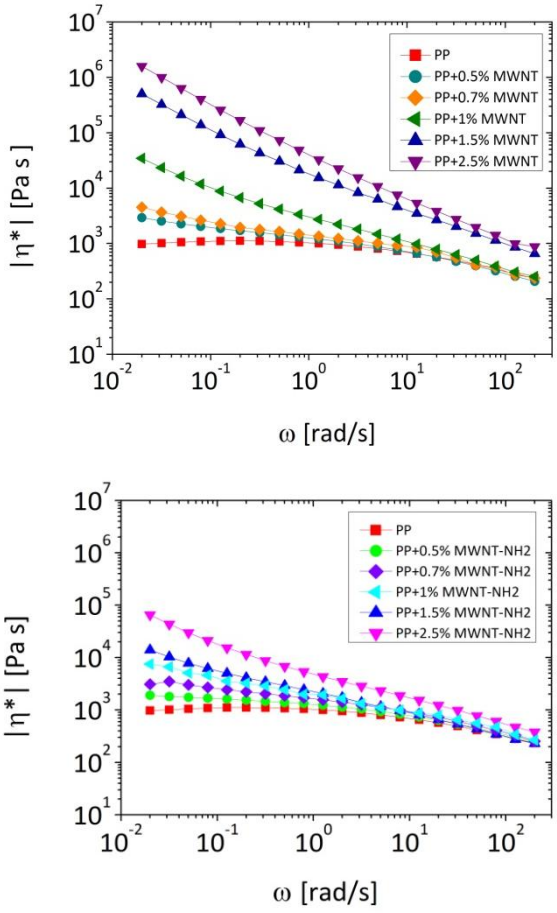

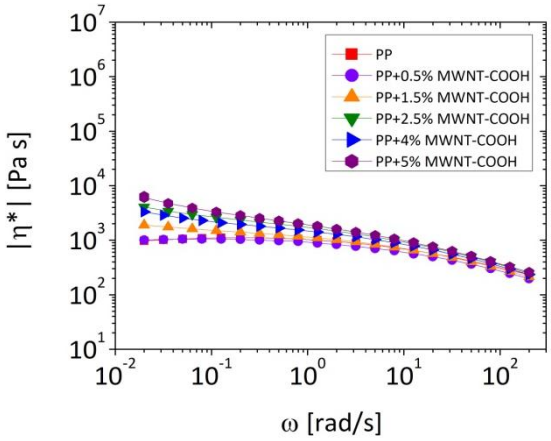

Fig. 4.18- Complex viscosities as angular frequency of: (a) MWNT; (b) MWNT-NH2; (c) MWNT-COOH.

4.6.3 Rheological percolation threshold

A graph, called "*Van Gurp-Palmen plot*", has been obtained by plotting the phase angle δ in function of complex modulus |G*|; through it, rheological percolation and material behavior can be defined [134]. In fact, in low |G*| region, when the phase angle is approximately near 90°, the material behavior is considered viscous; instead, a strong departure from 90° is commonly associated to the elastic behavior. A phase angle of 45° is taken, as the borderline between these two opposite ends [136, 137].

At this regard, Van Gurp-Palmen plots (Fig. 4.19) are utilized to identify rheological percolation thresholds, for each type of included carbon nanotubes.

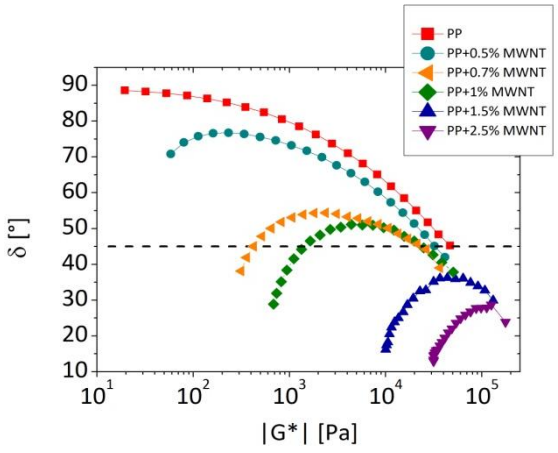

(a)

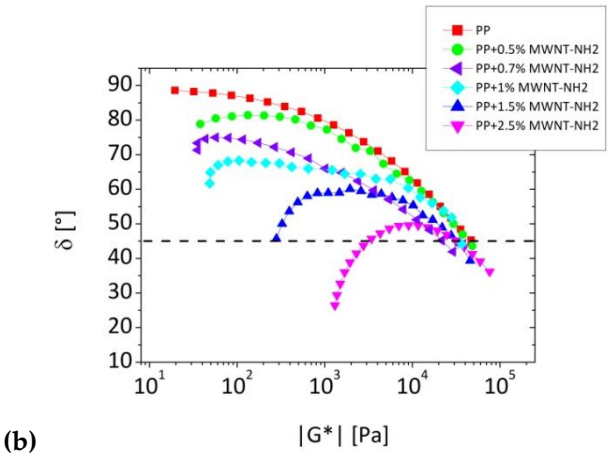

(b)

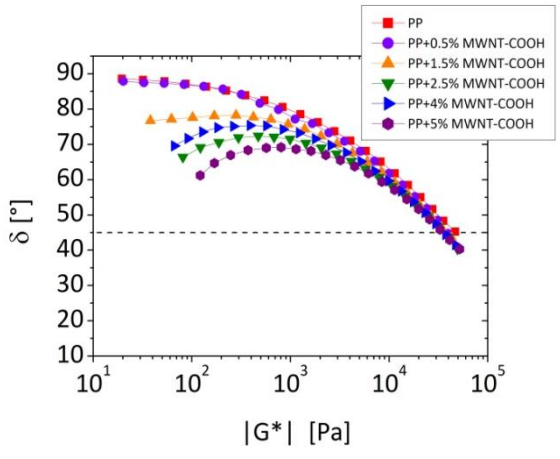

(c)

Fig. 4.19-Van Gurp-Palmen plot at a temperature of 190°C, for all investigated systems: (a) PP/MWNT; (b) PP/MWNT-NH$_2$; (c) PP/MWNT-COOH.

By increasing the filler content, the typical transition from viscous to elastic behavior could be observed at different volume fractions, depending on the type of included CNTs. In particular, the rheological percolation, in case of MWNT, is reached for a value, approximately equal to 0.65 vol.%, smaller than the one detected for MWNT-NH$_2$ (1.5 vol.%). Instead, for compounds containing MWNT-COOH, no percolation is reached up to 5% in vol. of filler amount. In this latter case, the material behavior appears almost viscous.

4.6.4 Physical Gelation: rule of the filler

A polymeric gel is a tridimensional network in which polymer chains are linked together through physical or chemical crosslink. By adding an amount of carbon nanotubes in the polymeric matrix, above the percolation threshold, tridimensional network of carbon nanotubes is realized by entanglements or Van deer Waals filler-filler and filler-matrix forces. This phenomenon could be associated to physical gelation, just studied in different cases like PVC/DOP and HDPE/POSS [138].

In this thesis, Winter and Chambon method [139] is used to study the "*gel-like*" behavior of nanocomposites, by plotting dissipation factor, at fixed frequencies, in function of carbon nanotubes content (Fig. 4.20).

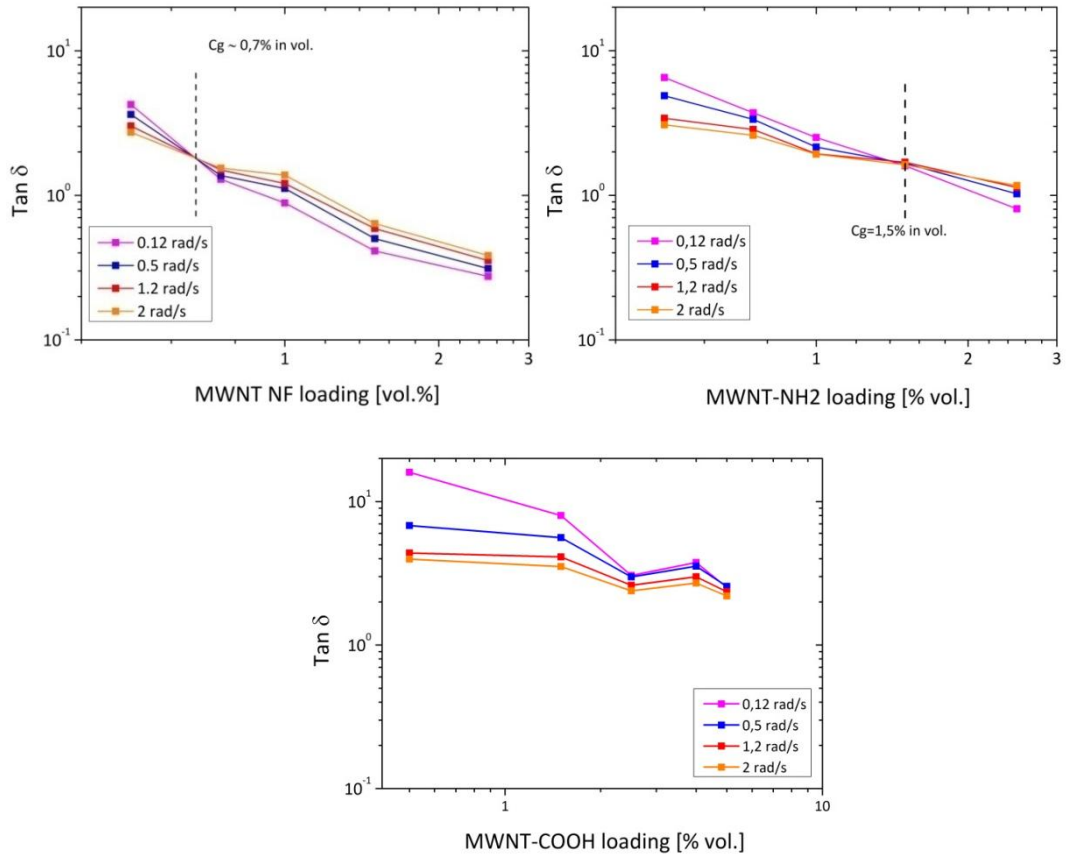

Fig. 4.20 -Dissipation factors, at different fixed frequencies and temperature of 190°C, in function of carbon nanotube loading.

The intersection point, among curves of each graph, is defined *gel point*; in correspondence of which the dissipation factor becomes frequency-independent.

In our case, the gel point is calculated around 0.7 vol.% and 1.5 vol.% in the case of MWNT and MWNT-NH_2, respectively. No intersection is detected for compounds filled with MWNT-COOH.

At the gel point, the "*shear relaxation modulus*" follows this constitutive equation:

$$G(t) = S_g t^{-n} \qquad 4.2)$$

where S_g is defined as the "*gel strength*" and n is the "*relaxation exponent*". These two parameters characterize the gel point. In particular, n reflects the compactness degree of the network: if n is small, a compact system with elastic behavior is prospected.

At the gel point, n and S_g are derived, by plotting G′ and $G''/Tan\left(\frac{n\pi}{2}\right)$ (Fig. 4.21) as a function of CNTs loading and by applying the following equation 4.3):

$$G' = \frac{G''}{Tan\left(\frac{n\pi}{2}\right)} = S_g \omega^n \Gamma(1-n)\cos\left(\frac{n\pi}{2}\right) \qquad 4.3)$$

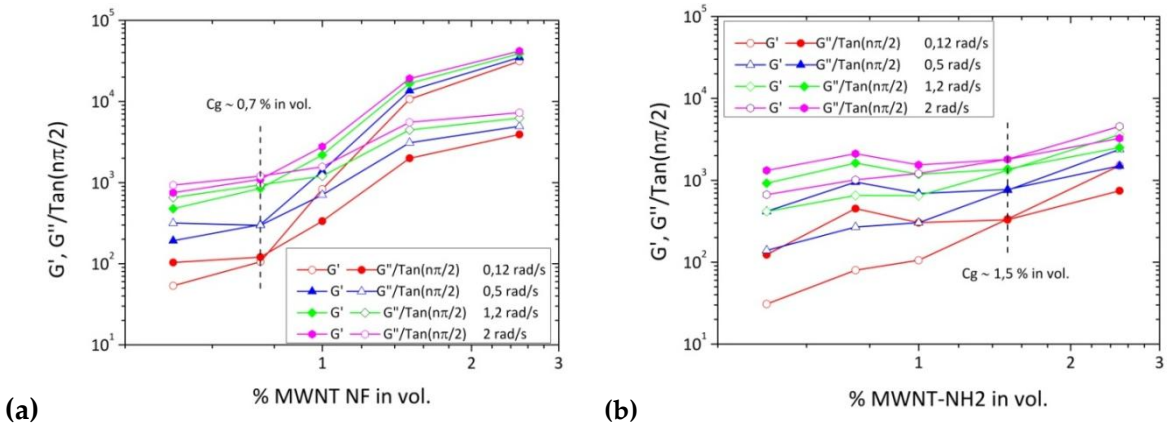

Fig. 4.21 - G′ and $G''/Tan\left(\frac{n\pi}{2}\right)$ trend in function of CNTs loading for nanocomposites: (a) PP/MWNT, (b) PP/MWNT-NH_2.

A lower relaxation exponent and higher gel strength are found in the case of MWNT-NH_2; see Tab. 4.4, which probably seem able to construct a more compact network with respect to MWNT ones.

	Gel point		
	Filler concentration for gel point	***n***	S_g $(Pa*s^n)$
PP/MWNT	0,7	0,7	620
PP/MWNT-NH2	1,5	0,6	1088

Tab. 4.4-Gel strength and relaxation exponent for investigated compound.

4.6.5 Effect of temperature on rheological behavior

In Fig.4.22, a comparison between rheological measurements at two different temperatures (190°C and 230°C), is reported in terms of normalized storage modulus and normalized complex viscosity as a function of carbon nanotubes loading.

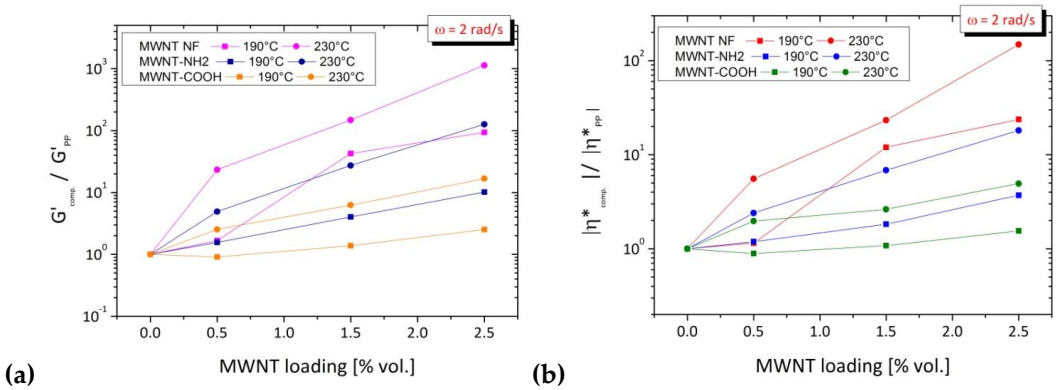

Fig. 4.22-Normalized value of storage modulus (a) and complex viscosity (b), for all nanocomposites, at temperature of 190°C and 230°C in function of filler content.

Normalized values of storage modulus and viscosity are higher for a temperature of 190°C with respect to those detected at 230°C, because of the G'

and η^* of the matrix decreasing with temperature. Consequently, it is clear that at a temperature of 190°C, the addition of carbon nanotubes results in a stronger enhancement of normalized parameter with respect to 230°C. For the same reason, at a higher temperature, also rheological percolation thresholds are reached at lower filler content: around 0.5 vol.% for MWNT, < 1.5 vol% for MWNT-NH_2 and approximately 2.5 vol.% for MWCNT-COOH, as can be seen in Fig. 4.23.

The influence of temperature on the rheological percolation can be explained with the fact that *liquid-like* to *solid-like* transition behavior takes place in correspondence of the network formation, related not only to filler-filler interactions but to a combined structure of polymer and filler. Consequently, since density and mobility of a polymer are influenced by temperature also percolated structures result affected by it.

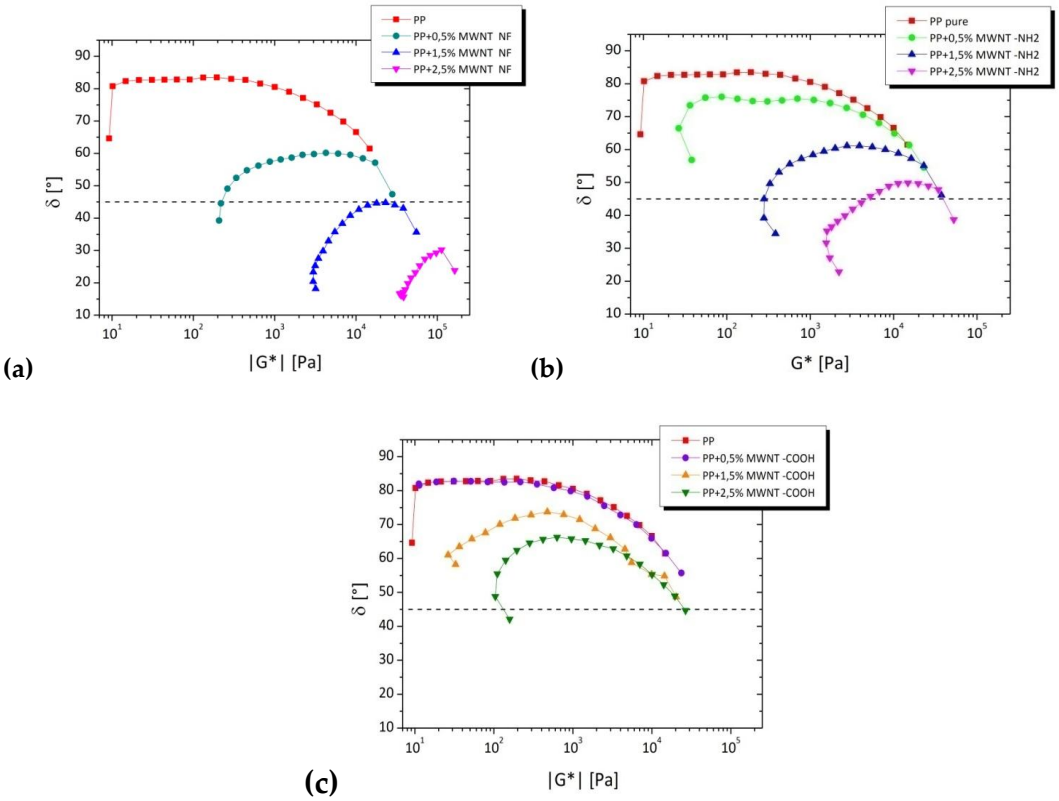

Fig. 4.23- Van Gurp-Palmen plot at a temperature of 230°C, for all investigated systems: (a) PP/MWNT; (b) PP/MWNT-NH_2; (c) PP/MWNT-COOH.

4.7 Flexural Properties

Nanocomposites containing up to 2.5% in vol. of amino-functionalized carbon nanotubes (MWNT-NH_2) and neat ones (MWNT), respectively, are tested in term of flexural properties. Results are summarized below in terms of typical stress-strain curves [140].

In all cases, maximum strain is limited at 5 %, as recommended by ASTM D790 normative, and no ultimate breaking is observed. Then, flexural modulus and strength as a function of the carbon nanotube contents have been estimated, as shown in Fig. 4.24.

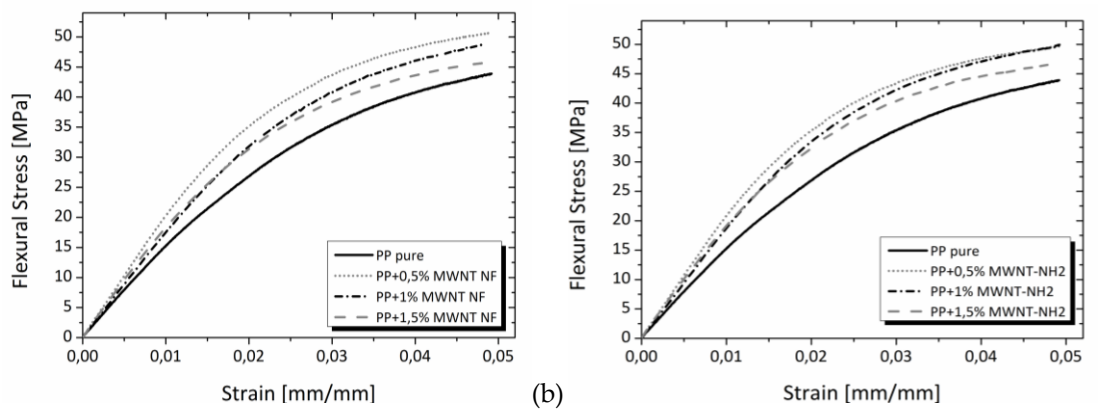

Fig. 4.24 - Stress-strain curves for nanocomposites containing MWNT (a) and MWNT-NH_2 (b) respectively

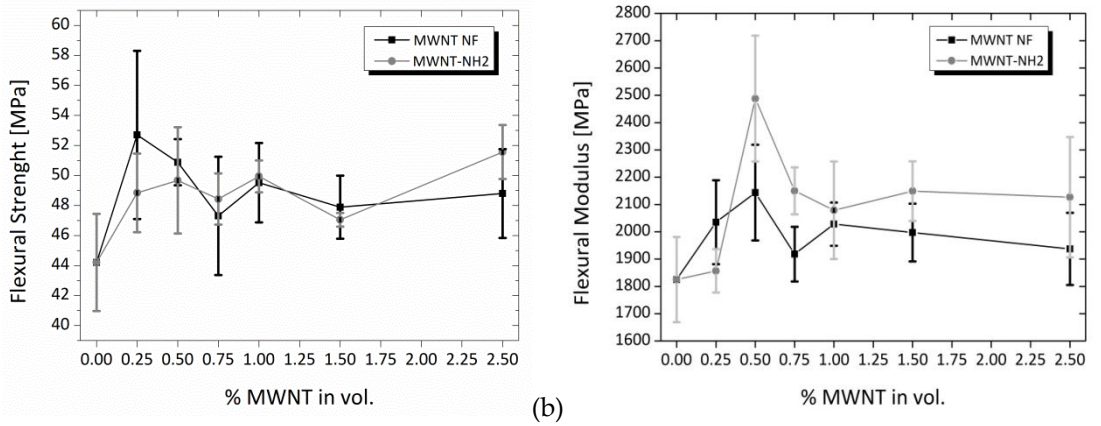

Fig. 4.25- a) Flexural modulus and b) flexural strength as a function of the MWNT content.

For each family of compounds, both flexural modulus and strength of matrix increase with the addition of carbon nanotubes, especially in the case of amino-functionalized fillers (MWNT-NH_2), showing a non monotonous trend. Probably, almost in the analyzed content range, amino-functionalization promotes a better dispersion, plausibly due to interactions with polymer, steric hindrance of functional groups, primary agglomerates different in size, porosity and cohesive strength.

In details, it is noted an increase, with respect to the neat matrix, of the averaged flexural strength approximately equal to 15.1% for compounds containing 0.5 vol. % of nanotubes with an effect apparently not influenced by the surface functionalization. Similarly, the flexural modulus increases approximately up to 17.4% and 36.3% in presence of 0.5% by volume of non-functionalized and amino-functionalized carbon nanotubes, respectively. However, further additions of the filler content, over 0.5% in vol., always induce slight reductions of these parameters probably for the formation of clusters or agglomerates, confirmed in SEM observation, resulting in lower properties at the interface with the hosting matrix and in a reduced interface area between CNTs and matrix. This state of dispersion promotes filler interactions and consequently shear delamination during test, in accordance with previous literature [141].

CHAPTER V-EXPERIMENTAL RESULTS AND DISCUSSION:

CHARACTERIZATION ON NEW POLYPROPYLENE-BASED HYBRID SYSTEMS

In this section, an attempt to further enhance the thermal conductivity of the nanocomposites containing carbon nanotubes, is tried. At this regard, hybrid systems are considered combining carbon nanotubes and another particle, together in polypropylene, in order to improve the number of heat transfer efficiency. So, this section reports on "binary" compounds based on not functionalized carbon nanotubes (MWNTs) and "ternary" or "hybrid" systems involving also a "secondary" or "additional" filler as ZnO, Talc, $CaCO_3$ and BN.

5.1 Thermal conductivity measurements on hybrid systems

Fig.5.1 compares thermal conductivity values of binary systems, containing up to 2.5% in vol. of CNTs, and ternary formulations, containing 1.5%vol. of CNTs and 10% in vol. of a secondary filler. For all investigated materials, thermal conductivity improvements, with respect to the hosting matrix, are reported in Tab.5.1.

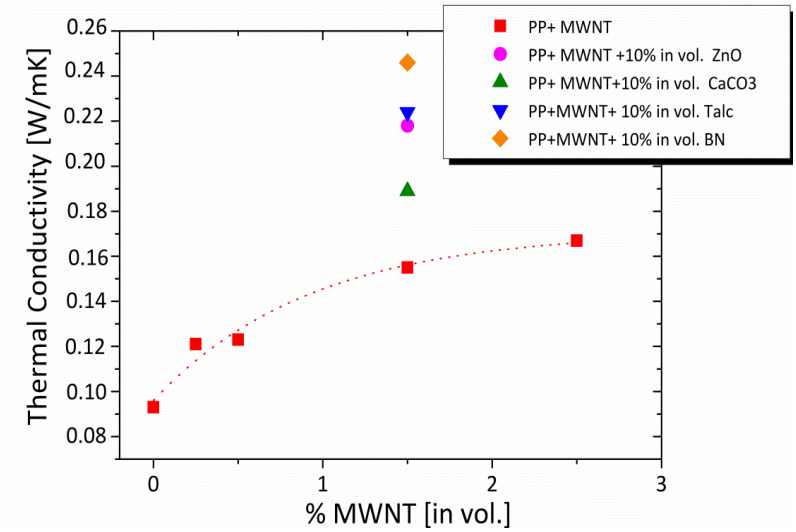

Fig. 5.1- Thermal conductivity of composites containing hybrid fillers.

Materials	Increase(%)
Processed Matrix (PP)	/
PP+1.5% MWNT	72%
PP+2.5% MWNT	79%
PP+1.5% MWNT+10% CaCO3	103%
PP+1.5% MWNT+10% ZnO	134%
PP+1.5% MWNT +10% Talc	141%
PP+1.5% MWNT+10% BN	165%

Tab. 5.1- Percentage increase in thermal conductivity obtained for hybrid composites at the same filler content.

For binary systems containing 1.5% in vol. of carbon nanotubes an increase in thermal conductivity, respect to neat matrix, approximately equal to 72%, is recorded. In presence of the secondary filler, the enhancement in thermal conductivity becomes remarkable even when compared to another binary system containing a higher amount of MWNT (2.5% in vol.).

From these results, the best hybrid solution, in term of thermal conduction, seems to be the combination of boron nitride (BN) and carbon nanotubes

(MWNT), allowing enhancements up to 165%. Thermal conductivity of systems containing zinc oxide, as secondary filler, is approximately equal to ternary formulations containing Talc. Instead, in the case of combined MWNT/$CaCO_3$, low benefits seems to be achieved.

5.2 Morphological observations by EDS/SEM analysis

Morphological observations with the help of the elemental EDS analysis tool provide information about mutual distribution of the two fillers in ternary formulations. For systems containing BN and MWNT, apparently, a good dispersion of both fillers is achieved with quite isolate or small aggregates of CNTs between platelets of BN (Fig. 5.2.a). Also in the case of composites containing ZnO and CNTs, an homogeneous distribution of both fillers seems to be verified (Fig. 5.2.b). EDS/SEM analysis, for systems containing Talc and MWNT (Fig. 5.2.c), allows to identify the presence of talc lamellas in sample and shows an apparently good dispersion of both fillers in matrix. In fact MWNTs seems to be quite isolate, while Talc appears probably exfoliate so to imply a possible interaction between two different fillers. On the contrary, for hybrid systems containing $CaCO_3$ (Fig. 5.2.d), a poor mutual dispersion is already observed with carbon nanotubes agglomerates separated sharply from $CaCO_3$ particles.

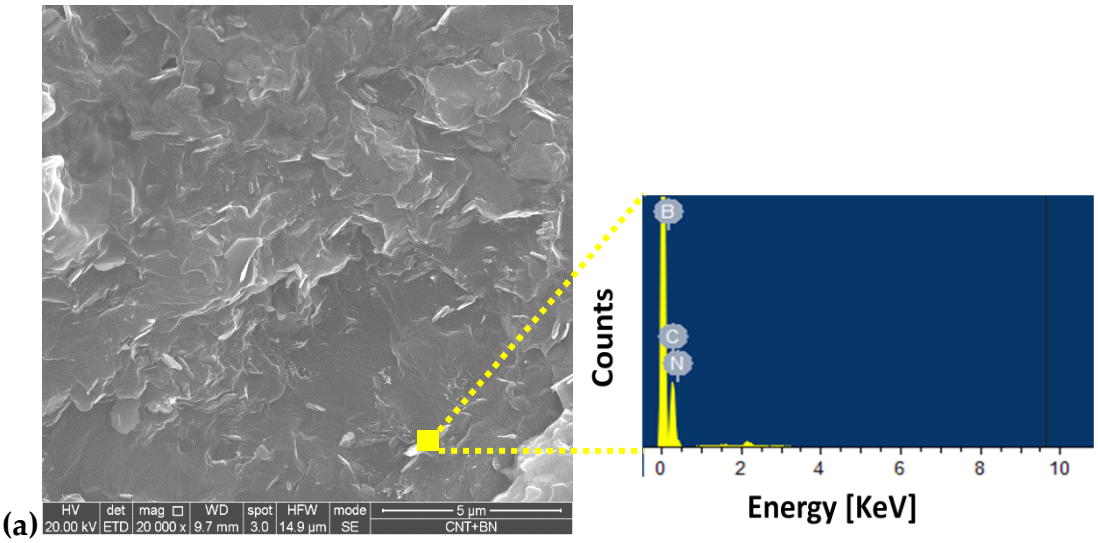
HV 20.00 kV
det ETD
mag 20 000 x
WD 9.7 mm
spot 3.0
HFW 14.9 µm
mode SE
5 µm
CNT+BN
B
C
N
Counts
0
2
4
6
8
10
Energy [KeV]

(a)

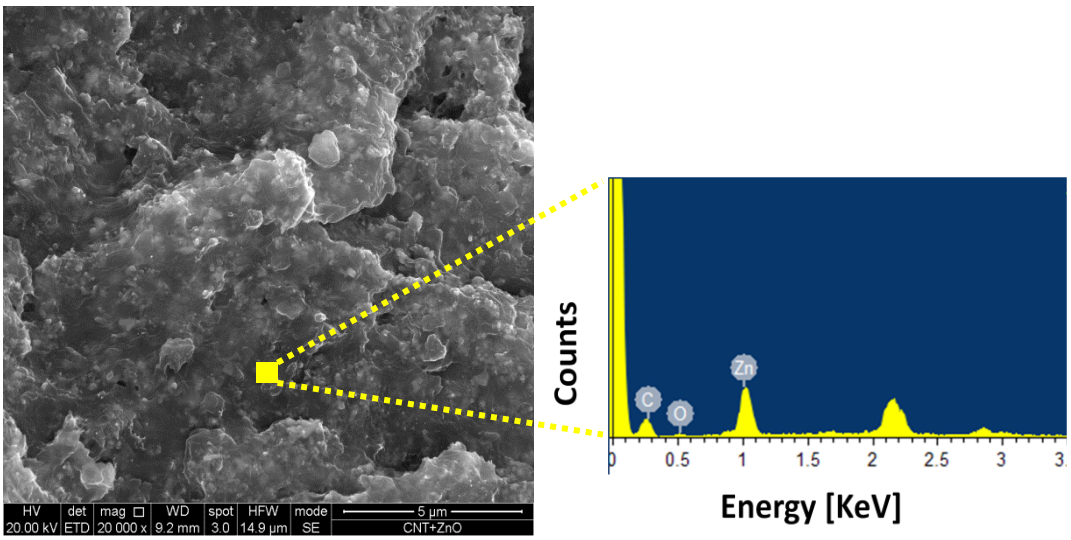
HV 20.00 kV
det ETD
mag 20 000 x
WD 9.2 mm
spot 3.0
HFW 14.9 µm
mode SE
5 µm
CNT+ZnO
Zn
C
O
Counts
0.5
1
1.5
2
2.5
3
Energy [KeV]

(b)

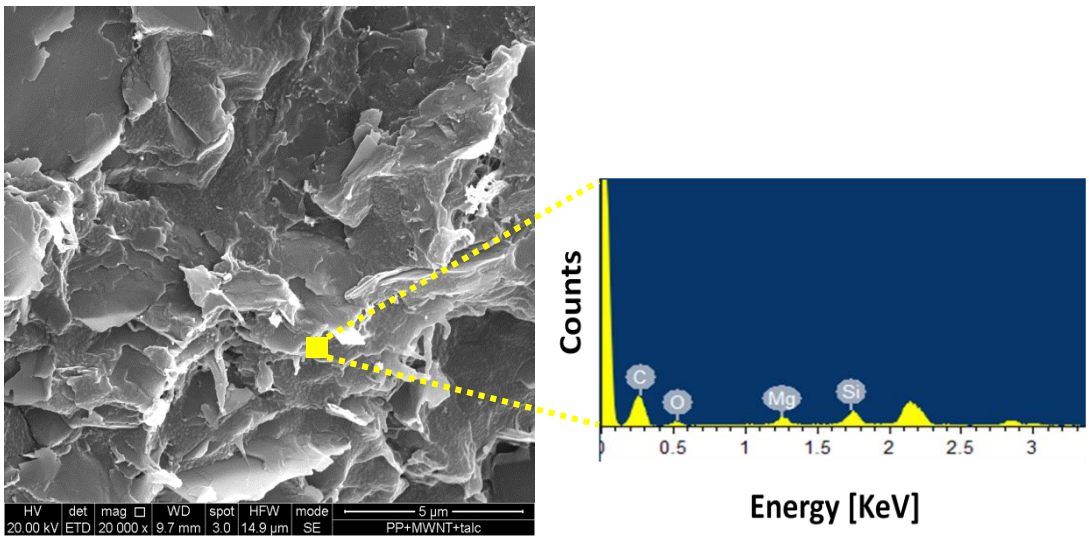
HV 20.00 kV
det ETD
mag 20 000 x
WD 9.7 mm
spot 3.0
HFW 14.9 µm
mode SE
5 µm
PP+MWNT+talc
C
O
Mg
Si
Counts
0.5
1
1.5
2
2.5
3
Energy [KeV]

(c)

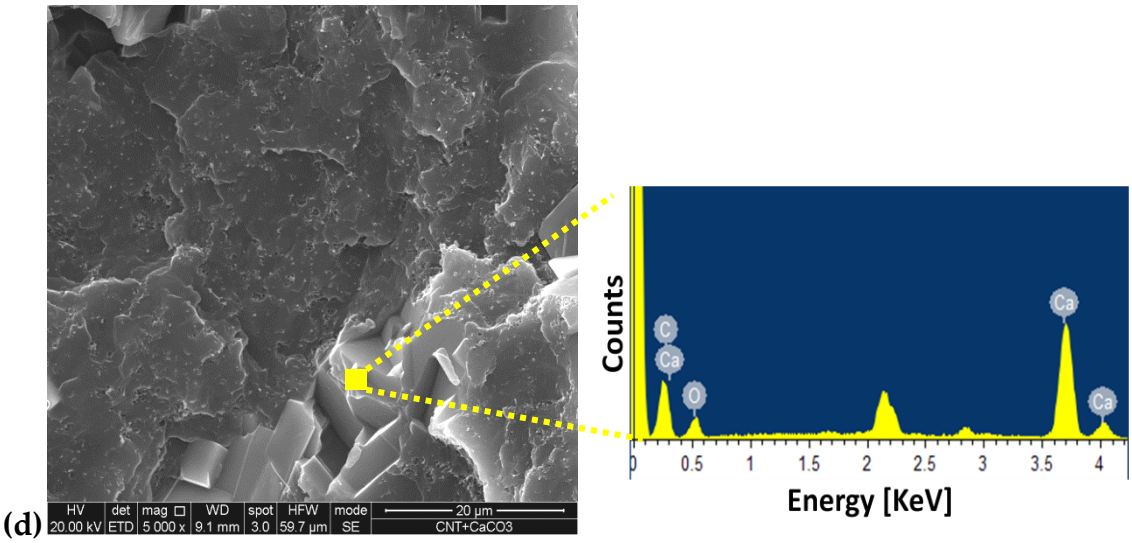

Fig. 5.2-SEM micrographs and relative EDS spectrum of hybrid systems: (a) PP/MWNT/BN; (b) PP/MWNT/ZnO; (c) PP/MWNT/Talc; (d) PP/MWNT/$CaCO_3$.

5.3 Thermogravimetric analysis on hybrid systems

Fig. 5.3 compares weight loss curves for all prepared hybrid systems while, in Tab. 5.2 their initial decomposition temperatures are indicated.

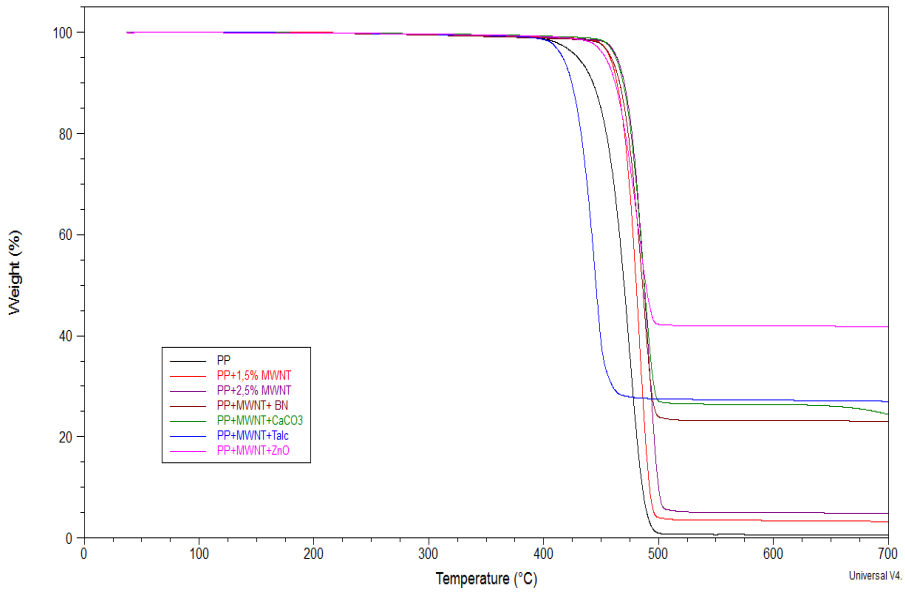

Fig. 5.3-Weight loss curves for investigated hybrid systems.

Materials	T_d at 5% weight loss (°C)
Extruded PP	420
PP+1.5 vol% MWNT	458
PP+2.5 vol% MWNT	464
PP+1.5 vol% MWNT+10% vol BN	459
PP+1.5 vol% MWNT+10% vol Talc	417
PP+1.5 vol% MWNT+10% vol CaCO3	463
PP+1.5 vol% MWNT+10% vol ZnO	464

Tab. 5.2-Initial decomposition temperature of investigated materials.

Clearly, the inclusion of particles increases the thermal stability of the matrix with exception of the case in which talc is used as the secondary filler. This effect could be just attributed to the mutual filler distribution. In fact, it is reported that clays have two opposites effects on the thermal stability of polymer nanocomposites: a barrier effect, which should improve the thermal stability, and a promoter effect, which would encourage the degradation process and decrease the thermal stability. While the first mechanism is predominant in the case of lower filler content and well dispersed, intercalated or exfoliated structures; by increasing the filler loading, the promoter effect becomes impressible [142].

5.4 Differential scanning calorimetric analysis on hybrid systems

Tab. 5.3. summarizes thermal parameters evaluated by calorimetric analysis of all investigated materials.

Results show that the addition of carbon nanotubes to matrix, alone or in combination with a secondary filler, do not significantly affect neither crystallization nor melting parameters. In fact, while melt temperature remains

almost equal to 168°C, the degree of crystallinity is approximately near 40%. These considerations allow to assess that, also of investigated hybrid systems, detected improvements in thermal conductivity could not be attributed to changes of matrix crystallinity.

Materials	First Heating			Cooling		Second Heating		
	T_m [°C]	ΔH_f^1 [J/g]	x_c^1	T_m [°C]	[J/g]	T_m [°C]	ΔH_f^2 [J/g]	x_c^2
PP	169	84.5	40 %	126	90.0	166	86.2	41 %
PP+1,5% MWNT	167	75,7	37 %	125	82,9	167	82,9	41 %
PP+2,5% MWNT	166	77,2	39 %	125	81,2	166	77,6	39 %
PP+1,5% MWNT+10% ZnO	168	46.8	39 %	126	49.4	168	62.1	40 %
PP+1,5% MWNT+10% CaCO3	169	59.2	39 %	127	65.8	169	61.9	41 %
PP+1,5% MWNT+10% Talc	168	59.7	40 %	123	67.2	168	62.2	41 %
PP+1,5% MWNT+10% BN	169	63.1	40 %	125	66.2	169	47.9	39 %
Avarage	**168.0**		**39.1**	**125.3**		**167.6**		**40.3**%
Dev.std.	**1.2**		**1.1**	**1.3**		**1.3**		**1.0**

Tab. 5.3 - Crystallization temperature (Tc), crystallization entalphy (ΔH_c), melting temperature (Tm), melting entalphy (ΔH_f), degree of crystallinity (Xc) of polypropylene based nanocomposites.

5.5 Torque measurements during mixing

In Fig. 5.4, curves of torque as a function of the processing time, recorded during the preparation of hybrid composites, are shown. For comparison, torque curves related to PP matrix and to binary systems, containing 1.5% and 2.5% in vol. of MWNT, are also reported. The trend of curves is qualitatively the same for each studied compound and reflects the operation mode. In particular, when the matrix is fed alone in the mixer chamber, the torque value reaches a peak and then decreases in correspondence of its melting temperature. After 2 min, fillers are added and, correspondingly, an increase in the torque value is recorded again. By changing fillers, not considerable discrepancies, between torque trends and values, are evident among compounds, suggesting a similar processing behavior.

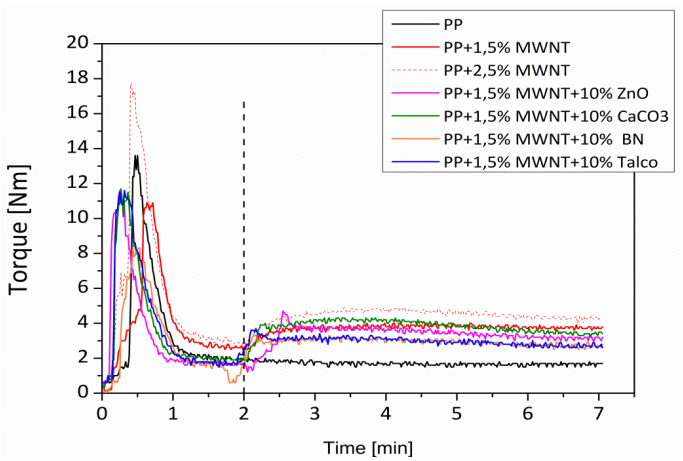

Fig. 5.4-Torque measurements during composites preparation.

The curves of torque have permitted the evaluation of the total mechanical energy (TME), as defined in Cap.II (see in Fig. 5.5). This parameter, being a direct function of the torque, can be assumed as a further indication of the actual processability of investigated materials. As expected, there is an evident increase of total mechanical energy of binary materials, by increasing the nanotube content. Anyway it is interesting to note that, with the inclusion of second fillers at the basic formulation containing 1.5% vol. of MWNT, the same parameter remains almost equal to the one detected for binary systems (PP+MWNT).

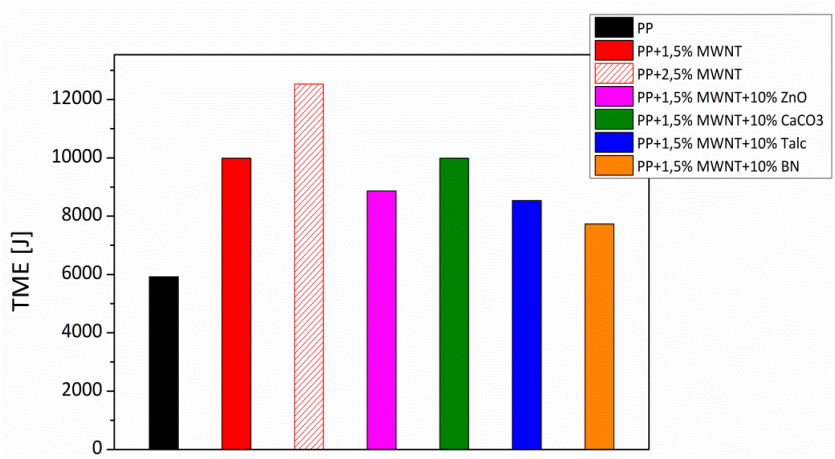

Fig. 5.5- Total mechanical energy for investigated compounds.

5.6 Rheological measurements on hybrid materials

5.6.1 Viscoelastic behavior of hybrid systems

The viscoelastic behavior of all hybrid systems is reported in Fig. 5.6, in terms of storage modulus as a function of the angular frequency, taking the neat PP processed under the same conditions, and binary formulations at 1.5% and 2.5% in vol. of CNTs, as reference materials.

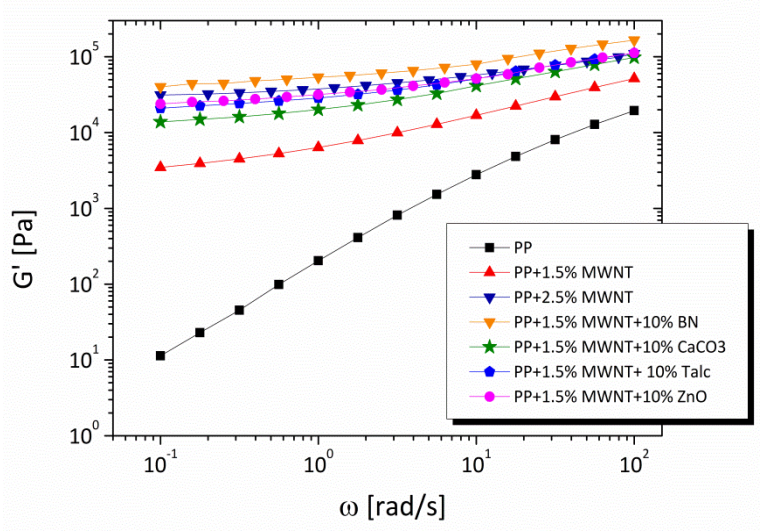

Fig. 5.6- Storage moduli in function of angular frequency for hybrids materials.

In details, at low frequencies, all composites show a solid-like behavior with storage modulus almost frequency-independent. This behavior is related to the formation of interconnected structures, due to filler-filler and filler-matrix interactions, characterized by a slow relaxation dynamics. At high frequencies, curves tend to collapse and converge on pure PP behavior, thus showing a negligible contribution of the filler to relaxation dynamics. These features are confirmed by dissipation factor (Tan delta) curves.

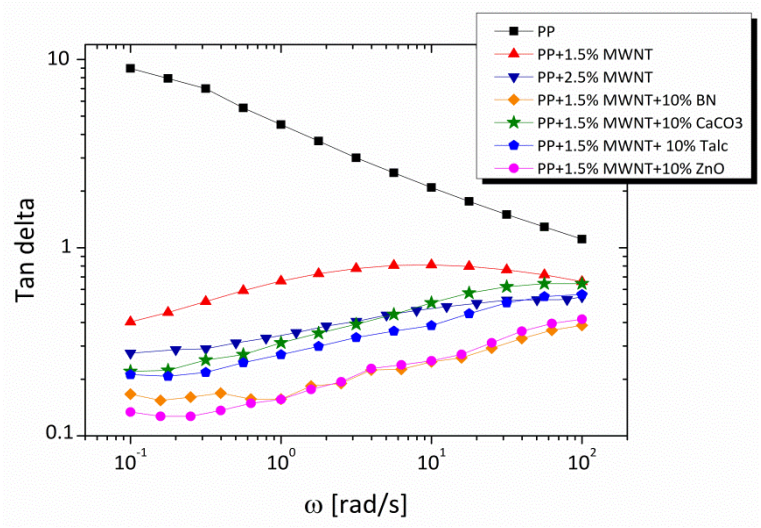

Fig.5. 7 -Dissipation factor in function of angular frequency for investigated composites.

5.6.2 Role of carbon nanotubes in ternary formulations.

In order to investigate how carbon nanotubes affect the melt behavior of compounds when combined with another filler, a comparison between storage moduli of ternary (PP/MWNT/secondary filler) and binary systems (PP/secondary filler), is given in Fig. 5.8.

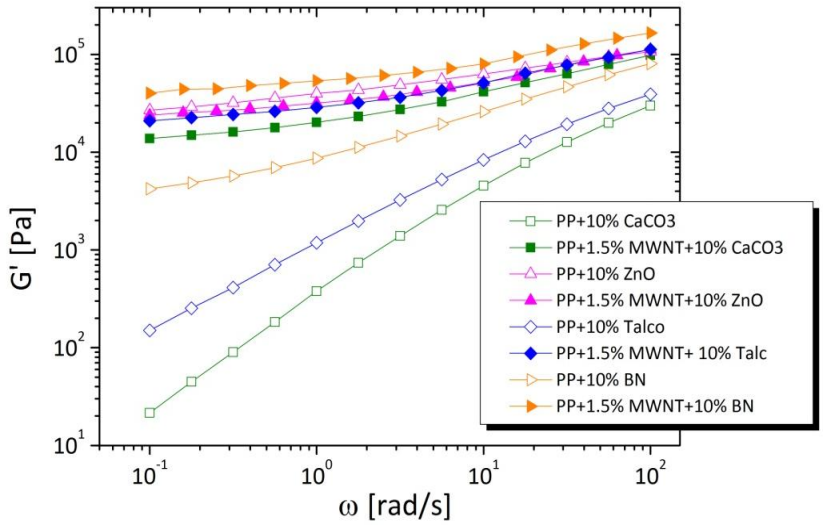

Fig. 5.8-Comparison between storage modulus, at a temperature of 190°C, of hybrid compounds, containing CNTs and additional filler, and those with *as-defined* additional fillers alone.

From this picture, it is clear that the inclusion of carbon nanotubes significantly changes melt behavior of binary systems in different way, depending on type and dimension of additional particles.

In details, at a frequency of 0.1 rad/s, storage modulus of binary systems containing $CaCO_3$ (< 30 μm), approximately equal to 20 Pa, is drastically improved by the inclusion of MWNT, becoming in the range of 10^4 Pa. Limited increases, but however remarkable, are recorded by decreasing the size of secondary fillers. In fact, in the case of BN (< 1 μm) and Talc (< 10 μm), respectively, the storage modulus of PP/secondary particles compounds is lower one or two order of magnitude, respectively, than the one detected for relative ternary formulations. No substantial variation can be observed in the case of ZnO (< 100 nm).

This behavior has been interpreted assuming that the inclusion of small nanofillers (MWNT) in microcomposite systems, promotes a number of interactions increasing with the difference in size between the different particles included.

Another possible way to analyze interactions between the two combined particles, is to check thermally viscoelastic behavior changes in PP-based materials. In fact, blending a polymer with carbon nanotubes, three networks can be expected: (i) the temporary polymer network formed by entanglements, (ii) a filler-filler network and (iii) a combined filler-polymer network. Differences in rheological properties, at different temperatures, can be explained by simple mixing laws between the entangled polymer network, whose properties shift considerably with temperature, and the filler–polymer network. It can be assumed that the mobility and characteristic structure of the chains, as well as the shortest distances among tubes are temperature dependent [134].

At this regard, rheological data are collected at two different temperatures, 170 and 230°C, respectively, on binary systems (PP/secondary particles) and their relative ternary formulations (PP/MWNT/secondary particles). Results are reported in Fig. 5.9 in terms of dissipation factors, measured at 170 and 230°C, in function of the angular frequency.

Dissipation factor results to be almost frequency independent for all hybrid materials. Therefore, it can be concluded that percolation is achieved everywhere.

About temperature effect, it is evident that for ternary formulations containing Talc or $CaCO_3$, tan delta curves at the two temperatures, roughly overlap; slight differences appear instead for ternary compounds involving BN or ZnO particles.

In conclusion, in hybrid systems, containing Talc or $CaCO_3$, dominant interactions are mainly between fillers, forming a network in a percolated structure. In the case of smaller secondary particles, as ZnO or BN, connections involve also matrix; consequently, it can be imagined that the percolated microstructure is constituted by entangled polymer-filler network.

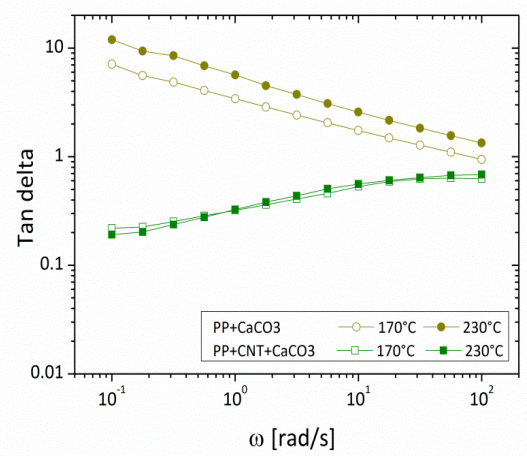

(a)

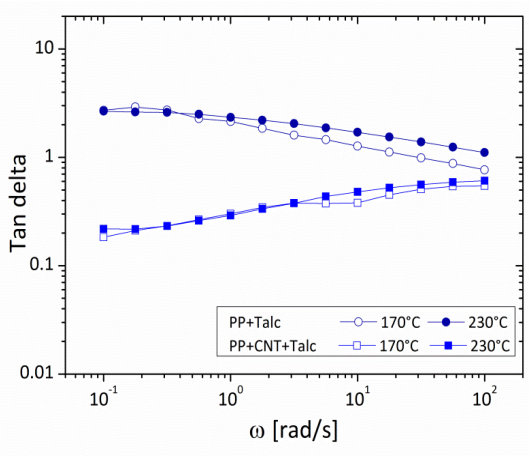

(b)

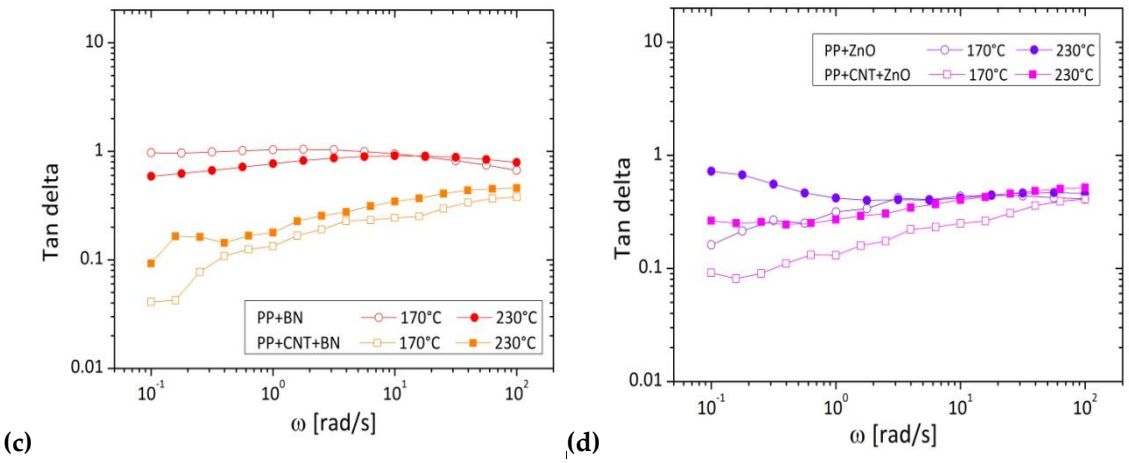

Fig. 5.9-Comparison between dissipation factors of hybrid materials and their respective binary systems without MWNT, at a temperature of 170 and 230°C, for different particles:(a) $CaCO_3$; (b) Talc; (c) BN; (d) ZnO.

5.6.3 Comparison between complex and shear viscosity

Finally, Fig 5.10 shows a comparison between rheological measurements both in steady-state and dynamic mode in terms of real and complex viscosity, for all prepared materials.

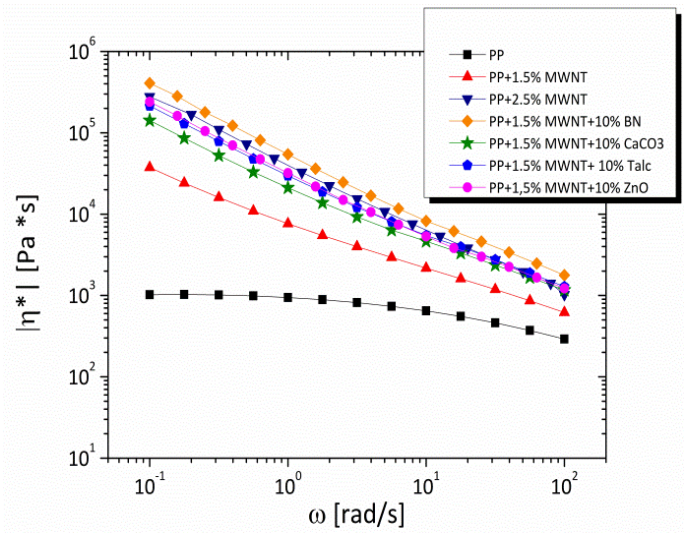

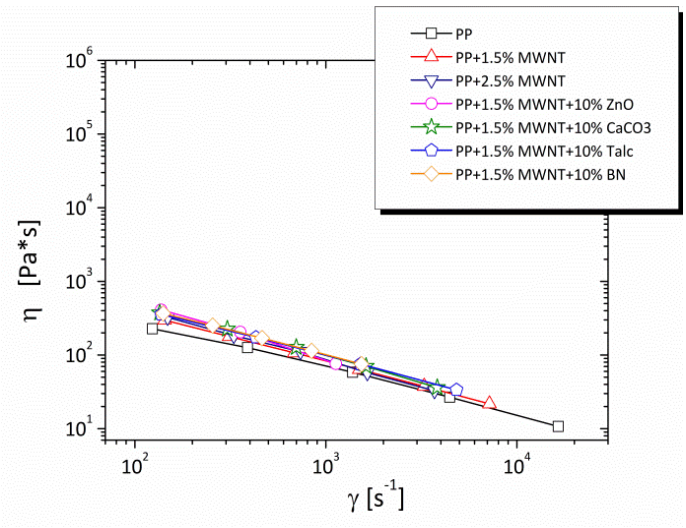

(b)

Fig. 5.10-Comparison between complex (a) and shear (b) viscosity

Concerning complex viscosity data (Fig. 5.10.a), while PP matrix exhibits a pseudo-Newtonian behavior in almost the whole detected range of angular frequency; for composite samples, the Newtonian plateau disappears and a higher complex viscosity values with a more pronounced shear thinning behavior is shown. It is obvious that the differences between rheological properties of composites are strongly affected by features of the percolated filler–filler network structures, in term of morphologies mainly governed by mutual fillers dispersion in polymer matrix [143].

On the contrary, Fig.5.10.b shows that the shear viscosity of all investigated compounds decreases almost linearly by increasing the shear rate. Yet, viscosity differences between composites and pure PP, at the high shear region, becomes small.

In general, the steady shear viscosity trend gives information about the processing of a material and it can be is estimated from complex viscosity value using the Cox-Merz rule [144]. This law states that the complex viscosity (η^*) is equal to the steady-shear viscosity (η) when the oscillatory frequency (ω) corresponds the shear rate ($\dot{\gamma}$) :

$$\eta^*(\omega) = \eta(\dot{\gamma}) \quad 5.1)$$

A material that follows this law will have the frequency at which the terminal region is reached in oscillatory measurements, identical to the shear rate at which the Newtonian region is reached in steady shear measurements. Although not universally obeyed, this law generally holds if steady shear does not change the structure of the investigated material [144], and consequently it fails for complex systems like composites [135].

Thus, expectedly, in our case, Cox-Merz relationship holds only for the neat polypropylene resin, for which, at an angular frequency of 100 rad/s, the complex viscosity value equal to 20 Pa*s, is approximately the same of PP shear viscosity at 100 s^{-1}.

Concluding, it is clear that even if dynamic results show considerable discrepancies between complex viscosity data of different samples, at typical process shear rates, their real viscosity appear quite similar. In conclusion, included fillers, at least in the range of contents analyzed so far, do not significantly affect the processability of the polypropylene matrix.

5.7 Electrical conductivity measurements for hybrid compounds.

Fig. 5.11 shows a comparison among electrical resistivity values of different compounds: hybrid formulations, bynary systems and neat processed matrix.

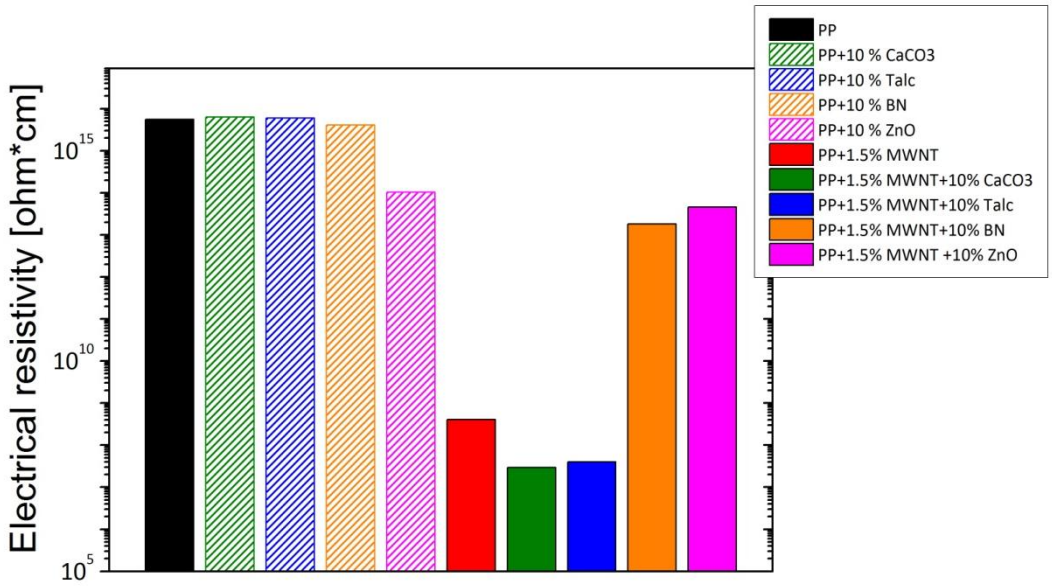

Fig. 5.11- Electrical resistivity measurements of binary and ternary composites.

These results display an electrical resistivity value for polypropylene matrix in the order of magnitude around 10^{15} ohm*cm, confirming expected properties of an insulator material.

The inclusion in matrix, exclusively, of secondary inert particles does not alter significantly the electrical resistivity, except in the case of ZnO, for which a lower value is recorded in the order of 10^{14} ohm*cm . On the contrary, when carbon nanotubes are added alone, the composite behavior drastically changes, assuming features of a conductor system with an electrical resistivity near to 10^{7} ohm*cm.

Different aspects can be highlighted for hybrid formulations. In details, the combination of $CaCO_3$/MWNT or Talc/MWNT, namely micrometric secondary particles, gives composites with electrical conductive features, i.e. an electrical resistivity equal to that recorded for binary systems containing only carbon

nanotubes. Instead, combining ZnO/MWNT or BN/MWNT, i.e. submicron secondary particles, insulator composites are realized with an electrical resistivity similar to that of matrix .

In conclusion, depending on secondary filler type and dimension, the mutual distribution, between included different particles in hybrid materials, favors or hinders the electrical conduction network, promoted by carbon nanotubes, modifying completely their features.

In the following picture (Fig. 5.12), dissipation factors of all investigated materials are reported as a function of frequency.

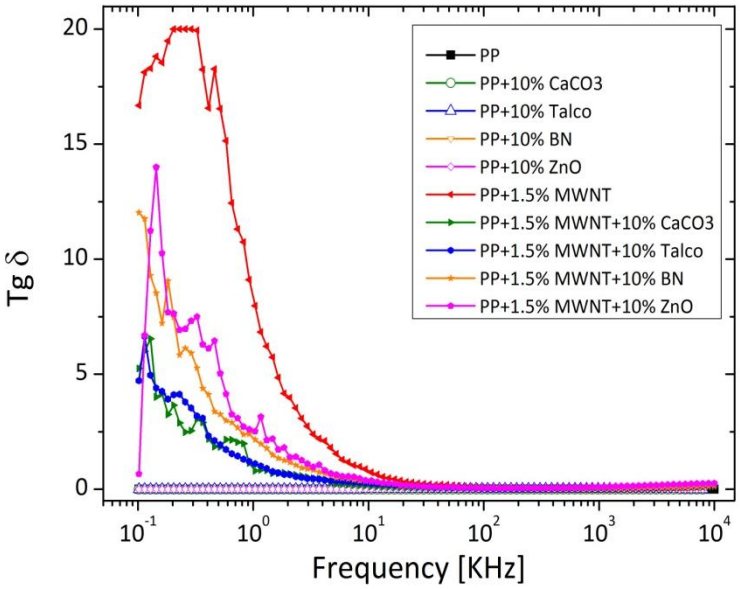

Fig. 5.12- Comparison among dissipation factors of binary and ternary formulations.

In general, the dissipation factor is the sum of different dielectric losses, attributed to conduction and/or hysteresis phenomena, which occur in a certain range of frequencies. In our case, both neat PP and binary systems, containing only secondary particles, show a dissipation factors almost frequency independent, clearly highlighting the lack of losses. Instead, in the case of PP/MWNT nanocomposites and hybrid formulations, over the frequency range

of 10^{-1}-10 kHz, a non monotonous trend of Tg δ is displayed, with a maximum particularly pronounced for PP/MWNT. Since conduction losses decrease as 1/ω; their contribution is neglected and Tg δ trends can be attributed to hysteresis phenomena, that seem to decrease by increasing the size of secondary particles, as the following sequence:

MWNT/CaCO3 < MWNT/Talco < MWNT/BN < MWNT/ZnO

Tg δ peak is found in the same frequencies range, at which a polarization mechanism gradually fades.

According to the Maxwell-Wagner model, this behavior is present also in the case of interfacial polarization, typical in composites. In this latter case, a remarkable increase of relative dielectric constant with respect to hosting matrix is recorded, as confirmed by a comparison between binary and ternary compounds reported in Fig. 5.13.

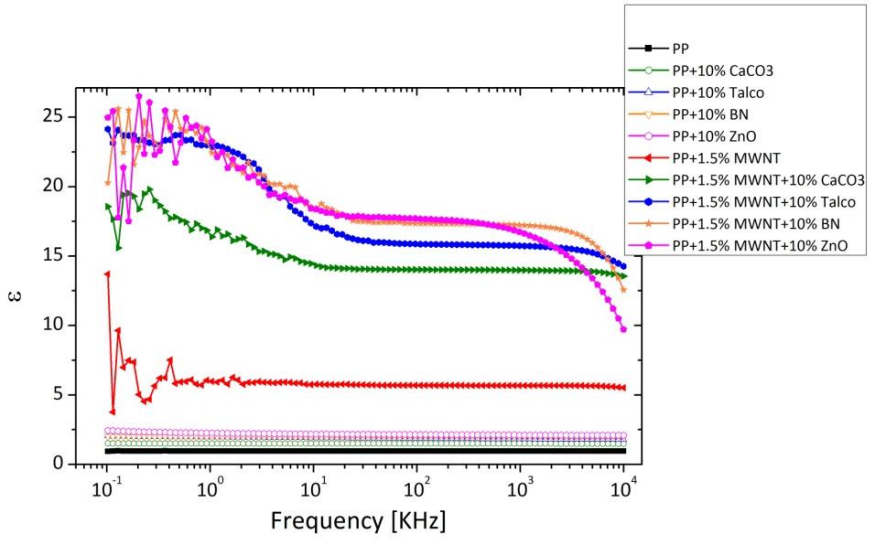

Fig. 5.13- Comparison between permittivity (ε) of binary and ternary systems.

In general, the permittivity, as the dissipation factor, is the result of different polarizations (dipolar, interfacial, atomic), identified in a specific frequencies range. In order to verify interfacial effects, our attention is paid on interfacial

polarization, restricted in the frequency range from 0.5 to 10 KHz and attributed to accumulation and orientation of electric dipoles along direction of the applied field, essentially near filler-polymer and filler-filler interphases. In the examined case, no polarization is verified, both for neat PP and for PP/secondary particles composites, being their permittivity always constant. In the case of PP/MWNT nanocomposites, the permittivity increases up to 5 and becomes higher with the addition of secondary filler, following again the same trend:

MWNT/CaCO3 < MWNT/Talco < MWNT/BN < MWNT/ZnO

This consideration can be assumed as an indication of the mutual distribution of two combined fillers in the resin. In fact, the introduction of another particle, besides carbon nanotubes, can lead to an increase of interfaces, inversely proportional to the state of their agglomeration in the composite. In fact, the filler's tendency to the agglomeration decreases the points of accumulation and orientation of dipoles with consequent reduction of the relative permittivity.

CONCLUSION

In this work, thermally conductive plastics are prepared by melt-blending, trough the inclusion of multi-walled carbon nanotubes (MWNT) in a commercial polypropylene resin (PP). Nanocomposites are prevalently characterized by thermal conductivity measurements and dispersion analysis (TEM, SEM, rheological test, OP, THz) but flexural and electrical characterization techniques are also considered to confirm the achieved actual filler dispersion and to gain more insights about the potentials of produced systems.

The effect of different variables as processing conditions, melt flow rate of the matrix, filler drying, addition of a compatibilizer, test temperature and surface functionalization (presence of amino or carboxyl groups) of included carbon nanotubes on thermal transport behavior of final products is analyzed.

About the mixing parameters, temperature of 190°C, rotational speed of 60 rpm, mixing time of 7 min are identified as optimized values for the preparation of selected materials. Thermal conductivity values of compounds, obtained by changing compression molding conditions, seem to be not affected by pressure

and dwell time but slightly influenced by the processing temperature. Significant improvements of the thermal conductivity are recorded by adopting a commercial polypropylene grade with a higher MFI. Probably, the high fluidity of the matrix may facilitate the polymer infiltration and consequently, the disintegration of CNTs primary agglomerates. Instead, lower performance are shown in presence of a compatibilizer agent and/or dried fillers.

Thermal conductivity data of all investigated nanosystems show a non linear trend with the filler content and could be well-fitted by a cubic polynomial equation. In details, three different regions are identified depending on filler concentration: for loadings up to 1.5% in vol., an increase of thermal conductivity is always detected with a more pronounced effect for amino-functionalized carbon nanotubes. Then, in the range of 1.5-3.7% in vol. of filler loadings, the thermal conductivity of systems including not functionalized carbon nanotubes (MWNT) remains almost constant, while a sharp reduction is recorded in presence of functionalized ones. Finally, an upward trend is shown for percentages in vol. up to 3.7% in vol. This trend is interpreted in terms of an average distance between agglomerates (AID), invoked in analogy to the well-known geometrical parameter "*average interparticle distance*" (AID). It can be reasonably assumed that this parameter is influenced by two competitive phenomena, occurring during the nanocomposites preparation: dispersion and re-agglomeration. In fact, these latter, being controlled by different parameters as melt viscosity, intrinsic features of CNTs primary agglomerates and their respective content, affect the filler distribution in a polymer, as well agglomerates sizes and the relative distance between them.

Rotational rheological response and morphological studies by TEM, on these developed materials, reveal that contrary to MWNT and MWNT-NH_2, MWNT-COOHs lead to systems with higher difficulties to form interconnected structures.

Further thermal analyses, by differential scanning calorimetric (DSC), highlight that carbon nanotubes do not significantly alter neither thermal parameters, related to melting and crystallization phenomena, nor the degree of crystallinity of the matrix.

A comparison, in terms of flexural features, of PP/MWNT-NH_2 and PP/MWNT nanocomposites, shows a non monotonous trend of elastic modulus and strength in function of the filler loading, with a maximum benefit in correspondence of 0.5% in vol. of CNTs content, especially in presence of surface functionalized nanotubes. This behavior is attributed to agglomeration phenomena, favoured by increasing the filler loading (as confirmed by SEM analysis), that reduce polymer/CNTs interfaces.

The actual state of the filler dispersion is quantitatively investigated by optical microscopy, on all investigated nanocomposites loaded with 0.5% in vol. of carbon nanotubes. Results highlight a worst dispersion index (~ 60%) in presence of not functionalized carbon nanotubes (MWNT), for which the highest number of aggregates is found. In the case of functionalized carbon nanotubes, instead, the dispersion index increases up to 86% and the smallest aggregates size is related to amino-functionalized carbon nanotubes (MWNT-NH_2).

In order to further analyze the level of filler dispersion achieved for each family of compounds, the use of the THz spectroscopy is also considered. Indeed, this latter seems an effective technique to evaluate sample homogeneity. Specific parameter, as refraction index (n) and adsorption coefficient (α) are correlated to experimental data, obtained by optical microscopy. Samples characterized by a higher number of aggregates of bigger dimensions, display also higher n and α values.

Moreover, melt-compounded hybrid composites involving not functionalized carbon nanotubes (MWNT) and another particle with different shape and sizes

as boron nitride (BN), zinc oxide (ZnO), calcium carbonate ($CaCO_3$) and talc, respectively, are also considered. An improvement of the thermal conductivity is always measured, especially for MWNT/BN hybrids (+165% with respect to the neat matrix). Capillary rheological tests and torque trends during mixing, reveal that the processability of hybrid compounds, in term of shear viscosity and total mechanical energy (TME), remains almost equal with respect to the neat matrix. Rotational rheological measurements show the formation of interconnected structures, realized essentially by filler-filler interaction in MWNT/talc and MWNT/$CaCO_3$ hybrid systems (i.e. micrometric secondary particles) or by also filler-polymer interactions in the case of MWNT/ZnO or MWNT/BN (i.e. submicronic secondary particles) hybrids.

Finally, electrical measurements confirm that the behavior of hybrid materials is completely different depending on type and dimension of secondary inert particles. In details, the introduction of micrometric secondary particles (talc or $CaCO_3$), does not alter electrical conductor features of PP/MWNT composites. On the contrary, submicronic particles (BN or ZnO), probably due to an efficient mutual dispersion with MWNTs, confirmed by a higher interfacial polarization, hinder electrical conductive pathways of carbon nanotubes and the material becomes an insulator.

Concluding, original contributions of this work can be summarized as following:

- polypropylene-based nanocomposites, useful for automotive applications, with enhanced thermal conductivity, are realized by melt blending in optimized conditions for heat transport;
- a cubic polynomial fitting of thermal conductivity data as a function of filler loadings is proposed, taking into account concomitant dispersion-agglomeration phenomena.

- the possibility of non-destructive technique (THz spectroscopy) to evaluate filler dispersion, is verified;
- insulator features can be achieved in thermally conductive compounds (PP/CNTs), by adding inert submicronic particles, without compromising the final processability of materials.

REFERENCES

[1] Ebadi-Dehaghani H., Branch S., Reiszadeh M , Chavoshi A., Nazempour M. ,Vakili M. H. *"The Effect of Zinc Oxide and Calcium Carbonate Nanoparticles on the Thermal Conductivity of Polypropylene"* Journal of Macromolecular Science Part B 53, 93-107, 2014.

[2] Weidenfeller B., Hofer M., Schilling F.R.*"Thermal conductivity, thermal diffusivity, and specific heat capacity of particle filled polypropylene*" Composites Part A Applied Science and Manufacturing 35, 423-429, 2004.

[3] Cheewawuttipong W., Fuoka D., Tanoue S., Uematsu H., Iemoto Y."*Thermal and Mechanical Properties of Polypropylene/Boron Nitride Composites"* Energy Procedia 34, 808-817, 2013.

[4] Zhang L. M., Dai G. C. *"Effect of interfacial treatment on the thermal properties of thermal conductive plastics"* eXPRESS Polymer Letters 1, 608-615, 2007.

[5] Huang X., Jiang P. ; Tanaka T. "*A review of dielectric polymer composites with high thermal conductivity"* IEEE Electrical Insulation Magazine 27, 8-16, 2011.

[6] Bhardwaj B.P. "*The Complete Book on production of Automobile Components of Allied Products*", 536 pp., 2004.

[7] Szeteiovà K. " *Automotive Materials plastics in automotive markets*"- Institute of Production Technologies, Machine Technologies and Materials, Faculty of Material and Technology in Trnava, Slovak University of Technology Bratislava. Hal : 27-33.

[8] Commission on Engineering and Technical Systems, Committee on Materials for High-Density Electronic Packaging, National Research Council, Division on Engineering and Physical Sciences, National Materials Advisory Board "*Materials for high-density electronic packaging and interconnection*", National Academies , 156 pp., 1990 .

[9] Zweben C. "*High performance thermal management materials*" Electronic Cooling 5, 36-42, 1999.

[10] Mortensen A. "Concise Encyclopaedia of Composite Material" Elsevier, 1050 pp., 2006.

[11] T'Joena C., Park Y., Wang Q., Sommers A., Hanc X., Jacobi A. "*A review on polymer heat exchangers for HVAC&R applications*" International Journal of refrigeration 32, 763-779, 2009.

[12] Seymour R.B. "*Conductive Polymers*" Springer Science & Business Media, 237 pp., 2012

[13] King J.A.; Tucker K.W.; Vogt B.D.; Weber E.H. & Quan C. "*Electrically and thermally conductive nylon 6,6"* Polymer Composites, 20, 643-654, 1999.

[14] Hu M.; Yu D. & Wei J. " *Thermal conductivity determination of small polymer samples by differential scanning calorimetry*" Polymer Testing 26, 333-337, 2007.

[15] Speight J.G. "*Lange's handbook of chemistry"* (16th ed.) McGraw-Hill, New York, 2794 pp., 2005.

[16] Gupta R. K., Kennel E., Kim K.-J."*Polymer Nanocomposites Handbook"* CRC Press, 566 pp., 2009.

[17] Hussain F., Hojjati M., Okamoto M., Goiga R.E. "*Review article: Polymer-matrix Nanocomposites, Processing, Manufacturing, and Application: An Overview*" Journal of composite materials 40, 1511-1575, 2006.

[18] Eatemadi A., Daraee H., Karimkhanloo H., Kouhi M., Zarghami N., Akbarzadeh A., Abasi M., Hanifehpour Y. and Joo S.W. "*Carbon nanotubes: properties, synthesis, purification, and medical applications*" Nanoscale Research Letters 9, 2014.

[19] Bauhofer W., Kovacs J.Z. "*A review and analysis of electrical percolation in carbon nanotube polymer composites*" Composites Science and Technology 69, 1486-1498, 2009.

[20] Min-Feng Yu, Oleg Lourie, Mark J. Dyer, Moloni K., Thomas F. Kelly, Rodney S. Ruoff "*Strength and Breaking Mechanism of Multiwalled Carbon Nanotubes Under Tensile Load*" SCIENCE 28, 637-640, 2000.

[21] Andrews R., Weisenberger M.C. "*Carbon nanotube polymer composites*" Current Opinion in Solid State and Materials Science 8, 31-37, 2004.

[22] Han Z., Fina A. "*Thermal conductivity of carbon nanotubes and their polymer nanocomposites: A review"* Progress in Polymer Science 36, 914–944, 2011.

[23] Sathyanarayana S., Hübner C. "*Thermoplastic Nanocomposites with Carbon Nanotubes*" Chapter Structural Nanocomposites Part of the series Engineering Materials 19-60 pp., 2013.

[24] Logakis E., Pollatos E., Pandis Ch., Peoglos V., Zuburtikudis I., Delides C.G., Vatalis A., Gjoka M., Syskakis E., Viras K., Pissis P. "*Structure–property relationships in isotactic polypropylene/multi-walled carbon nanotubes nanocomposites*" Composites Science and Technology 70, 328-335, 2010.

[25] Bikiaris D. "*Microstructure and Properties of Polypropylene/Carbon Nanotube Nanocomposites*" Materials 3, 2884-2946, 2010.

[26] Garzón C., Palza H. "*Electrical behavior of polypropylene composites melt mixed with carbon-based particles: Effect of the kind of particle and annealing process*" Composites Science and Technology 99, 117-123, 2014.

[27] Da Bao H, Guo ZX, Yu J. "*Effect of electrically inert particulate filler on electrical resistivity of polymer/multi-walled carbon nanotube composites"* Polymer, 49, 3826–3831, 2008.

[28] Palza H. , Garzón C., Arias O. "*Modifying the electrical behavior of polypropylene/carbon nanotube composites by adding a second nanoparticle and by annealing processes*" eXPRESS Polymer Letters 6, 639-646, 2012.

[29] Anderson D.R. "*Thermal conductivity of polymers*" Chem. Rev. 66, 677–690, 1966.

[30] Hansen D., Ho C.C. "*Thermal conductivity of high polymers*" Journal of Polymer Science; Part A 3, 659-670, 1965.

[31] Henry A. "*Thermal transport in polymers*" Ann. Rev. Of Heat Transfer 17, 485-520, 2013.

[32] Dashora P., Gupta G. "*On the temperature dependence of the thermal conductivity of linear amorphous polymers*" Polymer 37, 231-234, 1996.

[33] Rodney S. Ruoff , Dong Qian, Wing Kam Liu "*Mechanical properties of carbon nanotubes: theoretical predictions and experimental measurements*" C. R. Physique 4, 993–1008, 2003.

[34] Chunyu Li, Tsu-Wei Chou "*A structural mechanics approach for the analysis of carbon nanotubes*" International Journal of Solids and Structures 40, 2487–2499, 2003.

[35] Lukes J.R., Zhong H. "*Thermal Conductivity of Individual Single-Wall Carbon Nanotubes*" Journal of Heat Transfer 129, 705-712, 2007.

[36] Marconnet A.M.,. Panzer M.A, Goodson K. E. "*Thermal conduction phenomena in carbon nanotubes and related nanostructured materials"* Review of Moder Physics 85, 1295-1327, 2013.

[37] Wang Z., Tang D., Zheng X., Zhang W., Zhu Y. "*Length-dependent thermal conductivity of single-wall carbon nanotubes: prediction and measurements*" Nanotechnology 18, 475714-475758, 2007.

[38] Osman M. A. , Srivastava D**.** "*Temperature dependence of the thermal conductivity of single-wall carbon nanotubes*" Nanotechnology 12**,** 21–24, 2001.

[39] M Grujicic, G Cao, Bonnie Gersten *"Atomic-scale computations of the lattice contribution to thermal conductivity of single-walled carbon nanotubes"* Materials Science and Engineering: B 107, 204–216, 2004.

[40] Zhang W., Zhu Z., Wang F., Wang T., Sun L.,·Wang Z. "*Chirality dependence of the thermal conductivity of carbon nanotubes"* Nanotechnology 15, 936-939, 2004

[41] T.W. Takada T. "*Topological and SP³ defect structures in nanotubes*" Carbon 33, 973–978, 1995.

[42] Che J., Cagin T., Goddard W.A. "*Thermal conductivity of carbon nanotubes*" Nanotechnology 11, 65-69, 2000.

[43] Grandy B.P. "*CARBON NANOTUBE-POLYMER COMPOSITES Manufacture, Properties, and Application*" John Wiley & sons, Inc., Publication, 339 pp., 2011.

[44] Wu F., He X, Zeng Y., Cheng H.M. "*Thermal transport enhancement of multi-walled carbon nanotubes/high-density polyethylene composites*" Appl. Phys. A 85, 25-28, 2006.

[45] Chen X.G., He G.H., Du J.H., Pei S.F., Guo J.F. "*Investigation on the thermal conductivity of HDPE/MWCNT composites by laser pulse method*" Sci.China Ser. E 52, 2767-2772, 2009.

[46] Kim S., Kim J.K., Lee S.H., Park S.J., Kang K.H. *"Thermophysical properties of multiwalled carbon nanotube-reinforced polypropylene composites*" Int. J. Thermophys. 27, 152-160, 2006.

[47] Kashiwagi T., Grulke E., Hilding J., Groth K., Harris R., Butler K., Shields J., Kharchenko S., Douglas J. *"Thermal and flammability properties of polypropylene/carbon nanotube nanotube composites"* Polymer 45, 4227-4239, 2004.

[48] Yang, Y., Gupta M.C., Zalameda J.N. Winfree W.P. "*Dispersion behavior, thermal and electrical conductivities of carbon nanotube-polystyrene nanocomposites* " Micro Nano Letters 3, 35-40, 2008.

[49] Abbasi S., Carreau P.J., Derdouri A., Moan M. "*Rheological properties and percolation in suspension of multiwalled carbon nanotube in polycarbonate*" Rheol. Acta 48, 943-959, 2009.

[50] Cai D.Y., Song M. "*Latex technology as a simple route to improve the thermal conductivity of carbon nanotube/polymer composites*" Carbon 46, 2107-2112, 2008.

[51] Shenogin S., Xue L., Ozisik R., Keblinski P., Cahill D. G."*Role of thermal boundary resistance on the heat flow in carbon-nanotube composites"* J. Appl. Phys. 95, 8136, 2004.

[52] Srivastava G.P "*The Physics of Phonons"* CRC Press, 438 pp.,1990.

[53] Swartz E. T. and Pohl R. O. "*Thermal boundary resistance"* Rev. Mod. Phys. 61, 605, 1989.

[54] Mercader A.G., Castro E.A., Haghi A. K. *"Nanoscience and Computational Chemistry: Research Progress"* CRC Press, 488 pp., 2013.

[55] Lubrecht A. A., Dalmaz G. *"Transient Processes in Tribology:* Proceedings of the 30th Leeds-Lyon Symposium on Tribiology" Elsevier, 892 pp., 2004.

[56] Marconnet A.M., Yamamoto N., Matthew A. Panzer†, Brian L. Wardle, and Goodson E. K. "*Thermal Conduction in Aligned Carbon Nanotube–Polymer Nanocomposites with High Packing Density*" *ACS Nano*, 4818–4825, 2011.

[57] Prasher, R. S., Hu X. J., Chalopin Y., Mingo N., Lofgreen K., Volz S., Cleri F., Keblinski P. *"Turning Carbon Nanotubes from Exceptional Heat Conductors into Insulators"* Phys. Rev. Lett. 102**,** 2009.

[58] Zhong H., Lukes J.R. "*Interfacial thermal resistance between carbon nanotubes: molecular dynamics simulations and analytical thermal modelling*" Physical Review B 74, 125403, 2006.

[59] Alig I., Potschke, Lellinger D., Skipa T., Pegel S., Kasaliwal G.R., Villmow T. "*Establishment, morphology and properties of carbon nanotube networks in polymer melts*" Polymer 53, 4-28, 2012.

[60] Kasaliwal G.R., Pegel S., Göldel A., Pötschke P., Heinrich G., " *Analysis of agglomerate dispersion mechanism of multiwalled carbon nanotubes during melt mixing in polycarbonate*" Polymer 51, 2708-2720, 2010.

[61] Barber A.H., Cohen S.R., Wagner H. D. "*Static and Dynamic Wetting Measurements of Single Carbon Nanotubes"* Phys. Rev. Lett. 92, 186103, 2004.

[62] Kasaliwal G.R., Golden A., Pötschke P., Heinrich G. "*Influences of polymer matrix melt viscosity and molecular weight on MWCNT agglomerate dispersion*" Polymer 52, 1027-1036, 2011.

[63] Socher R., Krause B., Muller M.T., Boldt R., Pötschke P. "*The influence of matrix viscosity on MWCNT dispersion and electrical properties in different thermoplastic nanocomposites*" Polymer 53, 495-504, 2012.

[64] Krause B., Pötschke P., HauBler L. "*Influence of small scale melt mixing conditions on electrical resistivity of carbon nanotube-polyamide composites*" Comp. Sci. Techn. 69, 1505-1515, 2009.

[65] Yang Y., Grulke E.A., Zhang Z.G., Wu G."*Thermal and rheological properties of carbon nanotube-in-oil dispersions"* Journal of Applied Physics 99, 114307-114308, 2006.

[66] Jang B.-K., Sakka Y. *"Dispersion and Shortening of Multi-Walled Carbon Nanotubes by Size Modification"* Materials Transactions 51, 192 -195, 2010.

[67] Kasaliwal G., Göldel A., Pötschke P *"Influence of processing conditions in small-scale melt mixing and compression molding on the resistivity and morphology of polycarbonate–MWNT composites"* Journal of Applied Polymer Science 112, 3494–3509, 2009.

[68] Pegel S., Pötschke P., Petzold G. , Alig I. , Dudkin S.M, Lellinger D. *"Dispersion, agglomeration, and network formation of multiwalled carbon nanotubes in polycarbonate melts"* Polymer 49, 974-984, 2008.

[69] Ma P., Siddiqui N.A., Marom G., Kim J.K. "*Dispersion and functionalization of carbon nanotubes for polymer-based nanocomposites: A review*" Composites: Part A 41, 1345-1367, 2010.

[70] Thakur V. K., Thakur M. K. "*Chemical Functionalization of Carbon Nanomaterials: Chemistry and Applications"* CRC Press, 1101 pp., 2015.

[71] Yup Jeon, Dong Wook Chang, Nanjundan Ashok Kumar and Jong-Beom Baek "*Functionalization of Carbon Nanotubes"* DOI: 10.5772/18396, 2011.

[72] Spitalsky´ Z, Mateˇjka L, SˇloufM, Konyushenko EN,Kovarˇova J, Zemek J, Kotek J. "*Modification of carbon nanotubes and its effect on properties of carbon nanotube/epoxy nanocomposites*." Polym Compos 30, 1378-1387, 2009.

[73] Padgett C.W., Brenner D.W. *"Influence of Chemisorptions on the Thermal Conductivity of Single-Wall Carbon Nanotubes"* NANO LETTERS 4, 1051-1053, 2004.

[74] Szentes, Varga Cs., Horvàth G., Bartha L. Kònya Z., Haspel H., Szèl J., Kukovecz A. *"Electrical resistivity and thermal properties of compatibilized multi-walled carbon nanotube/polypropylene composites"* eXPRESS Polymer Letters 6, 494-502, 2012.

[75] Ezat G. S., Kelly A. L., Mitchell S. C., Youseffi M., Coates P. D. "*Effect of maleic anhydride grafted polypropylene compatibilizer on the morphology and properties of polypropylene/multiwalled carbon nanotube composite"* Polymer Composites 33, 1376-1386, 2012.

[76] Díez-Pascual A M, Naffakh M., Gómez M A, Marco C, Ellis G, González-Domínguez J M, Ansón A., Martínez M T, Martínez-Rubi Y, Simard B and Ashrafi B "*The influence of a compatibilizer on the thermal and dynamic mechanical properties of PEEK/carbon nanotube composites"* Nanotechology, 20, 315707, 2009.

[77] Pietrak K. , Wisniewski T.S. "*A review of models for effective thermal conductivity of composite materials"* Journal of Power Technologies 95, 14-24, 2015.

[78] Nan C.W., Liu G., Lin Y., Li M. "*Interface effect on thermal conductivity of carbon nanotubes composites*" Appl. Phys. Lett. 85, 3549, 2004.

[79] Bejan A. D. K. A., "*Heat transfer handbook"*, John Wiley & Sons, 2003.

[80] Stauffer D. *"Introduction of Percolation Theory"*; Taylor and Francis: London, UK, 1985.

[81] Bauhofer W., Kovacs J.Z. *"A review and analysis of electrical percolation in carbon nanotube polymer composite"* Composites Science and Technology, 69, 1486-1498, 2009.

[82] Shenogina N., Shenogin S., Xue L., Keblinsk P. "*On the lack of thermal percolation in carbon nanotube composites* "Appl. Phys. Lett. 87, 133106, 2005.

[83] Bonnet P., Sireude D., Garnier B., Chauvet O. "*Thermal properties and percolation in carbon nanotubes-polymer composites*" Appl. Phys.Lett. 91, 201910, 2007.

[84] Paleo A. J., García X., Arboleda-Clemente L., Van Hattum F. W., Abad M. J., Ares A. "*Enhanced thermal conductivity of rheologically percolated carbon nanofiber reinforced polypropylene composites"* Polym. Adv. Technol. 26, 369–375, 2015.

[85] Kole M., Tripathi D., Dey T.K. "*Percolation based enhancement in effective thermal conductivity of HDPE/LBSMO composites*" Bull. Mater. Sci. 35, 601-609, 2012.

[86] Zhang G, Xia Y, Wang H, Tao Y, Tao G, Tu S and Wu H "*A Percolation Model of Thermal Conductivity for Filled Polymer Composites"* Journal of Composite Materials 44, 963-970, 2010.

[87] Deng F., Zheng Q.S., Wang L.F. "*Effects of anisotropy, and non straightness of carbon nanotubes on thermal conductivity of carbon nanotube composites*" Appl. Phys. Lett. 90, 021914, 2007.

[88] Kickelbick G. "*Hybrid Materials: Synthesis, Characterization, and Applications"* John Wiley & Sons, 516 pp., 2007.

[89] Ashby M.F., Brechet Y.J.M. "*Designing hybrid materials*". Acta Mater 51, 5801-5821, 2003.

[90] Szeluga U., Kumanek B., Trzebicka B. "*Synergy in hybrid polymer/nanocarbon composites. A review"* Composites: Part A 73**,** 204-231, 2015.

[91] Leong Y.W., Mohd Z.A., Ariffin A. "*Mechanical and thermal properties of Talc and Calcium Carbonate filled polypropylene hybrid composites"* Journal of Applied Polymer Science 91, 3327, 2004.

[92] Bao H.-D., Guo Z.-X., Yu J. "*Effect of electrically inert particulate filler on electrical resistivity of polymer/multi-walled carbon nanotube composites"* Polymer 49, 3826, 2008.

[93] Ng H.Y., Lu X. "*Thermal conductivity, electrical resistivity, mechanical and rheological properties of thermoplastic composites filled with boron nitride and carbon fiber*" Polymer-Composites 26, 66-73, 2005.

[94] Müller M.T., Dreyße J., Häußler L., Krause B., Pötschke P. "*Influence of talc with different particle sizes in melt-mixed LLDPE/MWCNT composites"* Journal of Polymer Science: Part B 51, 1680-1691, 2013.

[95] Lee G.-W., Parka M., Kima J., Lee J. I., Yoon H. G. *"Enhanced thermal conductivity of polymer composites filled with hybrid filler"* Composites: Part A 37, 727-734, 2006.

[96] Pak S.Y., Kim H.M., Kim S.Y., Youn J.R. "*Synergistic improvements of thermal conductivity of thermoplastic composites with mixed boron nitride and multiwalled carbon nanotubes fillers*" Carbon 50, 4830, 2012.

[97] Choi S., Kim J. *"Thermal conductivity of epoxy composites with a binary-particle system of aluminum oxide and aluminum nitride fillers"* Composites Part B Engineering 51, 140-147, 2013.

[98] Srinivas K., Bhagyashekar M.S. "*Thermal Conductivity Enhancement of Epoxy by Hybrid Particulate Fillers of Graphite and Silicon Carbide"* Journal of Minerals and Materials Characterization and Engineering 3, 76-84, 2015.

[99] Yuan F.-Y., Zhang H.-B., Li X., Li X.-Z., Yu Z.-Z. "*Synergistic effect of boron nitride flakes and tetrapod-shaped ZnO whiskers on the thermal conductivity of electrically insulating phenol formaldehyde composites"* Composites: Part A 53, 137-144, 2013.

[100] Mahanta N.K., Loos M.R., Manas Zlocozawer I., Abramson A.R. "*Graphite-graphene hybrid filler system for high thermal conductivity of epoxy composites*" J.Mater.Res. 30, 959-964, 2015.

[101] Birnboim A., Carnel Y., Wilson Jr. O.C., Knowlton Lloyd J.K., Smith S., Campbell R."*Thermal Conductivity of Zinc Oxide: From Green to Sintered State"* Journal of American Ceramic society 85, 1249-1253, 2002.

[102] Huang X., Jiang P. "*A review of dieletric polymer composites with high thermal conductivity*" IEEE Electrical Insulation Magazine 27, 8-16, 2011.

[103] Ebadi-Dehaghani H., Reiszadeh M., . Chavoshi A, Nazempour M., Vakili M. H. "*The Effect of Zinc Oxide and Calcium Carbonate Nanoparticles on the Thermal Conductivity of Polypropylene"* Journal of Macromolecular Science, Part B: Physics 53, 93-107, 2014.

[104] Perry H., Green D.. "*Perry's Chemical Engineers' Handbook*" Seventh Edition. Mc Graw Hill International Editions, 1999.

[105] Clauser C., Huengens E. "*Thermal conductivity of rocks and minerals*". In: Ahrens TJ, editor. Rock physics and phase relations. A handbook of physical constant. American Geophysial Union Reference; 1995.

[106] Sichel E. K., Miller R. E., Abrahams M. S., Buiocchi C. J. "*Heat capacity and thermal conductivity of hexagonal pyrolytic boron nitride"* Phys. Rev. B 13, 4607-4611, 1976.

[107] Borges S.V., Dias M. L, Pita V. J., Azuma C., Dias M. V "*Processability, morphology and thermal behavior of poly(lactic acid)/synthetic mica nanocomposites obtained by melt blending"* Journal of Composite Materials, **48**, 1429–1440, 2014

[108] ASTM E1530-99 "*Standard Test Method for Evaluating the Resistance to Thermal Transmission of Materials by the Guarded Heat Flow Meter Technique".*

[109] Razavi-Nouri M., Ghorbanzadeh-Ahangari M., Fereidoon A., Jahanshahi M. "*Effect of carbon nanotubes content on crystallization kinetics and morphology of polypropylene*" Polymer Testing 28, 46-52, 2009.

[110] McNally T., Pötschke P. *"Polymer-Carbon Nanotube Composites: Preparation, Properties and Applications"* Woodhead Publishing, 848 pp., 2011.

[111] Pegel S. Ph.D.thesis. Materials Science Technical University Dresden. Dreden; 2010.

[112] M. Bernier, F. Garet, and J.L. Coutaz, "*Precise determination of the refractive index of sample showing low transmission bands by THz Time Domain Spectroscopy*", IEEE Trans. THz Science Techn. 3, 295-301, 2013.

[113] Kasaliwal G.R., Golden A., Pötschke P., Heinrich G. "*Influences of polymer matrix melt viscosity and molecular weight on MWCNT agglomerate dispersion*" Polymer 52, 1027-1036, 2011.

[114] Lee S.H., Cho E., Jeon S.H., Youn J.R. "*Rheological and electrical properties of polypropylene composites containing functionalized multi-walled carbon nanotubes and compatibilizer*" Carbon 45, 2810-2822, 2007.

[115] Yang B.X., Pramoda K.P., Xu G.Q., Goh S.H. "*Mechanical reinforcement of Polyethylene using polyethylene-grafted multiwalled carbon nanotubes*" Advanced Functional Materials 17, 2062-2069, 2007.

[116] Jin S.H., Kang C.H., Yoon K.H., Bang D.S., Park Y-B "*Effect of compatibilizer on morphology, thermal, and rheological properties of polypropylene/functionalized multi-walled carbon nanotubes composite*" Jour. of App.Poly.Sci. 111, 1028-1033, 2009.

[117] Benatar A., Gutowski T. G. *"Effects of moisture on interface modified graphite epoxy composites"* Polymer Composites 7, 84-90, 1986.

[118] Thomas J. A., Iutzi R. M., McGaughey Alan J. H. *"Thermal conductivity and phonon transport in empty and water-filled carbon nanotubes"* Phys. Rev. B 81, 2010.

[119] Hong W.T., Tai N.H. "*Investigations of thermal conductivity of composites reinforced with carbon nanotubes"* Diamond & Related Materials 17, 1577-1581, 2008.

[120] Patti A., Russo P., Acierno D., Acierno S. "*The effect of filler functionalization on dispersion and thermal conductivity of polypropylene/multi wall carbon nanotubes composites".* DOI 10.1016/j.compositesb.2016.03.072, Composites Part B: Engineering, 2016.

[121] Ling W., Gu A.J., Liang G.Z., Yuan L. "*New composites with high thermal conductivity and low dielectric constant for microelectronic packaging".* Polym. Comp. 31, 307-313, 2010.

[122] Logakis E., Pollatos E., Pandis Ch., Peoglos V., Zuburtikudis I., Delides C.G., Vatalis A., Gjoka M., Syskakis E., Viras k., Pissis P. "*Structure-property relationships in isotactic polypropylene/multi-walled carbon nanotubes nanocomposites*" Composites Science and Technology 70, 328-335, 2010.

[123] Avalos-Belmontes F., Ramos-deValle L. F., Ramírez-Vargas E., Sánchez-Valdes S., Méndez-Nonel J.,and Zitzumbo-Guzmán R. *"Nucleating Effect of Carbon Nanoparticles and Their Influence on the Thermal and Chemical Stability of Polypropylene"* Journal of Nanomaterials 2012 ,1-8, 2012.

[124] McNally T., Potschke P. "*Polymer-carbon nanotube composites-Preparation, properties and applications*" Woodhead Publishing, 848 pp., 2011.

[125] Bikiaris D. "*Microstructure and Properties of Polypropylene/Carbon Nanotube Nanocomposites"* Materials 3, 2884-2946, 2010.

[126] Casini R., Papari G., Andreone A., Marrazzo D., Patti A., Russo P. *"Dispersion of carbon nanotubes in melt compounded polypropylene based composites investigated by THz spectroscopy"*, Optics Express 23, 18181, 2015.

[127] Wietzke S., Jansen C., Reuter M., Jung T., Chatterjee S., Fischer B.M., and Koch M. "*Terahertz spectroscopy on polymers: a review of morphological studies*", J. Mol. Struct. 1006, 41-51, 2011.

[128] Wietzke S., Jansen C., Jung T., Reuter M., Baudrit B., Bastian M., Chatterjee, and Koch M., "*Terahertz time domain spectroscopy as a tool to monitor the glass* S. *transition in polymers*", Opt. Express 17, 19006-19014, 2009.

[129] Krumbholz N., Hochrein T., Vieweg N., Hasek T., Kretschmer K., Bastian M., Mikulics M., and Koch M., "*Monitoring polymeric compounding processes in line with THz time-domain spectroscopy*", Polym. Test. 28, 30-35, 2009.

[130] Rutz F., Koch M., Khare S., Moneke M., Richter H., and Ewert U., "*Terahertz quality control of polymeric compounds*", Int. J. Infr. Mill. Waves 27, 547-556, 2006.

[131] Prashantha K., Soulestin J., Lacrampe M.F., Krawczak P., Dupin G., Claes M. "*Masterbatch-based multi-walled carbon nanotube filled polypropylene nanocomposites: Assessment of rheological and mechanical properties*" Composites Science and Technology 69, 1756-1763, 2009.

[132] Pötschke P., Fornes T.D., Paul D.R. "*Rheological behavior of multiwalled carbon nanotubes/polycarbonate composites"* Polymer 43, 3247-3255, 2002.

[133] Zhang Q., Fang F., Zhao X., Li Y., Zhu M., and Chen D. "*Use of Dynamic Rheological Behavior to Estimate the Dispersion of Carbon Nanotubes in Carbon Nanotube/Polymer Composites*" J. Phys. Chem. B, 112, 12606-12611, 2008.

[134] Pötschke P., Abdel-Goad M., Alig I., Dudkin S., Lellinger D. "*Rheological and dielectrical characterization of melt mixed polycarbonate-multiwalled carbon nanotube composites*" Polymer, 45, 8863-8870, 2004.

[135] Shenoy A.V. "*Rheology of filled polymer systems*", Kluwer Academic Publishers, Dordrecht, 1999.

[136] Wu D., Wu L., Zhou W., Sun Y., Zhang M. "*Relations Between the Aspect Ratio of Carbon Nanotubes and the Formation of Percolation Networks in Biodegradable Polylactide/Carbon Nanotube Composites*", Journal of Polymer Science: Part B: Polymer Physics, 48, 479-489, 2010.

[137] Pan Y., Li L. "*Percolation and gel-like behavior of multiwalled carbon nanotube/polypropylene composites influenced by nanotube aspect ratio*", Polymer 54, 1218-1226, 2013.

[138] Joshi M., Butola B. S., Simon G., Kukaleva N. "*Rheological and Viscoelastic Behavior of HDPE/Octamethyl-POSS Nanocomposites*", Macromolecules 39, 1839-1849, 2006.

[139] Winter H.H., Chambon F. "*Analysis of Linear Viscoelasticity of a crosslinking polymer at the gel point*" Jounal of Rheology 30, 367-382, 1986.

[140] Patti A., Barretta R., Marotti de Sciarra F., Mensitieri G., Menna C., Russo P. *"Flexural properties of multi-wall carbon nano tube/polypropylene composites: experimental investigation and non local modeling"* Composite Structures 131, 282, 2015.

[141] Prashantha K., Soulestin J., Lacrampe M.F., Krawczak P., Dupin G., Claes M., *Masterbatch based multi-walled carbon nanotube filled polypropylene nanocomposites: assessment of rheological and mechanical properties*, Comp. Sci. Techn. 69, 1756-1763, 2009.

[142] Chrissafisa K., Bikiaris D. "*Can nanoparticles really enhance thermal stability of polymers? Part I: An overview on thermal decomposition of addition polymers*" Thermochimica Acta 523, 1-24,2011.

[143] Ferry J.D. "*Viscoelastic properties of polymers"* Wiley, New York, 1980.

[144] Grady B.P. *"Carbon Nanotubes-Polymer Composites Manufacture, Properties, and Applications"* John Wiley & Sons, 339 pp., 2011.